ABSTRACT

CAMACHO UMAÑA, MANUEL ERNESTO. Understanding and Addressing Weed Science Problems Using Soil Physics. (Under the direction of Drs. Ramon G. Leon and Travis W. Gannon).

In the literature, few studies have successfully integrated principles and concepts of soil sciences (specifically soil physics) and weed science, where knowledge gaps and research questions involving both branches of science have not been addressed from an interdisciplinary perspective. The main objective of the present dissertation was to evaluate the use of principles and concepts of soil physics aiming to develop a more comprehensive view of weed related issues to better inform the decision-making process when designing weed management strategies. A set of experiments was conducted to address three general objectives: 1) to assess the role of water potential on seed germination through comparisons among osmotic solutions and mineral soils, 2) to investigate the potential lateral movement of solutes in soils with textural anisotropy, using a field trial and numerical modeling approach, and 3) to characterize the potential carryover risk of two residual herbicides and its further effects on carinata (*Brassica carinata* A. Braun) establishment in two different soils of North Carolina.

When comparing total seed germination of four plant species using soils or polyethylene glycol (PEG) as germination substrate, dramatic differences in seed germination were observed, even when seeds were submitted to the same water potential. These results indicated that PEG did not reproduce accurately how the edaphic environment supplies water to seeds during germination. Furthermore, when exploring the role of soil unsaturated hydraulic conductivity (K_h) on seed germination, it was shown that the variability observed among soils and water potentials was better explained by K_h than PEG–generated osmotic potentials

A field study provided empirical evidence for lateral movement of a conservative tracer (Br^-), which moved along the surface horizon (Ap) following the soil slope. This movement was also modeled using HYDRUS 2D/3D, which allowed to visualize accurately this Br^- advancing along the boundary between horizons over time. Our findings demonstrated this component of the solute movement as formerly hypothesized in the literature and reinforced the potential use of HYDRUS 2D/3D as useful tool to predict the transport and fate of herbicides, and further assessment of pesticide off-target movement risk.

Field experiments confirmed that imazapic persisted in the soil for a longer time than flumioxazin and moved deeper into the soil profile. This movement was more evident when imazapic was applied to a sandy soil, where residues were detected between 15 and 20 cm depth. However, when assessing the potential carryover herbicide effect for both herbicides, our results suggested that *B. carinata* can be planted safely when either imazapic or flumioxazin are applied 12 months before planting interval or longer.

Understanding and Addressing Weed Science Problems Using Soil Physics

by
Manuel Ernesto Camacho Umaña

A dissertation submitted to the Graduate Faculty of
North Carolina State University
in partial fulfillment of the
requirements for the degree of
Doctor of philosophy

Crop Science

Raleigh, North Carolina
2021

APPROVED BY:

_____	_____
Dr. Ramon G. Leon Co-Committee Chair	Dr. Travis W. Gannon Co-Committee Chair
_____	_____
Dr. Aziz Amoozegar	Dr. Joshua L. Heitman

DEDICATION

I am dedicating this dissertation to my beloved family:

"Mi santa madre, mi tata, mis hermanitas y mis dos sobrinos"

Which patience, support, and endless love kept me focused on my studies, aiming to attain a better future for us. Thanks for being there always, no mattered the distance nor the time, during my happiest days and my saddest hours. The conclusion of all this wouldn't be possible without y'all.

I will dedicate this to "*Don Gonzalo*", who took his time to teach me the love for the agriculture and the nobleness of hard work and honesty. Thank you "Abuelito" for all those afternoons when we shared coffee, "revived" old parishioners, and told same old jokes. And overall, thanks for leading me into the right path, making me reach this crucial point in my life.

"¡Salve oh Patria! tu pródigo suelo,
dulce abrigo y sustento nos da;
bajo el límpido azul de tu cielo
¡vivan siempre el trabajo y la paz!"

Tomado del Himno Nacional de Costa Rica.

Hail, oh Homeland! Your prodigal soil
Gives us sweet shelter and sustenance
Under the limpid blue of your sky
May peace and labor live always.

Adapted from Costa Rican National Anthem

BIOGRAPHY

Manuel E. Camacho Umaña was born and raised in La Legua de Aserrí, province of San José in Costa Rica. Descendent of trailblazing families ("*Los Camachos*" and "*Los Umañas*") that long ago cleared that land and started coffee farms and cattle production, he grew up picking coffee beans, playing "Fútbol", and free-running in those sloped and beautiful landscapes. After obtaining a socioeconomic scholarship from the University of Costa Rica (UCR), he achieved his Bachelor of Science and Licentiate degrees in Agronomy at UCR, San Pedro de Montes de Oca. As part of his scholarship and following graduation, he worked for nine years as a lab assistant in the Natural Resources Lab, under the direction of Mr. Rafael Mata (M.Sc.), where his interest in Soil Genesis and Soil Physics flourished. Manuel continued his graduate school studies, working at the same lab in his alma mater (UCR), where he obtained a Master of Science in Soil Science. His thesis focused on the soil genesis and characterization of Oxisols in landscapes of Costa Rica and concluded this program on November 4th, 2016. Encouraged by his Soil Science professors at UCR to pursue the Doctorate degree, Manuel moved to the United States. In 2018 he joined Leon's Weed Biology and Ecology lab at North Carolina State University, where he found a "fertile ground" managed by an outstanding mentor, Dr. Ramon G. Leon. Under his mentorship, Manuel developed a broader perspective in agriculture and environmental sciences, as reflected in his Ph.D. dissertation. In addition, Manuel taught soils science under the supervision of Dr. Amy M. Johnson, giving him an opportunity to gain invaluable experience for his future career as a Soil Science Professor at UCR. While living in North Carolina, Manuel found joy and life balance in "Team bonding with Franklin" at Mitch's Tavern and D3, travelling within the state, tasting local breweries, and visiting the Mountains, the Sounds, and the Coast, in company of

wonderful people that he met in this blessed southern state. North Carolina took a little piece of his heart forever.

ACKNOWLEDGMENTS

I would like to express my deepest gratitude to my advisor Dr. Ramon G. Leon, not only for taking me on as his PhD student, but also to let me be part of his outstanding team. More than an advisor Ramon was a true mentor, always available to answer my questions or provide his best advice, and patient enough to deal with my frequent mistakes. But not limiting to the academic aspect, he propitiated a suitable environment for intellectual and personal growth during coffee time or team bonding. I will always be grateful for this opportunity.

¡Muchas gracias jefe!

In a very special way, I would like to thank my co-advisor Dr. Travis W. Gannon for his time, goodwill, and the support during this project, allowing me to learn about pesticide analysis and fate while working at his Pesticide and Trace Element Fate and Behavior Research Lab.

Thank you so much for everything, Dr. Gannon!

I would like to extend my appreciation to the other members of my committee: Dr. Aziz Amoozegar and Dr. Joshua L. Heitman, for their continuous support along these years as soil physics apprentice, for being always able to attend my questions and help me out with materials, equipment, and the most valuable thing: their knowledge and experience. Thanks for allowing me to attend the weekly lab meetings, where they made me feel as one soil physicist more.

Thank y'all for your goodwill!

I would like to acknowledge my former mentors at University of Costa Rica: Dr. Alfredo Alvarado, Rafael Mata, and Gilberto Cabalceta. They supported me from the beginning of this journey, and without their initial encouragement, I wouldn't be pursuing my PhD degree in North Carolina State University.

¡Muchas gracias queridos amigos!

My presence in North Carolina State University wouldn't be possible without Dr. S. Chris Reberg-Horton's help, who brough me initially as visiting scholar and allowed me to collaborate with his lab. I will always appreciate the opportunity that you gave me.

My appreciations to Dr. Theresa Reinhardt Piskackova, who became a role model during our times as graduate students. Thanks for all those long talks about science, society, arts, and providing "the word of the day". Similarly, my appreciation goes to my friend and colleague Eric. A. L. Jones, who was willing to offer selflessly his help and vast knowledge when I was "deep in the weeds". Thank you both for make this path less tortuous.

I would like to thank Adam Howard for his patience, valuable help with soil physical analyses, and his goodwill. In a very special way, I thank Daniel Freund and Khalied Ahmed for their assistance and invaluable advises and help with the sampling homogenization and the pesticide residue analysis.

Thanks to Sandy Ethridge, and Alyssa Zsido for their technical assistance during the germination experiments and the carinata field trials. Also, my gratitude goes to Ashley Pouncey, Alex Veverka and Haley Woolard for their support and help with the greenhouse bioassay and soil samples preparation. As well, many thanks to Dr. Raymond McCauley, Marty Parish for their assistance and invaluable help at the Lake Wheeler Turf Field Laboratory

Thanks to Dr. Amy M. Johnson for her support and trust during these three semesters that she honored me helping as TA in SSC 112. I really appreciate your goodwill and this teaching opportunity, Dr. Johnson.

Thanks to Angie Barefoot, for her constant support and goodwill with us, the graduate students. Thanks for being always willing to help and make sure we were in track.

Finally, I would like to extend my appreciation to all friends I made in this blesses state, who in one way or another made this journey more pleasant, and who I will try to name here: Marcela Alfaro, John Sawyer, Clara Tang, Angel Cruz, Sean Bloszies, Francesco Tiezzi, Steph Sosinski, Raymond McCauley, Wesley Childress, Henrique da Ross Carvalho, Esdras Carbajal, Alyssa Zsido, Axel Gonzalez, Susan Ramos, Roberto Cantor, Michael McKnight, Ariel Zelaya, Sandy Ethridge, Ashley Pouncey, Fernando Oreja, Bryan Muñoz, Guillermo Chacón, Sofia Feng, Nelida Agramont, Danielle Cooney, Cara Mathers, Luis Rivera, Marco Granadino, Diego Contreras, Marco Fajardo, Trip Rogers, Saket Chandra, Stephanie Proaño, Theresa Piskackova, Jan Piskacek, Thomas Falkenburger, among others whom want to remain anonymous here, but always present in my heart and mind.

I want to express a special appreciation to Alyssa M. Peavey, for her love, constant support, and patience. Thanks for being always there, especially in those moments where I needed you more. Thanks for this time together, walking during beautiful sunsets, discovering new places, getting new adventures.

¡Muchas gracias guapa!

¡Siempre estarás presente en mi mente y corazón!

TABLE OF CONTENTS

LIST OF TABLES

LIST OF FIGURES

CHAPTER 1: General introduction

Weed interference in agriculture

The world population is projected to rise to 9.7 billion people in 2050 (UN DESA 2019), which will require an increase in agricultural production to satisfy food demand (Anderson et al. 2020). However, despite that increases between 25 and 75% the current production would be sufficient to meet this demand (Hunter et al. 2017), it will be necessary to deal with trade-offs like water use and pest management.

Weed management is a critical factor must be addressed to achieve this global objective (Westwood et al. 2018). For instance, weed interference and further control in agricultural systems costs approximately $15 billion to the United States economy, and in developing countries the relative cost of could be even higher (Buhler et al. 2000).

Herbicides have become the dominant weed control method around the world due their effectiveness and versatility of use in multiple cropping systems (Buhler et al. 2000). However, overreliance on their use has resulted in multiple ecological and environmental problems such as the evolution of herbicide resistant species, contamination of land and water bodies, and soil degradation (Gevao et al. 2000; Green and Owen 2011; Peterson et al. 2018). Therefore, weed management should consider other control methods including mechanical, biological principles and tactics, and cultural practices (Buhler et al. 2000; Harker and O'Donovan 2013).

On this regard, knowledge of weed biology and ecology becomes a cornerstone for implementing an integrated weed management in agricultural systems. For instance, critical information about the seed bank ecology will include seed density, germination rate, and emergence time (Forcella et al. 1993).

Soil as key component in weed science

Weed growth and survival in cropping systems are highly dependent on the interaction between two main factors (Monaco et al. 2002): 1) *competitive factors* resulting from the interference among weed species, weeds, and crops, and 2) *environmental factors* including biotic, climatic, and physiographic. Within this physiographic component, the edaphic environment (soil) plays a fundamental role in weed biology and ecology, providing the seedbed and the environmental signals as well as inputs for weed seed germination, plant establishment, and further population growth in space and time (Forcella et al. 1993; Gallandt 2006).

Despite their importance for weed growth, soil properties and their contribution to weed management strategies are frequently disregarded. This could be associated with the lack of understanding about soil physics by weed scientists, who spent most of the efforts on weed chemical control during the early 1900's (Hamil et al. 2004). Though modern weed scientists consider a broader scope as integrated weed management, seems to be that soil fertility and conservation are the only soil components included in this scope (Hamil et al. 2004).

Soil properties such as texture and structure play important roles in herbicide dynamics and fate in the soil. For instance, the herbicide would follow several pathways within the soil matrix, including the adsorption in clay minerals or organic matter present in the soil, the movement through the soil porous space, or the molecule degradation by chemical or biological reactions (Gevao et al. 2000; Mehdizadeh et al. 2021). This degradation pathway is associated with herbicide persistence in the soil, which varies with changes in organic matter and soil texture (Marchesan et al. 2010). These two soil properties also affect the soil total porosity, which is related to herbicide movement through the soil matrix (Neto et al. 2017).

Furthermore, these movement and degradation processes contribute to herbicide persistence and potential damage to non-target plant species or susceptible crops due to carryover (York et al. 2000; Ulbrich et al. 2005; Price et al. 2020). This reinforces the need for more detailed information about how soils and their properties, in specific those included within the soil physical component influence weed growth as well as the efficacy and fate of weed control tools.

Soil physics as a tool for solving problems in weed science

Within soil science, the branch that deals with the physical properties of the soil is denominated soil physics. More precisely, this discipline studies the state and movement of matter, in addition to transformation and fluxes of energy within the soil (Hillel 1998). Soil physics is both a basic and applied science, which practice aims to improve and optimize soil management.

Soil physics contributes to the understanding of natural processes in other disciplines such as agronomy, hydrology, meteorology, and plant ecology. For instance, the concept of the soil-plant-atmosphere *continuum* (now on only referred as *continuum*) integrates the contribution of these three components into the energy and water balance approach (Evett et al. 2012).

The structure and functionality of this *continuum* under several gradients (spatial and temporal), is a fundamental objective for ecological research in different ecosystems (Penuelas and Sardans 2020), including agroecosystems. In the case of weed science, soil physics principles and applied procedures have the potential to increase our knowledge about fundamental processes in weed biology and ecology.

For example, seed dormancy release and germination are affected by external factors such as water potential and temperature within the soil-atmosphere boundary, and quantification of the response to different levels for both variables can be obtained from direct measurements and further modelling development using proper soil physics techniques (Camacho et al. 2021).

Soil physics also studies the flow of water within the soil under saturated or unsaturated conditions, denominated steady and transient flow, respectively (Hillel 1998).

Soil water flow is fundamental to understand soil water dynamics, including water distribution within the soil profile, water balance, nutrient uptake by plants, and other plant hydric relationships influencing the *continuum* (Hopmans and Bristow 2002; Evett et al. 2012). Soil water flow and its variability within the edaphic landscape are involved in soil moisture gradients. These soil moisture gradients could affect weeds growth, establishment, and competition across the landscape (Henry et al. 2009).

There is a branch of soil physics that studies the fundamentals of solute transport through the soil, which becomes the cornerstone when assessing edaphic contamination, or groundwater quality (Hillel 1998). This solute transport within the soil is a complex phenomenon, that includes reactions such as chemical transformations and adsorption into the most reactive particles such as clays and organic colloids (Radcliffe and Šimůnek 2010).

Despite this level of complexity, it is possible to characterize and predict the movement of herbicides within soils using the soil physics principles and methods. This kind of studies have improved our understanding of the dynamics and fate of herbicides in the environment (Carter 2000; Karim et al. 2021). On this regard, knowledge about herbicide fate and behavior in the soil will be fundamental for integrated weed management and further solving problems in weed science (Buhler et al. 2000; Monaco et al. 2002; Harker and O'Donovan 2013).

Soil physics, weed management, and modeling

Soil physics evolved from early qualitative description of soil properties to quantitative expressions that captured the dynamics within the soil physical processes. This was possible because of the development of computers and the use numerical methods to solve complex differential equations that represented the mass and energy transfer processes within the soil (Campbell 1985).

Simplifications of these quantitative mathematical expressions used in soil physics are denominated models. Although they do not include the total complexity of physical processes, many models, when properly generated, even with their simplified approach can lead to satisfactory results while addressing these physical processes (Hillel 1987). The uncertainty inherent to the models can be reduced through specific procedures such as model calibration and the identification of critical parameters through sensitivity analysis (Doherty 2015; Pujol 2017).

Models are useful to describe soil physical processes that are difficult to study through field measurements, or when laboratory procedures are impractical. For instance, the assessment of water flow under unsaturated conditions (transient flow) in the field is challenging using the existing available methods (e.g., sprinkling infiltration and impeding layer infiltration method), which require special equipment and continuous measurements for longer periods (Hillel 1998).

However, this transient flow can be addressed using mathematical models that involve soil parameters that can be more easily measure in situ (Radcliffe and Šimůnek 2010). Furthermore, models can be used to perform simulations of different soil physical processes that are relevant while addressing problems in weed biology and ecology.

For instance, it is possible to perform simulations of herbicide movement through the soil profile and residue persistence or modelling the soil water dynamics on different soils and its effect on plants establishment and distribution. On this regard, HYDRUS is an advanced and popular software used to model and simulate soil physical processes for a variety of soil physical and hydrological processes, including soil water flow, heat fluxes, and solute transport (Radcliffe and Šimůnek 2010).

HYDRUS has a robust history of applications and validation (Šimůnek et al. 2012), has been widely used in other studies about solutes and pesticides behavior within the soil (Boivin et al. 2006, Oliveira et al. 2019), and is considered user-friendly. Thus, this model could represent a useful tool to be considered for integrated weed management within the agroecosystem and other environmental studies associated with the use of herbicides.

Mathematical models could also be employed to assess other important processes of weed biology and ecology. For example, seed germination is a fundamental concept in weed management, which determines plant population and community dynamics The variation in germination can be described using hydrothermal time models, which integrate temperature and water potential to predict the germination timing and pattern for a specific population (Allen et al. 2000; Bradford 2002). Despite that this approach has a solid theoretical background and has been widely used, most of the experiments were conducted under laboratory conditions and using polymeric solutions as germinations substrates (Michel 1983). This last fact raises questions about how representative those polymers are of edaphic variability affecting soil water potential in mineral soils.

Objectives

An immense amount information is available in the literature about weed ecology and biology, weed management, or soil physical properties, when consulting them individually. However, few reports successfully achieved the integration of principles and concepts of soil sciences (in specific soil physics) and weed science, where there are still knowledge gaps and research questions that have not been addressed yet. The main objective of the present dissertation was to evaluate the use of different principles and concepts of soil physics to address specific problems and knowledge gaps in weed science, aiming to attain a more comprehensive approach for weed management in agricultural systems. Therefore, I established three distinct specific objectives: 1) to assess the role of soil physical processes and specific soil properties on the seed germination of crops and weed species, 2) to investigate the movement of solutes in different soils of North Carolina using field assessments and further a modelling approach, and 3) to evaluate the potential carryover risk of two residual herbicides widely used in crop rotations in the southeastern USA and further effects on carinata establishment in two different soils, aiming to assess changes in soil physical properties and their potential contribution to this herbicide carryover risk.

Objective 1 is covered in the chapter 2. Objective 2 is addressed in chapters 3 and 4. Objective 3 is covered in chapter 4.

Glossary of Key Concepts

As previously mentioned, this dissertation covers diverse topics that link principles from soil physics and weed science in a complementary fashion. Thus, the subsequent chapters will include diverse concepts that could be unfamiliar to the reader. The following is a list of concepts that are necessary to understand the research presented here.

Soil water potential: it refers to the difference in potential energy per unit of mass, volume, or weight of water, when it's compared with water under its standard state. This water standard state refers to water without solutes (pure), without forces acting over but gravity, at atmospheric pressure (P_0) and with reference height (z_0) and temperature (T_0).

Soil hydraulic conductivity: it is the soil ability to transmit liquids across it. Technically, soil hydraulic conductivity is the proportionality constant (K_s) that associates a water flux passing through a soil cross-sectioned area (Q/A) to a total soil water potential head gradient ($\Delta H/L$) as described by the Darcy's equation.

Soil water retention: it refers to the soil ability to hold or retain water. More technically, soil water retention is the relationship among the soil water content and the soil matric potential (soil matric suction).

Soil water flow: it refers to water movement occurring within the soil. This movement is predominantly vertical but also has components of lateral flow. Soil water flow can occur under both saturated (steady flow) or unsaturated conditions (transient flow). Water flow affects other important processes within the soil, including solute transport and water redistribution.

Polyethylene glycol (PEG): is a multiuse polymer utilized as solute in different aqueous mixtures. It has the property to retain water molecules within its polymeric chains, which allows to create very high osmotic pressure values (up to -2.0 MPa).

Modeling: is a group of procedures used to represent specific natural processes or fractions of them, using simplifications or reducing the number of factors involved. Generally, quantitative mathematical expressions used to describe the patterns found in those natural process are denominated models. Despite they do not encompass the total complexity of these processes, their simplified approach leads to obtain satisfactory and practical approximations.

Sensitivity analysis: it is a processes employed to estimate the contribution of individual inputs included in a specific model to the total uncertainty of the variable to predict. The sensitivity analysis computes all model inputs used and provide quantitative information about 1) the overall effect of each input in the model output (target variable) and 2) the effect of an interactive relationship between all the inputs assessed. Then, sensitivity analysis allows 1) to identify those model inputs which magnitude changes will result in a significant change of the final results, and 2) to reduce the number of model inputs by taking away inputs when identified as non-influential, increasing the model parsimony (model simplicity).

Model calibration: it is defined as a group of steps or processes employed to setting or tunning a model aiming to solve a specific problem. This tunning involves the manipulation of model inputs or the initial and boundary conditions under an acceptable range of values, with the objective to obtain simulated results close enough to observed values that considered as true.

Mathematical solutions in modeling: Two different approaches used to solve complex model are: 1) analytical solutions, which include a series of logical steps to solve the problem and finding the exact answer using the model, and 2) numerical solutions, which consist in iterative calculations where the model inputs are slightly changed in every run until the model output reaches a value that is considered as acceptable under certain level of error. The numerical solutions are preferred in models which complexity involves several inputs, where the analytical solutions fail to provide an answer that is considered reasonable. In addition, the advances in computer science have helped to perform the algorithms for numerical solution in a relatively shorter time.

HYDRUS 2D/3D: is a computer software widely employed to perform modeling and simulations of different processes in soil physics, hydrology, and other related disciplines. HYDRUS is based on fundamental theoretical equations and uses numerical solution to perform the calculations and further simulations of water flow, heat and solute transport under initial and boundary conditions selected by the user. This software is versatile enough to simulate several process in time and space.

Integrated weed management: is referred to the integration of a series of weed control approaches, which are used simultaneously or complementary to reduce weed populations to the point they are at ecologically and economically acceptable levels. This management is not limited to weed control using herbicides, but the adoption of cultural practices and an interdisciplinary approach including certain branches of soil science and agroecology.

Herbicide persistence: it is referred to the length of time that a particular herbicide molecule remains active (bioavailable). In general, it is expected that the herbicide persistence is long enough to ensure the weed control but allows the herbicide dissipation in the soil to inactivate the molecule and avoid further crop damage.

Herbicide carryover: it is defined as the potential phytotoxic effects that an herbicide could produce in a subsequent crops or seedlings just established. It is associated with intrinsic properties and behavior in the soil of the herbicide molecule.

References

Allen, P.S., Meyer, S.E. Khan, M.A. 2000. Hydrothermal time as a tool in comparative germination studies. In Black, M., Bradford, K.J., Vázquez-Ramos, J.(eds.). Seed Biology: Advances and Applications. Wallingford, U.K., CABI Publishing. pp 401–410.

Anderson, R., Bayer, P.E., Edwards, D. 2020. Climate change and the need for agricultural adaptation. Current opinion in plant biology 56: 197-202. https://doi.org/10.1016/j.pbi.2019.12.006

Boivin, A., Šimůnek, J., Schiavon, M., van Genuchten, M.T. 2006. Comparison of pesticide transport processes in three tile-drained field soils using HYDRUS-2D. Vadose Zone Journal 5(3): 838-849. https://doi.org/10.2136/vzj2005.0089

Bradford, K.J. 2002. Applications of hydrothermal time to quantifying and modeling seed germination and dormancy. Weed Science 50(2): 248-260. https://doi.org/10.1614/0043-1745(2002)050[0248:AOHTTQ]2.0.CO;2

Buhler, D.D., Liebman, M., Obrycki, J.J. 2000. Theoretical and practical challenges to an IPM approach to weed management. Weed Science 48(3): 274-280. https://doi.org/10.1614/0043-1745(2000)048[0274:TAPCTA]2.0.CO;2

Camacho, M.E., Heitman, J.L., Gannon, T.W., Amoozegar, A., Leon, R.G. 2021. Seed germination responses to soil hydraulic conductivity and polyethylene glycol (PEG) osmotic solutions. *Plant and Soil 462*(1): 175-188. https://doi.org/10.1007/s11104-021-04857-5

Campbell, G.S. 1985. Soil physics with BASIC: transport models for soil-plant systems. Elsevier. Amsterdam, The Netherlands.

Carter, A.D. 2000. Herbicide movement in soils: principles, pathways and processes. Weed Research 40(1): 113-122. https://doi.org/10.1046/j.1365-3180.2000.00157.x

Doherty, J. 2015. Calibration and uncertainty analysis for complex environmental models. Brisbane, Australia: Watermark Numerical Computing.

Evett, S.R., Prueger, J.H., Tolk, J.A., Huang, P. 2012. Water and energy balances in the soil–plant–atmosphere continuum. In Huang, P.M., Li, Y., Sumner, M.E. (Eds.), Handbook of Soil Sciences: Properties and Processes (2nd ed.). CRC Press, Boca Raton, Florida, USA. pp. 6-1-6-44

Forcella, F., Eradat-Oskoui, K., Wagner, S.W. 1993. Application of weed seedbank ecology to low-input crop management. Ecological Applications 3(1): 74-83. https://doi.org/10.2307/1941793

Gallandt, E.R. 2006. How can we target the weed seedbank? Weed Science 54(3): 588-596. https://doi.org/10.1614/WS-05-063R.1

Gevao, B., Semple, K.T., Jones, K.C. 2000. Bound pesticide residues in soils: a review. Environmental pollution 108(1): 3-14. https://doi.org/10.1016/S0269-7491(99)00197-9

Green, J.M., Owen, M.D. 2011. Herbicide-resistant crops: utilities and limitations for herbicide-resistant weed management. Journal of agricultural and food chemistry 59(11): 5819-5829. https://doi.org/10.1021/jf101286h

Hamill, A.S., Holt, J.S., Mallory-Smith, C.A. 2004. Contributions of Weed Science to Weed Control and Management1. Weed Technology 18(sp1): 1563-1565. https://doi.org/10.1614/0890-037X(2004)018[1563:COWSTW]2.0.CO;2

Harker, K.N., O'Donovan, J.T. 2013. Recent weed control, weed management, and integrated weed management. Weed Technology 27(1): 1-11. https://doi.org/10.1614/WT-D-12-00109.1

Henry, G.M., Yelverton, F.H., Burton, M.G. 2009. Asymmetric responses of *Paspalum* species to a soil moisture gradient. Crop science 49(4): 1473-1480. https://doi.org/10.2135/cropsci2008.08.0506

Hillel, D. 1987. Modeling in soil physics: A critical review. In Boersma L.L. (ed.). Future Developments in Soil Science Research. Soil Science Society of America. Madison, USA. pp. 35-42. https://doi.org/10.2136/1987.futuredevelopmentssoil.c5

Hillel, D. 1998. Environmental Soil Physics. Academic Press. San Diego, USA. 771 p.

Hopmans, J.W., Bristow, K.L. 2002. Current capabilities and future needs of root water and nutrient uptake modeling. Advances in agronomy 77: 103-183. https://doi.org/10.1016/S0065-2113(02)77014-4

Hunter, M.C., Smith, R.G., Schipanski, M.E., Atwood, L.W., Mortensen, D.A. 2017. Agriculture in 2050: recalibrating targets for sustainable intensification. Bioscience 67(4): 386-391. https://doi.org/10.1093/biosci/bix010

Karim, R., Reading, L., Dawes, L., Dahan, O., Orr, G. 2021. Transport of photosystem II (PS II)–inhibiting herbicides through the vadose zone under sugarcane in the Wet Tropics, Australia. CATENA 206: 105527.

Marchesan, E., dos Santos, F.M., Grohs, M., de Avila, L.A., Machado, S.L., Senseman, S.A., Massoni, P.F.S., Sartori, G.M. 2010. Carryover of imazethapyr and imazapic to nontolerant rice. Weed Technology 24(1): 6-10. https://doi.org/10.1614/WT-08-153.1

Mehdizadeh, M., Mushtaq, W., Siddiqui, S.A., Ayadi, S., Kaur, P., Yeboah, S., Tampubolon, K. 2021. Herbicide Residues in Agroecosystems: Fate, Detection, and Effect on Non-Target Plants. Reviews in Agricultural Science 9: 157-167. https://doi.org/10.7831/ras.9.0_157

Michel, B.E. 1983. Evaluation of the water potentials of solutions of polyethylene glycol 8000 both in the absence and presence of other solutes. Plant Physiology 72:66–70 https://doi.org/10.1104/pp.72.1.66

Monaco, T.J., Weller, S C., Ashton, F.M. 2002. Weed science: principles and practices. John Wiley & Sons, New York, USA. 671 p.

Neto, M.D.D.C., Souza, M.D.F., Silva, D.V., Faria, A.T., da Silva, A.A., Pereira, G.A.M., de Freitas, M.A.M. 2017. Leaching of imidazolinones in soils under a Clearfield system. Archives of Agronomy and Soil Science 63(7): 897-906. https://doi.org/10.1080/03650340.2016.1249471

Oliveira, L.A.D., Miranda, J.H.D., Grecco, K.L., Tornisielo, V.L., Woodbury, B.L. 2019. Atrazine movement in corn cultivated soil using HYDRUS-2D: A comparison between real and simulated data. Journal of Environmental Management 248: 1-8. https://doi.org/10.1016/j.jenvman.2019.109311

Penuelas, J., Sardans, J. 2021. Developing holistic models of the structure and function of the soil/plant/atmosphere continuum. *Plant and Soil 461*(1): 29-42. https://doi.org/10.1007/s11104-020-04641-x

Peterson, M.A., Collavo, A., Ovejero, R., Shivrain, V., Walsh, M.J. 2018. The challenge of herbicide resistance around the world: a current summary. Pest management science 74(10): 2246-2259. https://doi.org/10.1002/ps.4821

Price, K.J., Li, X., Price, A. 2020. Cover crop response to residual herbicides in peanut-cotton rotation. Weed Technology 34(4): 534-539. https://doi.org/10.1017/wet.2020.5

Pujol, G. 2017. Sensitivity: Global sensitivity analysis of model out-puts. Comprehensive R Archive Network. Retrieved from https://CRAN.R-project.org/package=sensitivity

Radcliffe, D.E., Šimůnek, J. 2010. Soil physics with HYDRUS: Modeling and applications. CRC press. Boca Raton, Fl. USA. 373 p. https://doi.org/10.1201/9781315275666

Ulbrich, A.V., Souza, J.R.P., Shaner, D. 2005. Persistence and carryover effect of imazapic and imazapyr in Brazilian cropping systems. Weed Technology 19(4): 986-991. https://doi.org/10.1614/WT-04-208R2.1

UN DESA. 2019. World Population Prospects 2019. Available: https://population.un. org/wpp/Download/Standard/Population/ Accessed 4 October 2021.

York, A.C., Jordan, D.L., Batts, R.B., Culpepper, A.S. 2000. Cotton response to imazapic and imazethapyr applied to a preceding peanut crop. Journal of Cotton Science 4: 210-216.

Westwood, J.H., Charudattan, R., Duke, S.O., Fennimore, S.A., Marrone, P., Slaughter, D.C., Zollinger, R. 2018. Weed management in 2050: Perspectives on the future of weed science. Weed Science 66(3): 275-285. https://doi.org/10.1017/wsc.2017.78

CHAPTER 2: Seed germination responses to soil hydraulic conductivity and polyethylene glycol (PEG) osmotic solutions

Published in *Plant and Soil*

Manuel E. Camacho[1]; Joshua L. Heitman[1]; Travis W. Gannon[1]; Aziz Amoozegar[1]; Ramon G. Leon[1,2,3]

1 Department of Crop and Soil Sciences, North Carolina State University, Campus Box 7620, Raleigh, NC 27695, USA.

2 Center for Environmental Farming Systems, North Carolina State University, Campus Box 7609, Raleigh, NC 27695, USA.

3 Genetic Engineering and Society Center, North Carolina State University, Campus Box 7565, Raleigh, NC 27695, USA.

Abstract

Aims Seed germination is one of the most important processes in plant biology and ecology because it determines the timing and magnitude of seedling emergence events every growing season influencing community dynamics. Our aim was to determine whether polyethylene glycol (PEG) solutions simulate soil water potential accurately and recreate germination responses to soil water availability.

Methods In this study, we compared seed germination of four plant species in PEG and four soils with different textures under six water potentials under controlled laboratory conditions.

Results Total seed germination for all species significantly differed between soil and PEG under the same water potentials, as well as among soil water potentials for each of PEG and soil materials. Due to the inconsistent total germination associated with soil water potential, we evaluated unsaturated soil hydraulic conductivity (K_h) as a predictor of germination. The germination of all species followed the same response to K_h. Germination rate (GR_{50}) was more directly related to water potential than total germination, but K_h provided a more robust description of GR_{50} across species and soils than PEG-osmotic potentials.

Conclusions Our findings showed that K_h is a more informative variable to predict both total seed germination and germination rate in soil, and caution must be used when considering results obtained using PEG solutions to infer germination behavior under field conditions.

Introduction

Seed germination is a fundamental process in the biology of plants determining population and community dynamics. This process is highly dependent on edaphic and environmental conditions, from which water and temperature are among the most important environmental factors (Koller and Hadas 1982; Walck et al. 2011; Bewley et al. 2013). As these two environmental factors are essential for germination, the integration of heat accumulation units and soil water availability as hydrothermal time is considered a useful approach to describe germination progression over time of seed lots or populations under field conditions (Allen et al. 2000; Bradford 2002; Bewley et al. 2013).

The use of hydrothermal time is based on the premise that seed germination rate is related to temperature (T) and water potential (ψ) around optimum conditions that are bound by lower and upper thresholds (Allen et al. 2000; Bradford 2002). Therefore, total germination and germination rate will occur as long as both conditions are met: 1) temperature is within the thresholds and 2) water potential is above the minimum. The longer the time these two conditions are met (i.e., hydrothermal time accumulation), the greater the germination. Mathematical models have been used to describe germination responses based on hydrothermal time accumulation to help predict germination timing and intensity in agricultural and natural systems (Allen et al. 2000; Bradford 2002).

Several laboratory studies have evaluated the cumulative seed germination of different plant species as a function of hydrothermal time accumulation (Allen et al. 2000; Bradford 2002; Bidgoly et al. 2018; Mobli et al. 2018; Abdellaoui et al. 2019). A common methodology in most studies using hydrothermal time is the use of polyethylene glycol (PEG) to generate different water potentials as described by Michel (1983).

PEG solutions have the advantages of maintaining relatively steady osmotic potentials equivalent to the desired water potentials as well as the simplicity with which a wide range of water potentials can be generated to determine germination thresholds (Bewley et al. 2013). However, it is questionable that homogeneous PEG solutions can realistically represent soil-water-seed interactions, which are also influenced by the intrinsic field soil variability (Peck et al. 1977). Therefore, the use of germination predictive models developed with water potential requirements determined with PEG solutions might not be appropriate to describe field seed germination, so direct soil water potential measurements might be needed (Bullied et al. 2012).

In the 1970s, at the same time that PEG solutions were starting to be used as a surrogate of soil water potential (Michel and Kaufmann 1973), other studies were suggesting that soil variables such as hydraulic conductivity, might play a more important role than water potential on seed germination (Dasberg 1971; Dasberg and Mendel 1971). Although those studies did not directly and systematically compare PEG solutions with soil with the same water potentials, they demonstrated that soil textural properties could influence the response of the seed to water potential, and this could result in different germination behaviours.

The simplicity and convenience of Michel's (1983) methodology quickly prompted a widespread adoption by the plant biology community. However, to the extent of our knowledge, no rigorous comparison between germination in PEG solutions and soil have been conducted to validate the use of this methodology as a mean to predict germination behaviour in the field, as many researchers have done over almost four decades.

Accurate and robust models of seed germination based on environmental variables are critical to understand and predict vegetation dynamics in response to changes in temperature and rainfall patterns. However, the lack of studies comparing seed germination as impacted by

specific water potentials under different soil physical conditions in place of using PEG solutions greatly limits our ability to use that information to understand plant biology and ecology under field conditions. The objectives of this study were (1) to compare the response of seed germination of four plant species under six different water potentials using both PEG solutions and four soils with contrasting texture as germination media, and (2) to develop indicators that properly describe germination responses under different soil water contents.

Materials and methods

Polyethylene glycol solutions and water potential measurement

Polyethylene glycol 8000 (PEG, Fisher Scientific, Pittsburgh, PA) solutions were prepared according to the procedure described by Michel (1983) to establish water potentials of -0.1, -0.3, -0.6, -0.8 and -1.2 MPa at 25°C. Water potential of each solution was measured with a WP4C dew point potential meter (Meter Group Inc., Pullman, WA) with a ± 0.05 MPa precision from 0 to −5 MPa.

Soil sampling and soil physical analysis

Bulk soil materials were collected from the top 10 cm at four agricultural fields in North Carolina with different soil textures. The soils at the fields were mapped as Cecil, Chewacla, Georgeville, and Herndon soil series. The textural classes of the soils were sandy loam, loam, clay loam, and silty loam for Cecil, Chewacla, Georgeville, and Herndon, respectively (**Table 1.1**). Soil materials were air dried for 6 weeks in a greenhouse and mixed every two days to ensure homogeneous dry conditions. Each soil material was then crushed through a 2 mm opening sieve. Three subsamples from each soil were used for particle size distribution analysis by the hydrometer method (Gee and Or 2002) and gravimetric soil water content (Topp and Ferré 2002).

Four subsamples of each soil material were sent to the soil testing lab at the Agronomic Services, North Carolina Department of Agriculture and Consumer Services (NCDA&CS) for soil fertility analysis. Soil pH was measured on 1:1 soil to water volume ratio. Humic matter (HM) content was determined through digestion with NaOH and further measurement through colorimetry (Mehlich 1984a). Mehlich-3 extracting solution (Mehlich 1984b) was used for P, K, Ca, Mg, S, Na, Mn, Cu, and Zn content determination. The elements extracted with this solution were analysed by plasma spectroscopy and quantified on volume basis (Mehlich 1984b; Tucker 1984). Cation exchange capacity (CEC) was estimated by adding the basic cations (Ca, Mg, Na, and K) and buffer acidity according with Mehlich et al. (1976) (**Table S1.1**).

Water retention was determined at five pressure levels corresponding to -0.1, -0.3, -0.6, -0.8 and -1.2 MPa). Soil water retention analysis was carried out using porous plates and pressure vessels following the methods described by Klute (1986). Soil samples were placed inside rubber rings over a porous plate (1 cm high, 5.1 cm inner diameter). The plates with soil samples were saturated for 24 h by setting them in a small tub and adding deionized water slowly until covering 0.5 cm above the plate surface. The plates with soil samples were then placed in a pressure vessel (Soil Moisture Equipment Corp., Santa Barbara, CA), and compressed air was applied to the vessel through a regulator. Soil samples remained under a constant pressure in the vessel until reaching equilibrium (no evidence of water draining from the vessel). The samples were then removed from the vessels and split into two subsamples. One subsample was processed to estimate gravimetric soil moisture content ($g\ g^{-1}$) following Topp and Ferré (2002) procedures. The other subsample was used to quantify water potential using a dew point potential meter WP4C (Meter Group Inc., Pullman, WA).

The above procedure was conducted for each pressure (i.e., soil water potential) using three replications for each soil. From soil water retention data, van Genutchen's equation parameters (van Genuchten 1980) were fitted through least squares regression for the four soils (**Figure S2.1**).

Each soil material was repacked into four 347.5 cm^3 volume cylinders at its natural bulk density. Then, saturated soil hydraulic conductivity (K_s) of each core was measured by maintaining the cylinders under a constant head pressure following the method described by Klute and Dirksen (1986) (**Table 1.1**). van Genutchen's equation parameters were then used to estimate unsaturated soil hydraulic conductivity (K_h) following Vogel et al. (2000).

Plant species and seed pretreatment

Two weed species, *Amaranthus palmeri* S. Watts and *Senna obtusifolia* H.S. Irwin & Barneby, and two cultivated species, *Lycopersicum esculentum* L. var. Cherokee Purple and *Triticum aestivum* L. cv. Shirley were selected to evaluate their seed germination.

Senna obtusifolia seeds were scarified with sandpaper to reduce physical dormancy and allow seed imbibition. Similarly, *A. palmeri* seeds were stratified under moist chilling conditions (3°C) for two weeks to reduce physiological dormancy. The tetrazolium test (International Seed Testing Association 1985) was performed to test seed viability before starting the germination experiments.

Germination experiments

Soils were autoclaved for 4 h at 121°C to reduce pathogen activity during the duration of the germination tests. Subsequently, based on soil water retention characteristics and initial gravimetric water content estimates, desired water potentials were generated by adding deionized water to each soil until reaching the corresponding target gravimetric water content. Water was

added to the ground soil with a spray bottle with careful and continuous soil mixing to ensure uniform moisture content. Then, sterile 9-cm diameter petri dishes (with bulk volume of 87 cm^3) were filled with a predetermined mass of the moistened soil samples corresponding to the desired natural bulk density of each soil (**Table 1.1**). The packing to achieve the desired bulk density in the petri dish was accomplished using a rubber stopper coated with parafilm®. Petri dishes corresponding to zero MPa pressure (saturated) were first filled with air dried soil and packed up to achieve the corresponding bulk density, and then were moistened with a volume of water estimated from soil porosity to generate saturation (**Table 1.1**).

Petri dishes corresponding to the PEG treatments were filled with 10 ml of corresponding PEG solution. A zero MPa water potential control treatment was included by filling the petri dishes with 15 ml of deionized water. Once all petri dishes were filled with PEG and soil, 50 seeds of the corresponding plant species were placed carefully on the surface, ensuring at least 70% of the seed surface was in direct contact with the PEG solution or soil matrix. This depth was chosen to ensure that there was a sufficient and uniform contact area between the seed and the germination matrix, proper oxygen availability, and avoid biases related to differences in pressure caused by matrix density and weight when the seed is fully buried. Petri dishes were sealed using Parafilm® and placed randomly in a germination chamber (Seedburo® Germinator) set to provide day (12 h) and night (12 h) temperature values of 30°C and 25°C, respectively.

Germinated seeds (i.e., with visible radicle) were counted and removed every other day. Petri dishes were sealed with parafilm after counting and placed back into the germination chamber. Petri dishes were weighed before and after seed counting to monitor any water loss and potential changes in water potential during the experiment. Soil and PEG solutions amounts were chosen such as water loss from the petri dish due to seedling removal represented less than 0.5%

of the weight variability, ensuring that water potential treatments were not influenced by seedling removal.

Experimental design and statistical analysis

Regression analysis was performed for the PEG calibration curve using the PEG solution concentration (g g^{-1} of H_2O) as independent variable and measured water potential as dependent variable. Those measurements were compared with nominal values estimated following Michell (1983) through linear regression analysis (**Figure S2.2**). From data obtained in soil water holding analysis, regression models were performed to fit the soil water retention curve.

Germination experiments were conducted twice as completely randomized designs with five replications. Total germination was normalized for each plant species to the corresponding average of maximum germination value. This was done to allow comparisons among the four species, which exhibited differences in total germination.

A factorial analysis of variance (ANOVA) was conducted for total normalized germination, with substrates (i.e., soils and PEG), water potential, and plant species treated as fixed effects and replications and experimental runs as random effects. Least significant differences were estimated using Tukey's HSD test ($\alpha = 0.05$) for treatment means separation.

Gompertz regression models were fitted to describe the relationship between total germination and the logarithm base ten of soil hydraulic conductivity ($\log_{10}(K_h)$) as independent variable for the soils within the same species. Linear regression models were also used to describe the response of the germination rate at 50% (GR_{50}) to $\log_{10}(K_h)$.

All statistical analyses were performed using R Studio 3.3.2 (2016-10-31) "Sincere Pumpkin Patch" (R Studio Team 2015). Regression models were optimized using SAS software (Statistical Analysis Systems version 9.4, Cary, NC 27513).

Results

Effect of water potential on total seed germination

All four plant species exhibited maximum total germination at water potentials of 0.0 to -0.3 MPa with no differences among soils and PEG (**Figure 2.1**). However, when the water potential decreased below -0.4 MPa, germination dropped for each plant species in a manner that was specific to each soil and PEG (**Figure 2.1**). Germination in PEG solutions differed from those obtained in soil when comparing with the corresponding water potentials (p-value = 0.0001; **Table S2.2** and **S2.3**). Total germination for the four plants species exhibited a similar trend in response to water potential when seeds were germinated in a sandy loam soil (**Figure 2.2**). In contrast, a more erratic and divergent response among species was observed when seeds were germinated in PEG. In the case of *T. aestivum*, these differences between soil and PEG were dramatic. For example, total germination in PEG was greater than 93% irrespective of water potential, while germination rapidly decreased as the water potential became more negative in the four soils (**Figure 2.1** and **2.2**).

Soil hydraulic conductivity and its effect on total germination

The lack of agreement in the germination patterns observed between soils and PEG suggests that PEG does not accurately represent the soil-water-seed dynamics that determine germination. This was particularly true when evaluating water potentials lower than -0.4 MPa. Because seeds require a balanced and constant water supply during different phases of the germination process, it is likely that determinants of water flow to the seed are as important as water potential for germination. In this regard, soil hydraulic conductivity is a measurement of the soil's ability to maintain the supply of water to the seed coat. Soil hydraulic conductivity can occur under both saturated (K_s) and unsaturated soil conditions (K_h), with the latter been the

most common in ecosystems with the exception of wetlands. Therefore, we hypothesized that K_h could account for the variability observed in response to water potential across species and soils.

The response in total seed germination was considerably more consistent across species and soil types when using K_h rather than water potential as a predictor (**Figure 2.1** and **2.3**). In general, total germination reached the maximum values within the highest K_h. It seems that there was a critical K_h threshold, and when hydraulic conductivity decreased (soil K_h decreases as soil water potential decreases) and reached a critical value, the germination decreased significantly (**Figure 2.3**).

Interestingly, the critical K_h germination threshold was characteristic for each soil and was similar for the four plant species. For instance, total germination exhibited a steep decline in the four species when $\log_{10}(K_h) \cong -3.31$ in the silty loam soil, while in the sandy loam germination decreased when $\log_{10}(K_h) \cong -6.53$. The loam soil presented the lowest threshold K_h (-7.11).

Effect of water potential and K_h on seed germination rate

In addition to total seed germination, it is important to understand how rapidly seeds are taking up water for the germination process. Therefore, we evaluated how water potential affected the rate to reach 50% germination (GR_{50}) expressed as the inverse of the time (d) to reach this percentile ($1/t_{50}$) for each soil and species combination (Pedroso et al. 2019). We hypothesized that GR_{50} was more sensitive than total seed germination to water potential because of the direct effect of this factor on uptake of water in direct contact with the seed coat. Unlike total germination (**Figure 2.1**), GR_{50} was indeed more sensitive to changes in water potential for all soils and species exhibiting a quasi-linear decline as water potential decreased (**Figure 2.4**). It is worth noting that the small seeds of *A. palmeri*, exhibited almost the same GR_{50} for all soils

and PEG, while as seed size increased vis-à-vis the other species, the differences in the GR_{50} among soils and PEG increased (**Figure 2.4**). For example, the GR_{50} of *T. aestivum* (i.e., largest seed) in PEG, was almost five-fold higher than in soils at water potential from 0.0 to -1.2 MPa.

When assessing the effect of K_h on GR_{50}, unique responses were observed depending on soil and plant species (**Figure 2.5**), but differences between soil types were not as marked as those observed when considering water potential only. The GR_{50} decreased proportionally to reductions in K_h, and those reductions were similar across species for each soil, with some exceptions for *S. obtusifolia* and *T. aestivum*, which exhibited steeper slopes than the other species in silty loam and loam, respectively (**Figure 2.5** and **Table 1.2**).

Discussion

The role of K_h and water potential on seed germination

Most studies on seed germination response to water potential, including hydrothermal time requirements, have been done using polymers and salts (e.g. PEG) as osmolites to generate germination media with specific water potentials that are, in their totality, dependent on osmotic potential. These osmotic solutions are easy to prepare and allow studying a wide range of water potentials (Hardegree and Emmerich 1994; Boddy et al. 2013; Bakhshandeh et al. 2017; Mobli et al. 2018; Abdellaoui et al. 2019). There are few reports of the use of hydrothermal time to describe seed germination using actual soils (Bullied et al. 2012). Therefore, it is difficult to determine how applicable to field conditions those results obtained using polymers as germination media are.

The differences observed in the present study between soils and PEG solutions might be related to a balance between physical processes driving the movement of water towards the seed and the ability of the seed to absorb the water that has already reached the seed coat. Comparing

osmotic and matrix potentials using PEG solutions as well as soil matrices with different soil particle sizes, Hadas (1977) determined that water potential is important for seed germination as long as soil moisture content is not limiting, but as soon as water content or water diffusivity decrease, soil physical properties influencing water supply to the seed will play a more important role.

While seeds are in direct contact with the water using PEG solutions, in soils the seed will present different angles and points of contact with the free water due to the arrangement of soil particles (**Figure 2.6**; Collis-George and Hector 1966; Kauffman and Ross 1970; Hadas and Russo 1974). The heterogeneous composition of the soil matrix is in contrast with the homogeneity of a polymer solution. Soil matrix includes both the solid and the pore phases, and the intrinsic variability of the combined phases affects the water dynamics such as water flux and holding phenomena through the soil volume. On the other hand, PEG solutions correspond to uniform media, where the water potential remains constant due the osmotic forces (osmotic potential, Ψ_o) exerted by the solutes (polymers). The relation between solutes concentration and total water potential (Ψ_T) follows a simple polynomial pattern (**Figure 2.6**; Michel 1983), which depends on the molarity, the molecular weight of PEG, and temperature ultimately affecting viscosity (Michel and Kauffmann 1973; Michel 1983; Money 1989). The PEG molecules in the solution form an arrangement of rigid helical segments, sporadically with disordered sections where the water forms hydrogen bonds with oxygen atoms in the PEG molecule creating the retention that is responsible for the osmotic effect (Michel and Kauffmann 1973). Conversely, soil Ψ_T is not only dependent on osmotic forces, but also dynamics in water - soil solid matrix interactions, and pressure of external gas and gravity, which are dependent on soil texture and structure (Hillel 1998). In addition, wettability plays an important role on soil-water relations,

specifically when soil dries out and reaches lower soil water content, therefore, the soil presents lower potential (Davis et al. 2009). This relationship between soil water potential and soil water content (**Figure S2.1**) is represented in the soil water holding retention curve, where soil wettability could be restricted in the region of the curve with the lowest water potential. This is particularly true in soils with soil water repellence (hydrophobicity), due to long C-chain organic substances coating soil particles (Roy and McGill 2000). For example, in the present study, the silty loam soil exhibited some level of hydrophobicity during the beginning of the wetting process to set the different water potentials, showing the formation of water drops with some degree of resistance to move into the soil and wet the particles.

Soil water potential by itself was insufficient to explain the variation observed in the germination of different species clearly indicating that other soil properties involved in the continuum soil-water-seed must be considered (Collis-George and Sand 1959; Wuest et al. 1999). Hydraulic conductivity is the transmitting property of soils as the conducting medium of water that moves due to a hydraulic gradient (Klute and Dirksen 1986; Hillel 1998). Soil hydraulic conductivity has different behaviour under saturated and unsaturated flow. Thus, under unsaturated conditions, K_h describes the water flow through the soil when soil pores are not completely filled with water and tend to decrease as the water potential becomes more negative (**Figure S2.3**). In a soil wetted to obtain a specific water potential according to the soil water retention curve, the degree of water resupply to the soil surface (with air boundary conditions) and further movement to the seed coat is affected by the magnitude of hydraulic conductivity (Hillel 1972). This is a common situation because most soils do not remain completely saturated (except for some wetland soils during a specific periods of the year), and their water dynamics

depend directly on rainfall (intensity, distribution, seasonality) or irrigation (Porporato et al. 2004; Vepraskas and Caldwell 2008).

Previous studies concluded that seed germination is not exclusively affected by soil water potential itself, and suggested the importance of considering other soil physical properties such as soil hydraulic conductivity (Collis-George and Sand 1959; Williams and Shaykewich 1971; Hadas and Russo 1974). Our data suggest that GR_{50} seems to be more sensitive to changes in the magnitude of soil hydraulic conductivity than soil water potential. Soil-seed contact, which is the area between soil particles and seed where the water moves towards and reaches the seed coat, should be large enough to allow enough water to get into the seed at a rate similar or higher than the potential imbibition rate of the seed (Rogers and Dubetz 1980). Seed initial water content, temperature, and the rate of seed hydration control is fundamental during the seed imbibition and the subsequent germination process (Collis-George and Melville 1975; Vertucci 1989). Seed hydration rate is affected by changes in water supply from the germination media; in the case of soils, changes in soil hydraulic conductivity will control the water supply (Collis–George and Sands 1959; Williams and Shaykewich 1971; Ward and Shaykewich 1972). In addition, K_h interacts with seed-water impedance, which is the resistance that water experiences to get inside the seed due to differences in soil matrix and seed coat. Impedance tends to increase with a decrease in K_h due to the decline in water content or the reduction in the soil water potential. Consequently, when soil K_h decreases, the impedance increases and the rate of seed imbibition is reduced, which leads to germination rate decline (Hadas and Russo 1974). Therefore, seed germination rate is not only dependent on soil water potential, but also on soil water flow determined by soil hydraulic conductivity.

Applications to plant physiology and ecology

The use of PEG solutions is a practical way to determine relative differences in water use between species, genotypes, or seed lots, but it is not an adequate system to determine accurate germination responses to water availability, which seems to be the aim of many studies. Our results do not invalidate previous research conducted with PEG solutions, but it highlights that the interpretation of that research must be done considering the limitations of its applicability to field conditions. A clear example of this was observed here for *T. aestivum*, which exhibited almost 100% germination at -1.2 MPa in PEG and only 20% in a sandy loam soil at the same Ψ_T (**Figure 2.2**). If one were to make planting and irrigation recommendations for germination based on the PEG data, it is likely that serious seedling emergence failure would be observed for this crop. Furthermore, our results illustrate how research seeking to understand seed and plant responses to soil water availability should consider the possibility that environmental factors other than Ψ_o or Ψ_T might play important roles in how the plant senses and adapt to soil water limitations. This is especially important when searching for genes and developing/breeding traits related to drought stress tolerance.

Soil hydraulic conductivity thresholds identified in the present study, represent a useful parameter to be included in seed germination and seedling emergence studies, because it provides a clear limit to germination potential for multiple species as a function of soil physical properties. Disturbance by natural or human causes of environmental and soil factors could lead to drastic changes in seed banks and consequently plant community dynamics and management (Forcella 1992; Buhler et al. 1997).

For example, changes in temperature and rainfall can directly influence the number of seeds germinating in the seed bank and seedling emergence timing, determining the probability of a given species to acquire resources and outcompete other species (Ooi et al. 2009; Walck et al. 2011; Mondoni et al. 2012; Ooi 2012).

Knowledge about seed germination thresholds based on environmental factors becomes fundamental in plant biology and ecology, even more with current climate change and its effect on the world's temperature and precipitation patterns (Walck et al. 2011; Bewley et al. 2013). Thresholds in seed germination could be used to predict changes in the spatial distribution of the species under drought or wet scenarios due to changes in rainfall patterns. Therefore, using soil survey data (e.g. K_h), in addition to long-term and real-time rainfall data, it might be possible to predict the periods and the areas in which a given species would be able to germinate. In other words, combining soil physical properties, climate data, temperature, and K_h-germination requirements could allow determining stability and changes in geospatial and ecological boundaries for the establishment of a given species. This information has important implications for conservation efforts of wild plant species, management of weedy and invasive plant species, and development of resilient crops.

Conclusions

The dramatic differences between germination responses to water potential in soil vs. PEG clearly indicate that caution is needed when trying to infer seed germination behaviours under field conditions using water potential thresholds determined in the laboratory with PEG or other osmotic solutions. Furthermore, water potential in itself did not provide a consistent description of germination when seeds were in soil. Conversely, K_h explained the variability in both total germination and GR_{50} among the four species evaluated.

Our results suggest that K_h is the driving force of maximum germination potential by regulating water flow towards the seed, while water potential might play a more important role for the ability of the seed to absorb water that is in direct contact with the seed coat. As shown here, different soil textures have different K_h thresholds below which water flow to the seed is impeded and germination collapses. The use of K thresholds can be an important tool to describe vegetation dynamics in response to climate change including geographic distribution, seasonality and desertification.

Funding

This research was funded by USDA-NIFA Grants 2017-6505-26807, 2018-70006-28933, 2019-68012-29818, and Hatch Project NC02653.

Acknowledgements

We would like to thank Adam Howard for his valuable help with soil physical analyses. We also thank Dr. Theresa Reinhardt Piskackova, Sandy Ramsey, Joseph Hunter III and Alyssa Zsido for technical assistance.

References

Abdellaoui R, Boughalleb F, Zayoud D, Neffati M, Bakhshandeh E (2019) Quantification of *Retama raetam* seed germination response to temperature and water potential using hydrothermal time concept. Environ Exp Bot 157:211–216

Allen PS, Meyer SE, Khan MA (2000) Hydrothermal time as a tool in comparative germination studies. In: Black M, Bradford KJ, Vizquez-Ramos J (eds) Seed Biology: Advances and Applications. CABI Publishing, Wallingford, UK

Bakhshandeh E, Jamali M, Afshoon E, Gholamhossieni M (2017) Using hydrothermal time concept to describe sesame (*Sesamum indicum* L.) seed germination response to temperature and water potential. Acta Physiol Plant 39:250

Bewley JD, Bradford KJ, Hilhorst HWM, Nonogaki H (2013) Environmental regulation of dormancy and germination. In: Bewley JD, Bradford K, Hilhorst H (eds) Seeds: Physiology of development, germination and dormancy. Springer, 3rd ed.

Bidgoly RO, Balouchi H, Soltani E, Moradi A (2018) Effect of temperature and water potential on *Carthamus tinctorius* L. seed germination: Quantification of the cardinal temperatures and modeling using hydrothermal time. Ind Crops Prod 113:121–127

Boddy LG, Bradford KJ, Fischer AJ (2013) Stratification requirements for seed dormancy alleviation in a wetland weed. PLoS One 8:e71457

Bradford KJ (2002) Applications of hydrothermal time to quantifying and modeling seed germination and dormancy. Weed Sci 50:248–260

Buhler DD, Hartzler RG, Forcella F (1997) Implications of weed seedbank dynamics to weed management. Weed Sci 45:329–336

Bullied WJ, Van Acker RC, Bullock PR (2012) Hydrothermal modeling of seedling emergence timing across topography and soil depth. Agron J 104:423–436

Collis-George N, Hector JB (1966) Germination of seeds as influenced by matric potential and by area of contact between seed and soil water. Aust J Soil Res 4:145–146

Collis-George N, Melville MD (1975) Water absorption by swelling seeds. I. Constant surface boundary condition. Soil Res 13:141–158

Collis-George NJ, Sands E (1959) The control of seed germination by moisture as a soil physical property. Aust J Agric Res 10:628–636

Dasberg S (1971) Soil water movement to germinating seeds. J Exp Bot 22:999-108

Dasberg S, Mendel K (1971) The effect of soil water and aeration on seed germination. J Exp Bot 22:992-998

Davis DD, Horton R, Heitman JL, Ren T (2009) Wettability and hysteresis effects on water sorption in relatively dry. Soil Sci Soc Am J 73:1947–1951

Forcella F (1992) Prediction of weed seedling densities from buried seed reserves. Weed Res 32:29–38

Gee GW, Or D (2002) Particle size analysis. In: Dane JH, Topp GC (eds) Methods of soil analysis. Part 4. Physical methods. SSSA, pp 255–293

Hadas A (1977) Water uptake and germination of leguminous seeds in soils of changing matric and osmotic water potential. J Exp Bot 28:977-985

Hadas A, Russo D (1974) Water uptake by seeds as affected by water stress, capillary conductivity, and seed-soil water contact. II. Analysis of experimental data. Agron J 66:648–652

Hardegree SP, Emmerich (1994) Seed germination response to polyethylene glycol solution depth. Seed Sci Technol 22:1–7

Hillel D (1972) Soil moisture and seed germination. In: Kozlowski TT (ed) Water deficits and plant growth, vol. 3. Academic Press, pp 65–89

Hillel D (1998) Environmental soil physics. Academic Press.

International Seed Testing Association (1985) International rules for seed testing. Seed Sci Technol 13:300–520

Kaufmann MR, Ross KJ (1970) Water potential, temperature, and kinetin effects on seed germination in soil and solute systems. Am J Bot 57:413–419

Klute A (1986) Water retention: Laboratory methods. In: Klute A (ed) Methods of soil analysis. Part 1. Physical and mineralogical methods. SSSA pp 635–662

Klute A, Dirksen C (1986) Hydraulic conductivity of saturated soils. In: Klute A (ed) Methods of soil analysis. Part 1. Physical and mineralogical methods. SSSA pp 694–700

Koller D, Hadas A (1982) Water relations in the germination of seeds. In: Lange OL, Nobel PS, Osmond CB, Ziegler H (eds) Physiological plant ecology II. Encyclopedia of plant physiology. New series vol. 12B, pp 401–431

Mehlich A (1984a) Photometric determination of humic matter in soils, a proposed method. Commun Soil Sci Plant Anal 15:1417–1422

Mehlich A (1984b) Mehlich-3 soil test extractant: A modification of Mehlich-2 extractant. Commun Soil Sci Plant Anal 15:1409–1416

Mehlich A, Bowling SS, Hatfield AL (1976) Buffer pH acidity in relation to nature of soil acidity and expression of lime requirement. Commun Soil Sci Plant Anal 7:253–263

Michel BE (1983) Evaluation of the water potentials of solutions of polyethylene glycol 8000 both in the absence and presence of other solutes. Plant Physiol 72:66–70

Michel BE, Kaufmann MR (1973) The osmotic potential of polyethylene glycol 6000. Plant Physiol 51:914–916

Mobli A, Ghanbari A, Rastgoo M (2018) Determination of cardinal temperatures of flax-leaf alyssum (*Alyssum linifolium*) in response to salinity, pH, and drought stress. Weed Sci 66:470–476

Mondoni A, Rossi G, Orsenigo S, Probert RJ (2012) Climate warming could shift the timing of seed germination in alpine plants. Ann Bot 110:155–164

Money NP (1989) Osmotic pressure of aqueous polyethylene glycols: relationship between molecular weight and vapor pressure deficit. Plant Physiol 91:766–769

Ooi MK (2012) Seed bank persistence and climate change. Seed Sci Res 22:S53–S60

Ooi MK, Auld TD, Denham AJ (2009) Climate change and bet-hedging: interactions between increased soil temperatures and seed bank persistence. Glob Change Biol 15:2375–2386

Peck AJ, Luxmoore RJ, Stolzy JL (1977) Effects of spatial variability of soil hydraulic properties in water budget modeling. Water Resour Res 13:348–354

Pedroso RM, van Kessel C, Neto DD, Linquist BA, Boddy LG, Al-Khatib K, Fischer AJ (2020) ALS inhibitor–resistant smallflower umbrella sedge (*Cyperus difformis*) seed germination requires fewer growing degree days and lower soil moisture. Weed Sci 68:51–62

Porporato A, Daly E, Rodriguez-Iturbe I (2004) Soil water balance and ecosystem response to climate change. Am Nat 164:625–632

R Studio Team (2015) RStudio: Integrated Development for R. RStudio, Inc., Boston, MA Available in http://www.rstudio.com/.

Rogers RB, Dubetz S (1980) Effect of soil-seed contact on seed imbibition. Can Agric Eng 22:89–92

Roy JL, McGill WB (2000) Flexible conformation in organic matter coatings: An hypothesis about soil water repellency. Can J Soil Sci 80:143–152

Topp GC, Ferré PA (2002) The soil solution phase. In: Dane JH, Topp GC (eds) Methods of soil analysis. Part 4. Physical methods. SSSA pp 417–1074

Tucker MR (1984) Volumetric measures for routine soil testing. Commun Soil Sci Plant Anal 15:833–840

van Genuchten MTh (1980) A closed-form equation for predicting the hydraulic conductivity of unsaturated soils. Soil Sci Soc Am J 44:892–898

Vepraskas MJ, Caldwell PV (2008) Interpreting morphological features in wetland soils with a hydrologic model. Catena 73:153–165

Vertucci CW (1989) The kinetics of seed imbibition: Controlling factors and relevance to seedling vigour. In: Stanwood PC, MacDonald MB (eds) Seed moisture. CSSA pp 93–115

van Genuchten, M. T. (1980), A closed-form equation for predicting the hydraulic conductivity of unsaturated soils, Soil Sci. Soc. Am. J., 44,892 – 898.

Vogel T, van Genuchten MTh, Cislerova M (2000) Effect of the shape of the soil hydraulic functions near saturation on variably-saturated flow predictions. Adv Water Resour 24:133–144

Ward J, Shaykewich CF (1972) Water absorption by wheat seeds as influenced by hydraulic properties of soil. Can J Soil Sci 52:99–105

Walck JL, Hidayati SN, Dixon KW, Thompson KEN, Poschlod P (2011) Climate change and plant regeneration from seed. Glob Change Biol 17:2145–216

Williams J, Shaykewich CF (1971) Influence of soil water matric potential and hydraulic conductivity on the germination of rape (*Brassica napus* L.). J Exp Bot 22:586–597

Wuest SB, Albrecht SL, Skirvin KW (1999) Vapor transport vs. seed–soil contact in wheat germination. Agron J 91:783–787

Figures

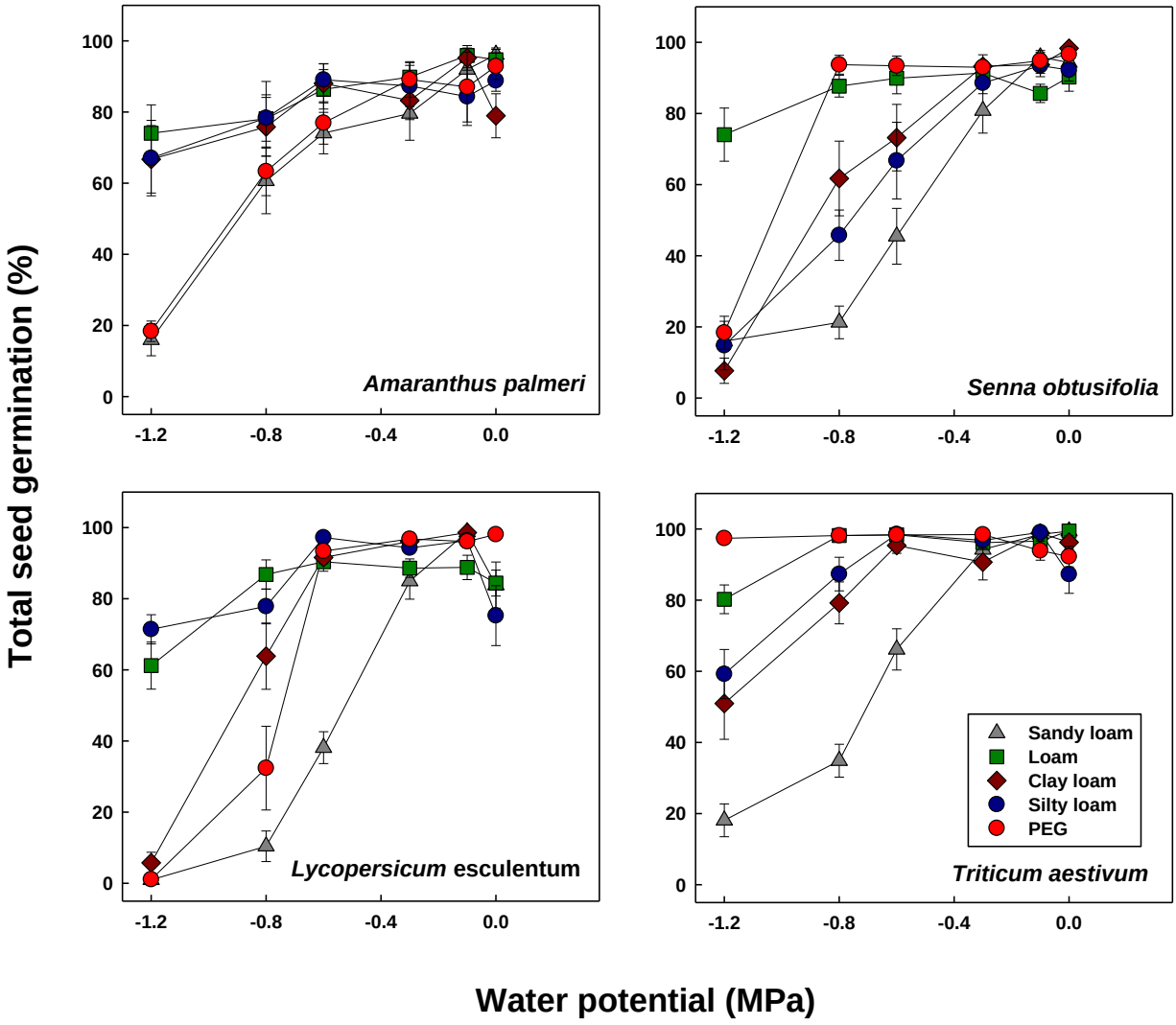

Figure 2.1 Total seed germination of four plant species after incubation under six water potentials in five substrates for 15 days. Error bars represents the standard error of the mean (n=10).

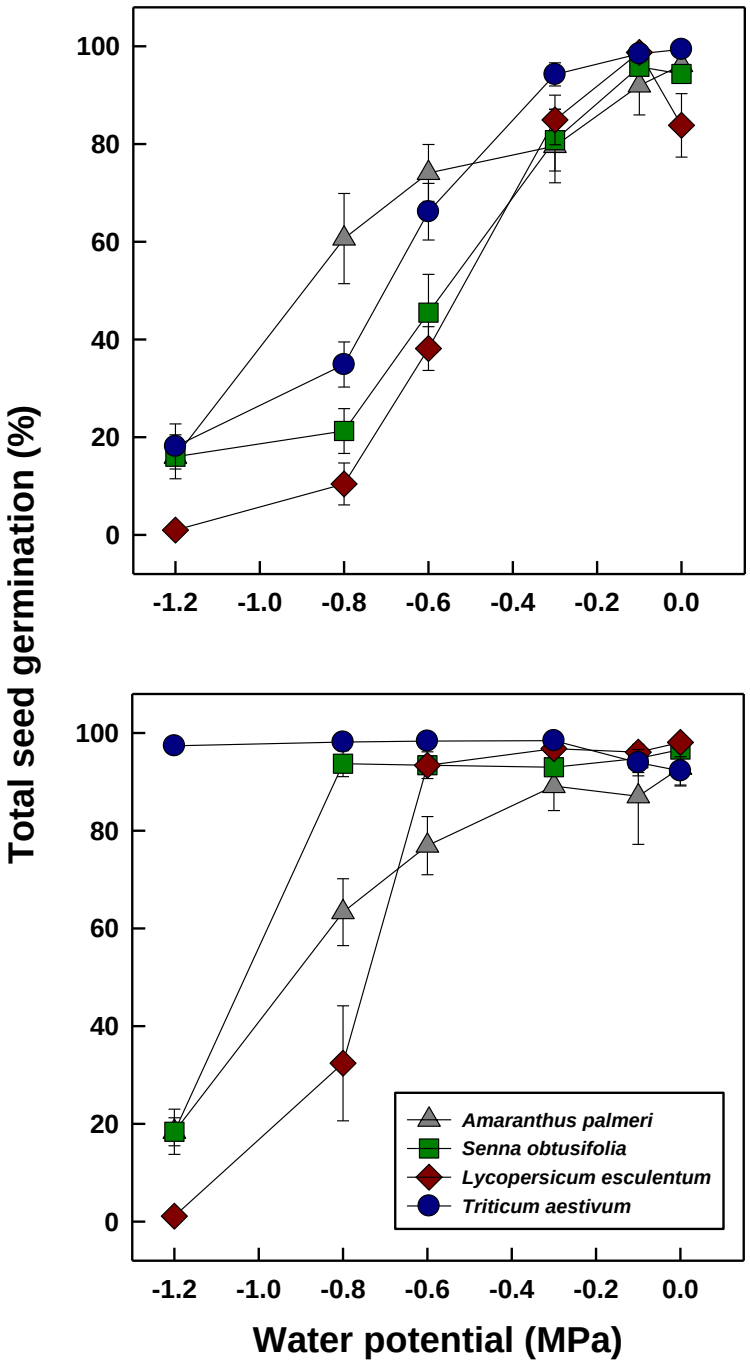

Figure 2.2 Total seed germination of four plant species in sandy loam soil (upper graph) and polyethylene glycol solutions (lower graph) with six water potentials. Error bars represents the standard error of the mean (n=10).

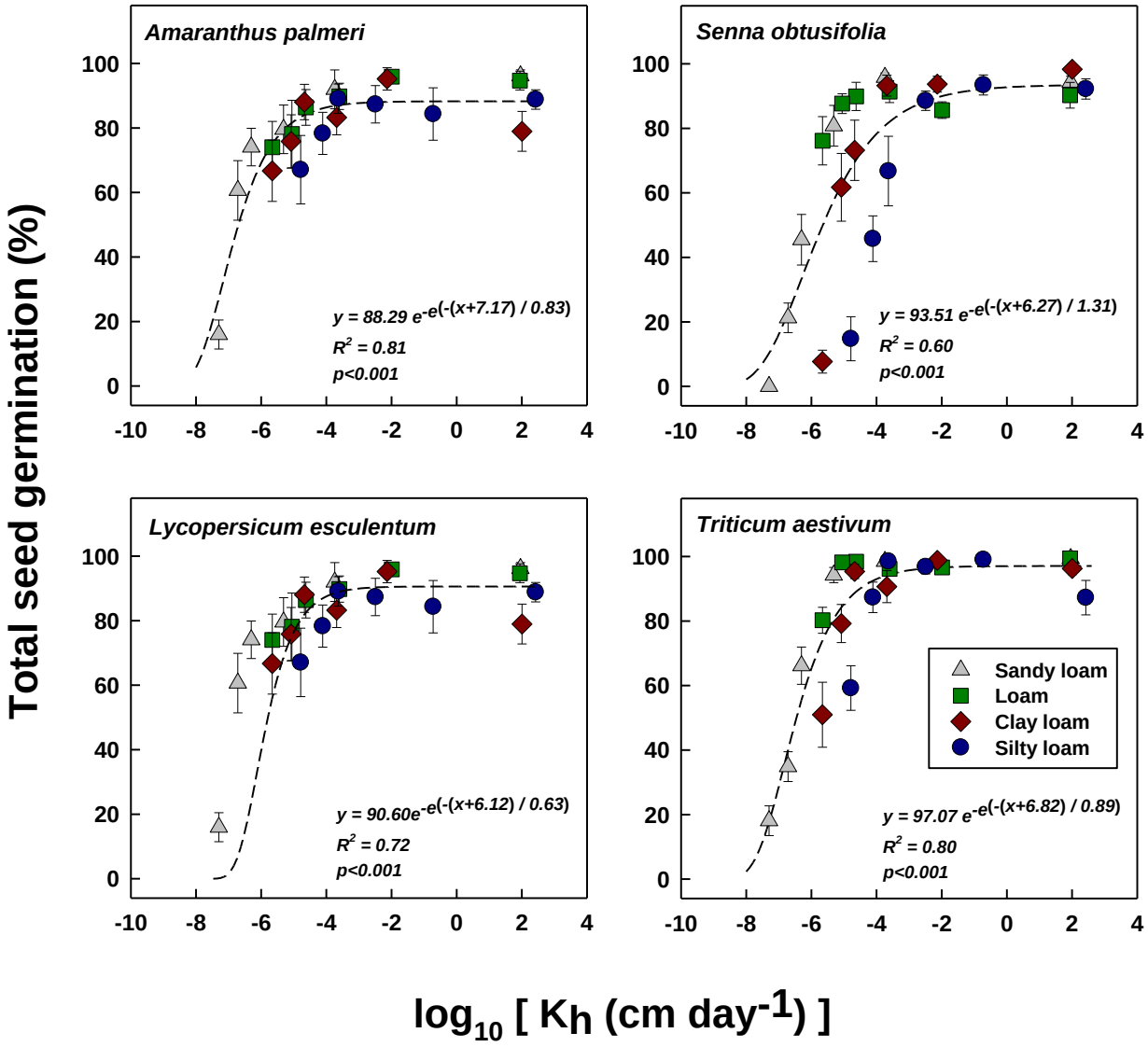

Figure 2.3 Seed germination of four plant species in response to unsaturated soil hydraulic conductivity (K_h) in four soils differing in texture. Error bars represents the standard error of the mean (n=10). Discontinuous line represents the best-fit model (Gompertz regression model).

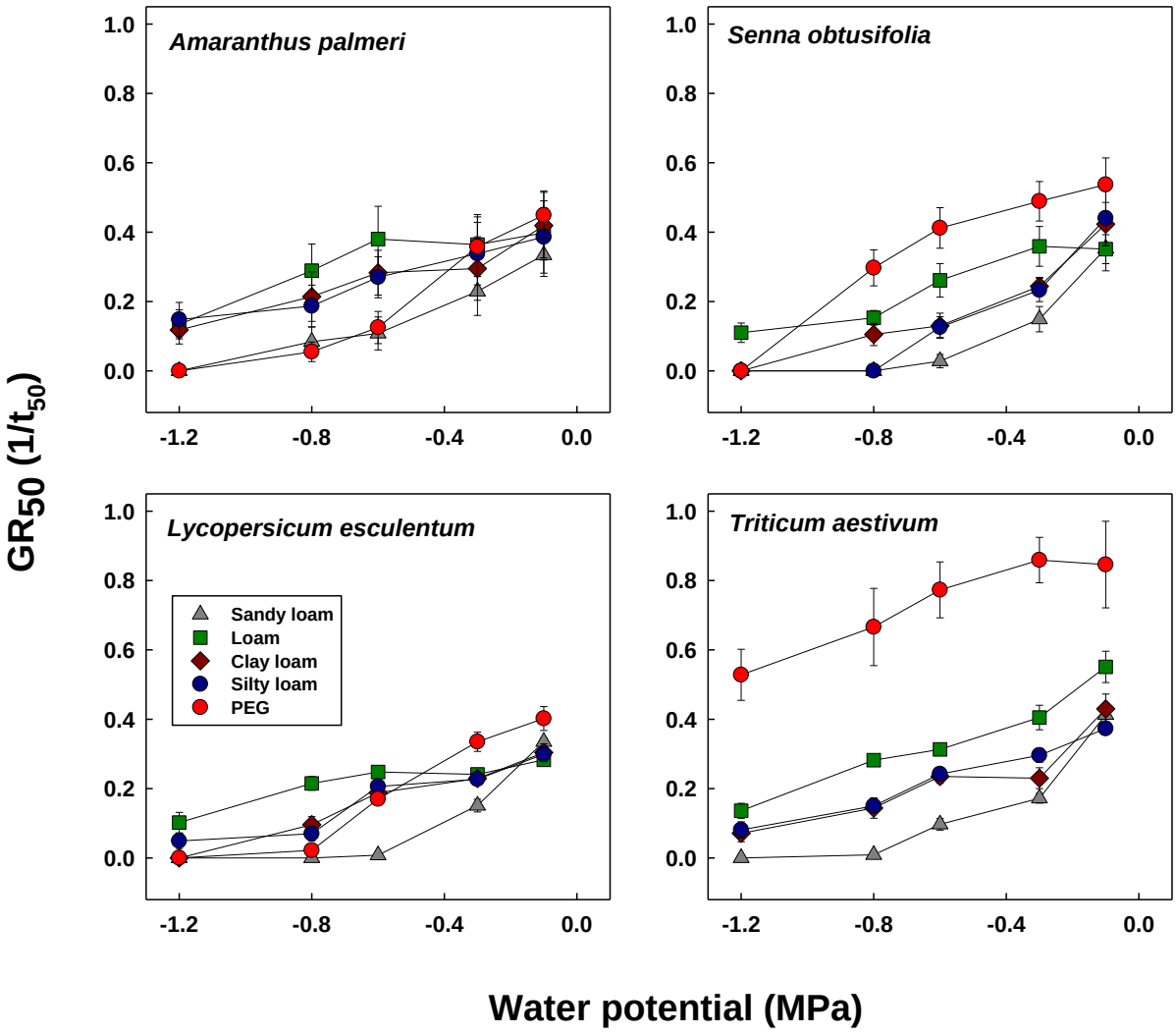

Figure 2.4 Seed germination rate measured in time to reach 50% germination (GR_{50}) of four plant species after incubation under six water potentials in five substrates for 15 days. Error bars represents the standard error of the mean (n=10).

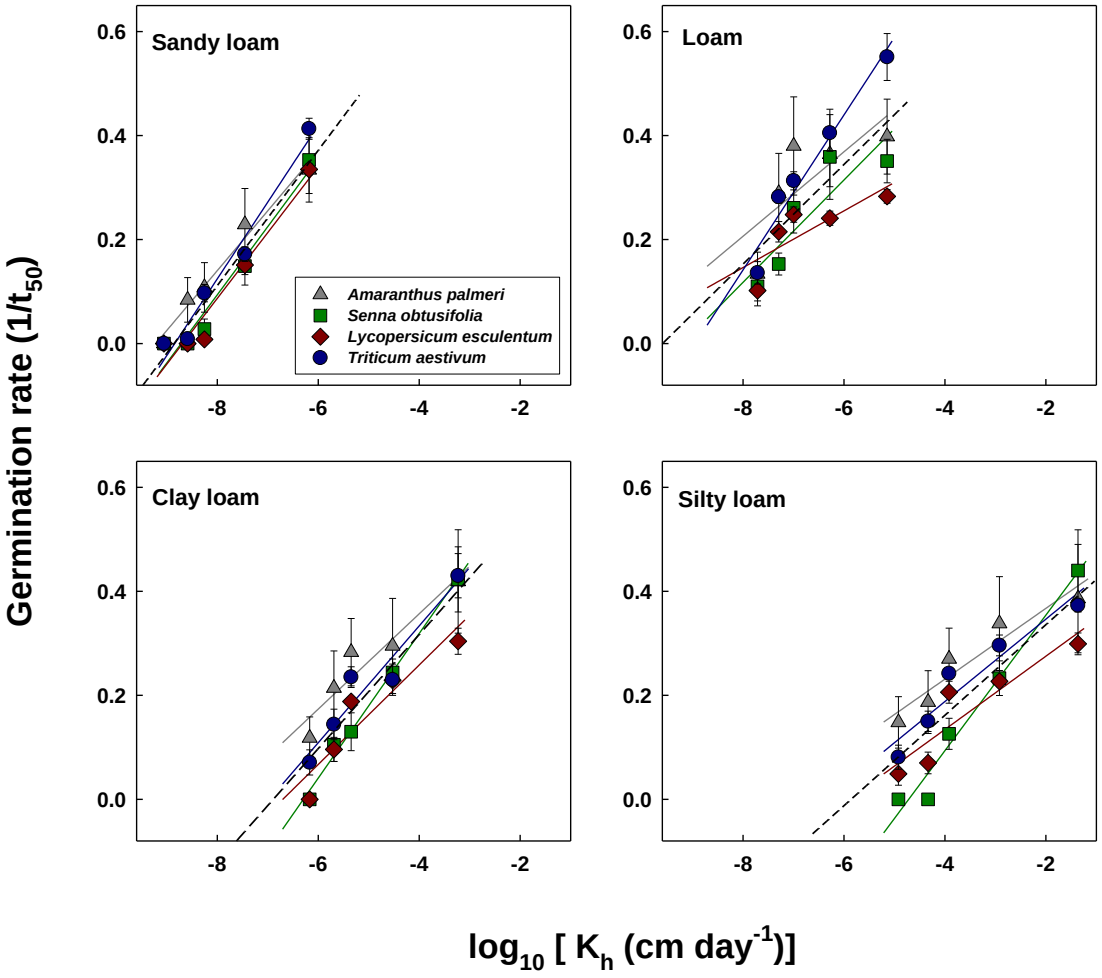

Figure 2.5 Unsaturated soil hydraulic conductivity (K_h) effect on seed germination rate measured in time to reach 50% germination (GR_{50}) of four plant species in four different soil textures. Error bars as standard error (n=10). Distinct color lines represent the best-fit model for its corresponding plant species (**Table 1.2**). Discontinued black line represents the best fit model for overall data points (**Table 1.2**).

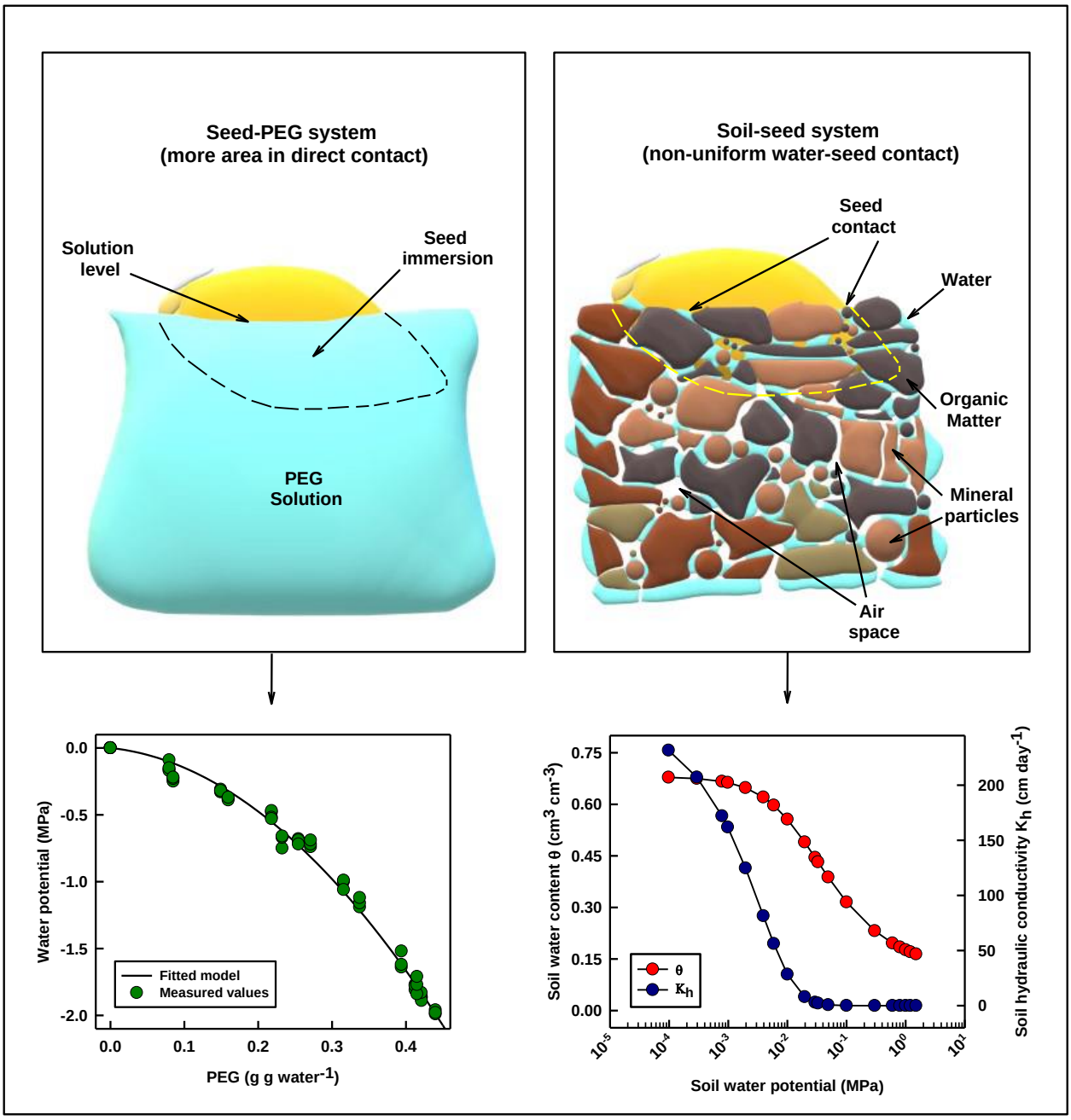

Figure 2.6 PEG solutions have uniform contact with the seed surface (top left), so they can easily and consistently expose the seed to different water potentials created by changing PEG concentration (bottom left). Conversely, in soil, the points of contact between water and the seed coat are determined by the physical properties of the soil matrix (top right), and complex non-linear interactions between unsaturated soil hydraulic conductivity (Kh), water potential, and soil water content.

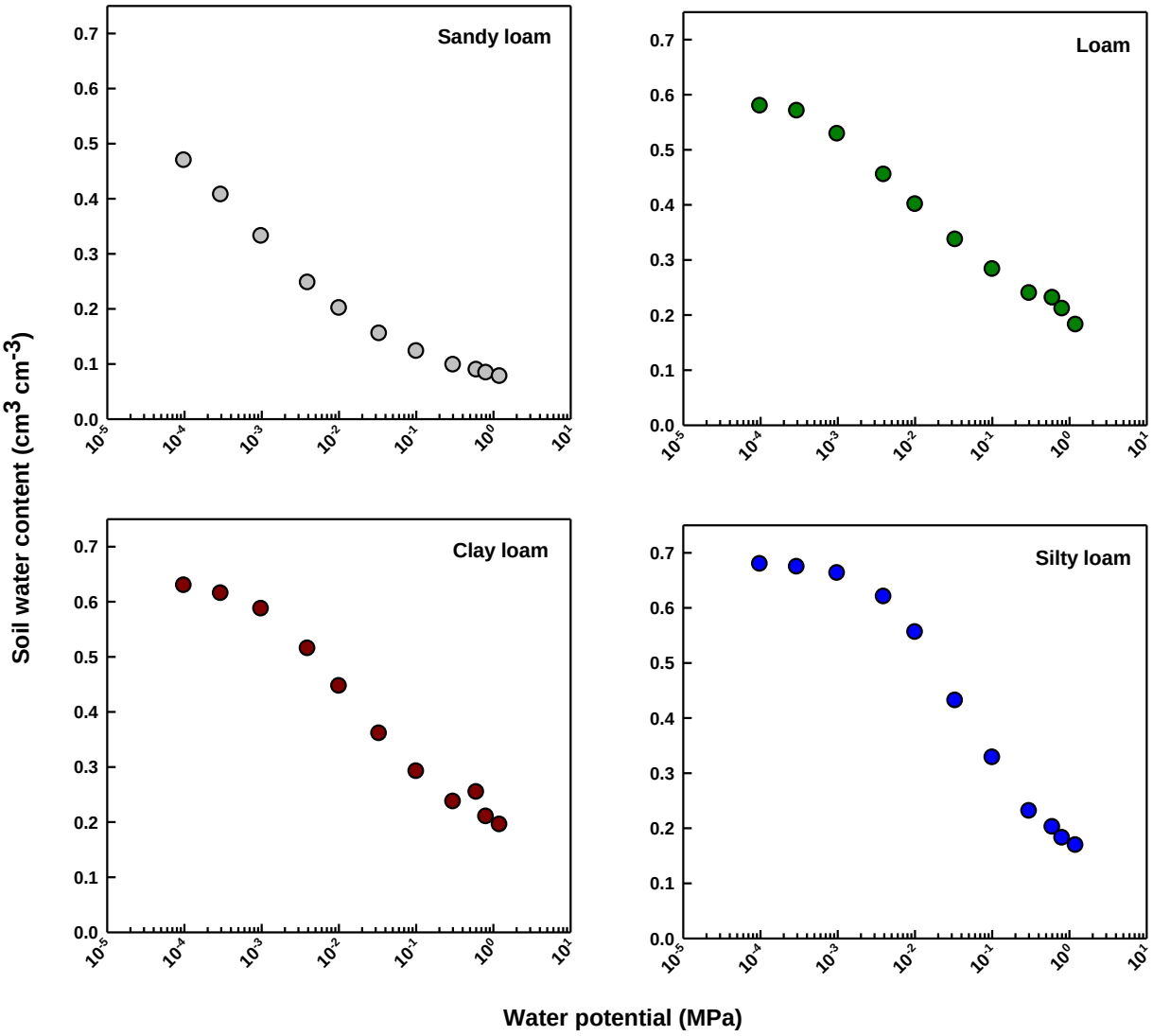

Figure S2.1 Soil water holding curves obtained for the four soils used in present study. Model parameters (van Genuchten 1980) fitted through least squares regression method from soil water potential values measured following Klute (1986) procedures.

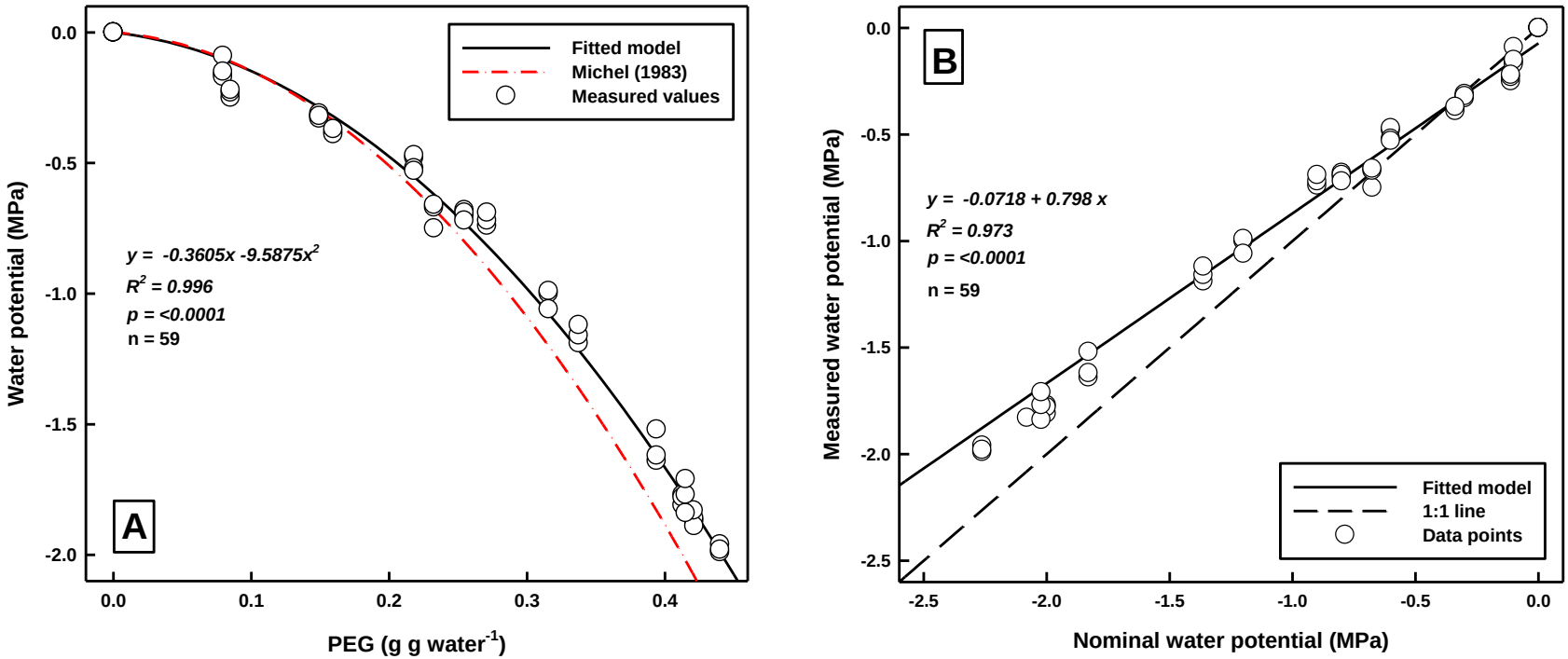

Figure S2.2 A) PEG calibration curve for present study compared with the model (in red line) proposed by Michel (1983). B) Regression model for nominal value following Michel (1983) and measured water potential values. PEG solutions were prepared and kept at 25°C.

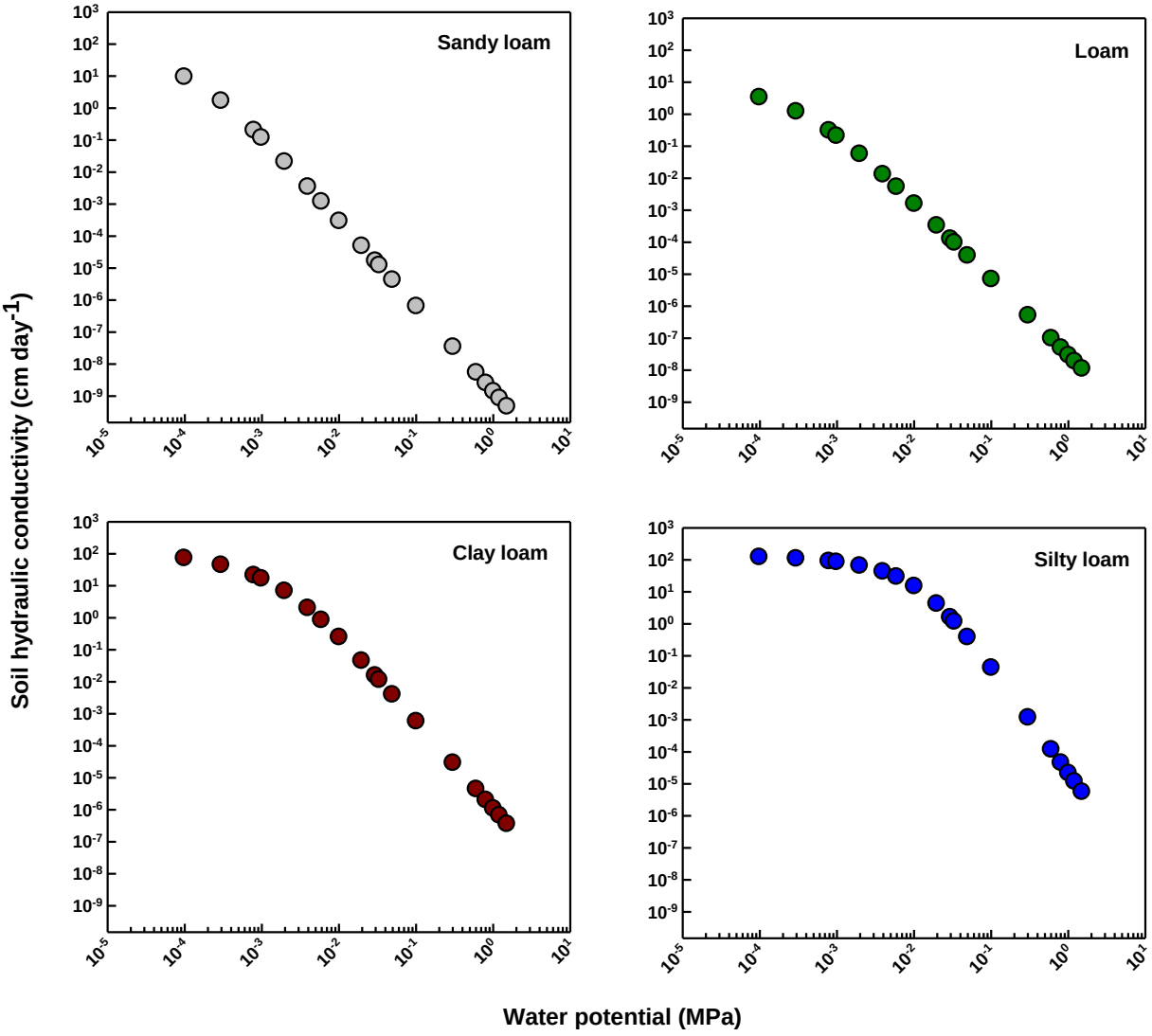

Figure S2.3 Estimated soil hydraulic conductivity corresponding to each soil water potential on four soils used on present study. Values calculated following Vogel et al. (2000) using measured K_s (Klute and Dirksen 1986) and van Genuchten's model parameters (van Genuchten 1980).

Tables

Table 2.1 Soil series and physical properties determined for soils used in the present study.

Soil series	Soil taxonomic family	Sand	Silt	Clay	Water content	Bulk density*	Total porosity†	Hydraulic conductivity‡	Textural class
		g g^{-1}				g cm^{-3}	cm cm^{-3}	cm day^{-1}	
Cecil	Fine, kaolinitic, thermic Typic Kanhapludults	0.74	0.10	0.16	0.01	1.33	0.50	157.93	Sandy loam
Chewacla	Fine-loamy, mixed, active, thermic Fluvaquentic Dystrudepts	0.45	0.40	0.15	0.02	1.06	0.60	45.39	Loam
Georgeville	Fine, kaolinitic, thermic Typic Kanhapludults	0.32	0.41	0.28	0.03	0.98	0.63	189.07	Clay loam
Herndon	Fine, kaolinitic, thermic Typic Kanhapludults	0.29	0.58	0.14	0.03	0.86	0.68	142.17	Silty loam

* Bulk density after packing soil into the petri dish.

† Calculated from bulk density value and a particle density value = 2.65 g cm^{-3}.

‡ Measured in saturated conditions.

Table 2.2 Regression model and fit parameters to predict seed germination rate measured as the time to reach 50% germination (GR50) of four plant species growing on four contrasting soil textures, using unsaturated soil hydraulic conductivity (Kh).

Soil	Plant species	Model*	β_0	β_1	R^2	p-value	AIC‡
Sandy loam	*A. palmeri*	Linear	1.060 ± 0.173†	0.115 ± 0.022*	0.37	<0.0001	-40.32
	S. obtusifolia	Linear	1.142 ± 0.121	0.131 ± 0.015	0.61	<0.0001	-76.09
	L. esculentum	Linear	1.099 ± 0.050	0.126 ± 0.006	0.89	<0.0001	-165.05
	T. aestivum	Linear	1.305 ± 0.056	0.147 ± 0.007	0.90	<0.0001	-153.14
	All	Linear	1.151 ± 0.057	0.130 ± 0.007	0.62	<0.0001	-341.03
Loam	*A. palmeri*	Linear	0.856 ± 0.257	0.081 ± 0.038	0.09	0.03859	4.38
	S. obtusifolia	Linear	0.905 ± 0.145	0.098 ± 0.021	0.31	<0.0001	-53.28
	L. esculentum	Linear	0.582 ± 0.074	0.055 ± 0.011	0.34	<0.0001	-120.07
	T. aestivum	Linear	1.334 ± 0.099	0.149 ± 0.015	0.68	<0.0001	-90.90
	All	Linear	0.919 ± 0.085	0.096 ± 0.013	0.23	<0.0001	-162.37
Clay loam	*A. palmeri*	Linear	0.723 ± 0.165	0.092 ± 0.032	0.14	<0.0100	1.42
	S. obtusifolia	Linear	0.875 ± 0.080	0.139 ± 0.016	0.62	<0.0001	-70.64
	L. esculentum	Linear	0.641 ± 0.044	0.096 ± 0.009	0.72	<0.0001	-130.79
	T. aestivum	Linear	0.783 ± 0.069	0.112 ± 0.013	0.59	<0.0001	-86.26
	All	Linear	0.755 ± 0.052	0.110 ± 0.010	0.37	<0.0001	-192.30
Silty loam	*A. palmeri*	Linear	0.503 ± 0.098	0.068 ± 0.026	0.12	0.01317	0.28
	S. obtusifolia	Linear	0.615 ± 0.053	0.130 ± 0.014	0.63	<0.0001	-60.78
	L. esculentum	Linear	0.416 ± 0.030	0.070 ± 0.008	0.61	<0.0001	-118.50
	T. aestivum	Linear	0.505 ± 0.026	0.079 ± 0.007	0.72	<0.0001	-130.70
	All	Linear	0.510 ± 0.031	0.087 ± 0.008	0.35	<0.0001	-190.27

* Linear model: $y = \beta_0 + \beta_1 * x$

† Model parameter ± standard error

‡ Akaike information criterion (AIC)

Table S2.1 Soil chemical properties determined for the four studied soils.

Soil Series	HM	BS	W/V	pH	Ac	CEC	Na	P	K	Ca	Mg	S	Mn	Cu	Zn
	%		g cm^{-3}		$cmol_c$ kg^{-1}			ppm							
Cecil	0.97	77.00	1.17	5.50	1.80	7.90	0.10	110	145	851	176	51	61	5	11
Chewacla	0.60	89.00	0.95	5.90	2.00	18.00	0.10	75	189	2229	538	51	418	2	14
Georgeville	1.02	84.00	0.94	5.50	2.60	16.00	0.10	68	277	1684	518	41	157	1	9
Herndon	0.56	95.00	0.92	6.70	1.00	20.80	0.10	72	166	3276	359	50	994	4	12

Table S2.2 Analysis of variance for seed germination**.**

Factor	Degrees of freedom	F value	Pr (>F)
Plant species (PS)	3	249.56	<0.0001
Substrate (S)*	4	93.81	<0.0001
Water potential (WP)	5	311.94	<0.0001
PS x S	12	12.72	<0.0001
PS x WP	15	10.35	<0.0001
S x WP	20	21.00	<0.0001
PS x S x WP	60	6.26	<0.0001
Residuals	1080		

*Substrate includes four soils and PEG.

Table S2.3 Normalized total seed germination of four plant species under six water potentials and five substrates.

Water potential	Substrate	*A. palmeri*				*S. obtusifolia*				*L. esculemtum*				*T. aestivum*			
Mpa		Germination (%)*															
0.00	Sandy loam	96.16	±	1.86[§]	a[ǂ]	94.34	±	1.81	a	83.84	±	6.50	a	99.39	±	0.61	a
	Loam	94.70	±	2.91	a	90.25	±	3.98	a	91.22	±	3.29	a	99.45	±	0.41	a
	Clay loam	78.96	±	6.18	b	98.31	±	1.13	a	53.66	±	11.3	b	96.27	±	1.84	ab
	Silty loam	88.83	±	3.00	ab	92.23	±	3.15	a	75.26	±	8.42	ab	87.27	±	5.34	b
	PEG	92.87	±	3.71	ab	96.62	±	1.69	a	98.09	±	0.94	a	92.25	±	2.89	ab
-0.10	Sandy loam	91.97	±	6.02	a	95.82	±	1.35	a	98.76	±	0.62	a	98.50	±	0.65	a
	Loam	95.92	±	1.55	a	85.65	±	2.57	a	96.12	±	3.32	a	96.61	±	1.14	a
	Clay loam	95.23	±	3.47	a	93.71	±	2.46	a	98.58	±	0.78	a	98.83	±	0.68	a
	Silty loam	84.34	±	8.12	a	93.46	±	3.11	a	96.34	±	1.90	a	99.06	±	0.52	a
	PEG	87.04	±	9.83	a	94.81	±	2.89	a	96.08	±	1.54	a	93.93	±	2.69	a
-0.30	Sandy loam	79.60	±	7.53	a	80.80	±	6.31	a	84.94	±	5.07	b	94.26	±	2.37	a
	Loam	89.81	±	4.08	a	91.39	±	3.39	a	95.63	±	1.93	ab	96.16	±	1.38	a
	Clay loam	83.25	±	5.37	a	93.25	±	3.26	a	96.10	±	1.74	a	90.68	±	4.98	a
	Silty loam	87.34	±	5.79	a	88.56	±	3.00	a	94.28	±	1.54	ab	96.82	±	2.22	a
	PEG	89.15	±	5.02	a	92.99	±	1.76	a	96.81	±	1.81	a	98.45	±	0.86	a
-0.60	Sandy loam	74.09	±	5.83	a	45.48	±	7.84	b	38.14	±	4.48	b	66.16	±	5.79	b
	Loam	86.39	±	5.54	a	89.91	±	4.36	a	96.59	±	2.09	a	98.39	±	0.97	a
	Clay loam	88.05	±	5.47	a	73.20	±	9.34	ab	91.60	±	1.73	a	95.37	±	2.21	a
	Silty loam	89.08	±	4.54	a	66.75	±	10.79	ab	97.23	±	1.60	a	98.55	±	1.28	a
	PEG	76.94	±	5.95	a	93.41	±	2.73	a	93.39	±	1.87	a	98.34	±	0.54	a
-0.80	Sandy loam	60.65	±	9.23	a	21.26	±	4.59	c	10.42	±	4.30	b	34.87	±	4.62	c
	Loam	78.12	±	10.48	a	87.67	±	3.06	a	93.22	±	3.79	a	98.16	±	0.99	a
	Clay loam	75.83	±	8.27	a	61.73	±	10.50	b	63.86	±	9.32	a	79.23	±	5.90	b
	Silty loam	78.33	±	6.53	a	45.78	±	7.09	bc	77.85	±	4.92	a	87.34	±	4.72	ab
	PEG	63.34	±	6.85	a	93.71	±	2.65	a	32.39	±	11.77	b	98.16	±	1.29	a
-1.20	Sandy loam	15.99	±	4.49	b	0.00	±	0.00	c	0.98	±	0.65	b	18.11	±	4.61	d
	Loam	74.05	±	7.98	a	76.16	±	7.48	a	66.99	±	6.83	a	80.24	±	4.03	ab
	Clay loam	66.72	±	9.48	a	7.68	±	3.55	c	5.77	±	2.96	b	50.96	±	10.08	c
	Silty loam	67.06	±	10.61	a	14.77	±	6.82	bc	71.40	±	4.11	a	59.23	±	6.91	bc
	PEG	18.38	±	2.88	b	32.78	±	4.63	b	1.11	±	0.76	b	97.39	±	1.08	a

* Germination was normalized based on relative to the maximum germination value at the end of the experiment for each experiment

§ mean ± standard error

ǂ different within water potential and within plant species letters denote significant differences according to HSD Tukey's ($\alpha = 0.05$)

CHAPTER 3: Modeling lateral transport of solutes in a sloped anisotropic soil with HYDRUS 2D: A case study in turfgrass

Formatted for *Agricultural Water Management*

Manuel E. Camacho[1,2], Carlos A. Faúndez Urbina[3], Aziz Amoozegar[2], Travis W. Gannon[2], Joshua L. Heitman[2], and Ramon G. Leon[2,4,5].

1 Centro de Investigaciones Agronómicas (CIA), Universidad de Costa Rica, 11503-2060 San Pedro, Costa Rica.

2 Department of Crop and Soil Sciences, North Carolina State University, Campus Box 7620, Raleigh, NC 27695, USA.

3 Instituto de Ciencias Agroalimentarias, Animales y Ambientales, Universidad de O'Higgins, Ruta 90 Kilómetro 3, San Fernando, Chile.

4 Center for Environmental Farming Systems, North Carolina State University, Campus Box 7609, Raleigh, NC 27695, USA.

5 Genetic Engineering and Society Center, North Carolina State University, Campus Box 7565, Raleigh, NC 27695, USA.

Abstract

Despite best management practices and efforts to avoid off-target pesticide movement in turfgrass landscapes, subsurface lateral flow under some weather and topographic conditions may cause vegetation injury and potentially pollute nearby water bodies. Lateral subsurface transport of solutes along boundaries between horizons, enhanced by irregular topography and textural anisotropy, however, is not fully understood. A field study was conducted to investigate the potential subsurface lateral transport of solutes in sloped soils with anisotropic horizons. To track solute transport, bromide (Br^-), a conservative tracer, was used as a proxy for modeling purposes. HYDRUS 2D/3D was used to model the potential subsurface lateral movement and predict soil water content and solute transport dynamics using soil and climatic parameters determined under experimental conditions. In addition, a global sensitivity analysis was conducted to identify the most influential HYDRUS 2D/3D input parameters for selecting the proper values for the parameters required for calibration and improvement of model performance. Field data confirmed the subsurface lateral movement of solutes following the soil slope direction, which advanced along the boundary between horizons over time. Simulations performed with HYDRUS 2D allowed visualization of this lateral movement, represented as changes in Br^- concentration within the soil profile and its lateral distribution in time and space. Our analysis indicated that the modeled subsurface lateral flow and transport was most influenced by parameters associated with soil water retention (van Genuchten parameters) and soil water evaporation occurring between rainfall/irrigation events. We recommend conducting further studies to assess the role of lateral water flow along horizon boundaries into pesticide dynamics and fate.

Introduction

Pesticide use has become a fundamental tool for pest management in agricultural and non-agricultural systems (Racke 2000; Oerke 2006). However, there is concern about the risk of pesticide off-target movement in terrestrial and aquatic systems, generating negative health, economic, and environmental consequences (Haith and Rossi 2003; Lee et al. 2011). Off-target movement can occur in diverse forms like drift, leaching through soils, and runoff over the land surface. Runoff is most frequently reported as one of the main pathways where pesticides move off-target after application (Haith and Rossi 2003). For instance, in turfgrass, herbicides with differing water solubility and soil adsorption affinity exhibited runoff movement along the soil surface, and this runoff was increased under sloped conditions and heavy rainfall events (Leon et al. 2016).

In some cases, off-target herbicide damage has been observed on downslope turfgrass landscapes, but interestingly, runoff transport was not responsible for displacement of the herbicides from the original application area. It has been hypothesized that downslope subsurface lateral movement of water and solutes is responsible for pesticide displacement from upslope areas and accumulation downslope. This could be even more evident if the slope of the landscape decreases downslope.

Subsurface lateral flow has been previously reported in forestry and perennial systems (Kim et al. 2005; Kahl et al. 2007), and it is more likely to occur in soils with distinct horizons which create anisotropy on its hydraulic properties (McCord et al. 1991; Filipović et al. 2018). However, the mechanisms of subsurface lateral flow and its role on pesticide movement have not been described in turfgrass landscapes where its consequences are easily detected with changes in aesthetics and turfgrass integrity.

An approach to elucidate this subsurface lateral flow is the use of mathematical models that describe water and solute interactions with soil particles in the vadose zone. HYDRUS 2D/3D (Šimůnek et al. 2016) is a widely used modelling software for studies of hydrologic processes such as soil water flow (McCoy and McCoy 2009; Bufon et al. 2012) and solute transport (Boivin et al. 2006; Filipović et al. 2019; Varvaris et al. 2021), with weather and soil properties measured onsite as inputs. In addition, sensitivity analysis allows identification of critical parameters which could have the highest impact on the magnitude of the model output (Saltelli et al. 2008), and further assist calibration and parameter optimization (Urbina et al. 2019; 2021) to increase the accuracy and precision of the model.

Filipović et al. (2018) performed HYDRUS 2D simulations to assess the subsurface lateral flow in hillslope soils, aiming to understand its fundamental role in solute transport in agricultural settings. They theorized that lateral flow is more likely to occur under sloped conditions and within soil horizons with hydraulic anisotropy, where the lateral flow will be favored over the vertical flow. Despite their efforts conducting simulations of conservative tracer to assess the solute movement, they did not conduct any actual measurements of solute transport under similar field conditions to confirm the accuracy of the simulations.

The objectives of our study were to: 1) investigate the potential subsurface lateral movement of solutes in a sloped soil with anisotropic hydraulic properties using field measurements, 2) assess HYDRUS 2D/3D modelling performance for predicting subsurface solute lateral movement under these conditions in turfgrass.

Materials and Methods

Field experiment

A field experiment was conducted during the months of January and May, 2021, in a field plot at the Lake Wheeler Turf Field Laboratory in Raleigh, NC. The soil for this facility has been mapped as Cecil sandy loam (fine, kaolinitic, thermic Typic Kanhapludult). The Ap horizon (sand texture) is on average 0.18 m thick, overlaying the Bt horizon (clay texture) that is more than 0.35 m thick (**Table 3.1**). The plot and surrounding area has 12% slope covered with hybrid bermudagrass "Tifway 419", which was dormant at the time of the experiment. A 3 m × 3 m area was established as the experimental plot and was divided into four equal sections (**Figure 3.1**). The sides and middle borders were marked with nylon strings for use as guides for installing sensors for water content monitoring and collecting samples for solute transport assessment.

Soil physical properties

Using 7.62 cm diameter and 7.62 cm long aluminum cylinders (347.5 cm^3) in a Uhland soil sampler (Blake and Hartge 1986), undisturbed soil cores were collected from six different locations surrounding the experimental plot. Two undisturbed soil cores were collected from each soil horizon at each sampling locations. These soil cores were trimmed and transported to the laboratory for analysis. The soil cores were divided into two groups, one used to quantify saturated hydraulic conductivity and the other for soil water retention analysis after slowly saturating them from the bottom over a 24-h period. In addition, three disturbed samples collected from each soil horizon were used for particle size distribution analysis by the hydrometer method (Gee and Orr 2002).

Saturated hydraulic conductivity (K_s) of the undisturbed soil cores (from first group) was measured by maintaining a constant head of water following the method described by Klute and Dirksen. (1986). In situ K_s was also measured in the field with a compact constant head permeameter (CCHP) following Amoozegar (1989).

Intact soil cores (from the second group) were used to generate water retention curve following the procedure described by Dane and Hopmans (2002). The analysis was divided into high-water potential (0 to -0.033 MPa) and low-water potential (-0.1 to -1.5 MPa). For the high-water potential, saturated soil cores were placed inside Buchner funnels connected to an air pressure device. Seven pressure levels between 0.00035 to 0.333 MPa (approximately equivalent to 3.5, 5, 10, 30, 50, 100, and 333 cm of water head) were applied incrementally. The volume of outflow was measured after reaching equilibrium for each pressure. After measuring the outflow volume at 0.333 MPa pressure, all soil cores were weighed and dried in an oven at 105°C for 24 h to determine their bulk density as well as final water content following methods described by Grossman and Reinsch (2002) and Topp and Ferré (2002), respectively.

For low soil water potential, the analysis was carried out using disturbed soil samples, porous plates, and pressure vessels (Soil Moisture Equipment Corp., Santa Barbara, CA) following the methods described by Klute (1986). The gravimetric soil water content for these samples was estimated following Topp and Ferré (2002) procedures. Soil water content obtained at each pressure was used to develop a water retention curve for each soil horizon.

Weather data and soil water content monitoring

Two rain gauges (one analogic Stratus® RG-202, and another digital Onset® RG3-M Borne, MA) were installed close to the experimental plot (**Figure 3.1A**) to accurately monitor rainfall. Soil water content was monitored every 15 min at an average depth of 7 cm (Ap horizon) and 21 cm (Bt horizon) using EC-5 soil moisture sensors (Onset Computer Corporation ® Bourne, MA). Eight monitoring points were established in a concentric arrangement. At each monitoring location an auger hole (7.5 cm diameter, 0 to 40 cm depth) was dug for horizontally installing the two soil moisture sensors into each soil horizon (**Figure 3.1B**). These sensors were connected to HOBO U30 data loggers (Onset Computer Corporation®) supported by individual solar panels. The auger holes were filled back with the original soil and then allowed to settle for one month prior to the initiation of the experiment. Daily minimum and maximum temperature, precipitation, and evapotranspiration values were obtained from the Lake Wheeler Rd Field Lab ECONET – Tower (35.72816, -78.67981) weather station, which can be accessed online through North Carolina Climate Office. A summary of the weather data is presented in **Figure 3.2**.

Solutes application and post irrigation treatment

Wednesday, 17 February of 2021, was selected as the solute application date following three consecutive rainfall events (> 1.5 cm) (**Figure 3.2**), aiming to ensure enough water had entered the soil to potentially reach near soil saturation conditions at the boundary between Ap and Bt horizons. One liter of potassium bromide (KBr) solution, at a concentration of 180.9 g L^{-1}, was uniformly applied by hand to a 0.38-m^2 circular area at the center of the plot as shown in **Figure 3.1**. The solute was applied using a CO_2 pressurized backpack sprayer with a flat-fan spray nozzles (XR; TeeJet®, XR11002VS, Spraying Systems Co., Wheaton, IL). This equipment was calibrated to deliver 280.2 L ha^{-1} of solution at 214 kPa of pressure. Three hours after the

solute application, the entire 9 m^2 plot was irrigated with 1.26 cm of water in three events (113. 6 L of water split into three applications; 49.2, 45.4, and 18.9 L) that were spaced one hour apart to leach the KBr into the soil. This amount of irrigation was chosen to supplement rainfall events to ensure soil saturation while avoiding surface runoff following KBr application. Irrigation was carried out using a hose coupled with a wand with an electronic water meter GPI® 01N31GM (Great Plains Industries Inc, Wichita, KS).

Soil sampling for Br^- extraction and measurement

Soil samples were collected at 5, and 46 days after the solutes application (DASA). Those dates were selected based on the amounts and the distribution of the rainfall received after the application (**Figure 3.2**), aiming to allow enough time to detect Br^- movement through the soil without losing the solutes to leaching below the sampling depth. Samples were systematically collected in a 60 x 60 cm grid to characterize lateral movement of the solutes. Soil samples were taken at four depth intervals (0-15, 15-30, 30-40, and 40-50 cm) for the first sampling date, and five depth intervals (0-5, 5-10, 10-15, 15-30, 30-45 cm) for the second sampling with a bucket auger (20 and 7.62 cm of length and diameter, respectively). The samples were placed in labelled Ziploc® bags (0.940 L volume) and sealed. The auger was washed twice with a brush and a solution of ammonia-water, rinsed with water, and dried with paper towel after each sampling to avoid solute cross contamination among samples and depths.

Bromide quantification in soil samples was performed following Abdalla and Lear (1975). A total of 120 g of soil per sample was mixed with 240 mL of deionized water in a mason jar (473 mL capacity) and vigorously shaken for 30 min using a reciprocal shaker (Eberbach Corporation®, Michigan, USA) at 240 oscillations min^{-1}.

The samples were allowed to settle overnight, and the supernatant was filtered using Whatman No. 42 filter paper. Bromide concentration was measured using an Oakton® pH 450 (pH/mV meter) and a Cole-Parmer® combination Ion-Selective Electrode (ISE).

HYDRUS-2D/3D modelling

Theoretical analysis and fundamental equations

HYDRUS-2D/3D software package (Šimůnek et al. 2016, 2018) was used to simulate the potential lateral flow and solute movement for soils with textural anisotropic conditions. A complete description of the processes and theoretical background underlying HYDRUS-2D/3D functions can be found in Šejna et al. (2018) and Šimůnek et al. (2012a), respectively. Here, we will describe the most relevant governing equations used in the present study to quantify water and solute lateral movement. For solving the two-dimensional variably saturated flow solution numerically by Galerkin finite element method, the Richards equation is presented by (Boivin et al. 2006):

$$\frac{\partial \theta}{\partial t} = \frac{\partial}{\partial x_i}\left[K\left(K_{ij}^{A}\frac{\partial h}{\partial x_j} + K_{iz}^{A}\right)\right] - S \qquad \text{(i, j = 1, 2) [1]}$$

where θ is the volumetric soil water content ($L^3\ L^{-3}$), t is time (T), h is the pressure head (L), x_i (i = 1, 2) corresponds to the position coordinates in the space (L) [i.e., $x_1 = x$ and $x_2 = z$], K is the unsaturated hydraulic conductivity ($L\ T^{-1}$), K_{ij}^{A} are the components of the dimensionless anisotropy tensor K^A, and S corresponds to the sink term for root water uptake (T^{-1}). For the present study, we assumed isotropic conditions within each soil horizon.

Unsaturated soil hydraulic conductivity (K_h) and the water retention (θ_h) functions were fitted for each soil horizon using the van Genuchten (1980) model:

$$\theta_h = \begin{cases} \theta_r + \frac{\theta_s - \theta_r}{[1+|\alpha h^n|]^m} & , h < 0 \\ \theta_s & , h \geq 0 \end{cases} \qquad [2]$$

$$K_h = K_s S_e^l \left[1 - (1 - S_e^{1/m})^m\right]^2 \quad [3]$$

$$S_e = \frac{\theta - \theta_r}{\theta_s - \theta_r} \quad [4]$$

where θ_s and θ_r are the saturated and residual water contents ($L^3\ L^{-3}$), respectively; K_s is saturated hydraulic conductivity ($L\ T^{-1}$); α (L^{-1}) and n (unitless) are empirical fitting parameters; m is related to n by $m = 1 - 1/n$ (unitless); and S_e is the soil effective saturation. The parameters θ_s, θ_r, α, and n were fitted from the soil water retention data generated as described above through nonlinear least-squares optimization with the RETC program (Leij et al. 1991). The same parameters were used together with K_s to estimate K_h following Eq. [3]. For the Bt horizon, a -2 cm air entry potential was assigned as recommended for fine-textured soils (Vogel et al. 2001).

Solute transport for Br^- was predicted employing the advection-dispersion equation (ADE; Boivin et al. 2006):

$$\frac{\partial(\theta c + \rho_b s)}{\partial t} = \frac{\partial}{\partial x_i}\left(D_{ij}\frac{\partial c}{\partial x_j}\right) - \frac{\partial q_i c}{\partial x_i} \quad (i, j = 1,2) \quad [5]$$

where c ($M\ L^{-3}$) corresponds to solute concentration in the soil solution, s ($M\ M^{-1}$) represents concentration in solid phase; ρ_b represents the soil bulk density ($M\ L^{-3}$), D_{ij} are the components of the dispersion tensor ($L^2\ T^{-1}$), q_i is the water flux density ($L\ T^{-1}$), and x_i, for i = 1 and 2, represent the horizontal (x) and vertical (z) dimensions as described above. The D tensor for the solute is computed into the software using three terms: transversal and longitudinal dispersivity (L) and molecular diffusion into the water phase ($L^2\ T^{-1}$). For Br^-, we used 10.0 and 1.0 cm as longitudinal and transversal dispersivity, respectively (Boivin et al. 2006), and a molecular diffusion coefficient in free water of 1.6 $cm^2\ d^{-1}$.

We did not consider K_d for bromide, an anion, because it is considered to be a non-reactive (i.e., non-adsorbing), conservative tracer with low risk of attenuation by soil materials (Shinde et al. 2001; Abit et al. 2008).

Soil domain, initial and boundary conditions, and numerical implementation

The soil domain was represented into the model by a finite element grid, composed of 8147 non-uniform triangular elements and 4202 nodes, and mesh-refined around the surface to produce a relatively fine grid pattern for the Ap horizon and a relatively coarse grid pattern for the Bt horizon, including a slope angle of 6.89° (**Figure 3.3**).

Two initial conditions (IC) for pressure head corresponding to the two genetic soil horizons were set in the model. The Ap horizon had a linear distribution with depth and slope in the x-direction, and top and bottom pressure head ICs of -780 and -400 cm, respectively. The Bt horizon had a linear distribution with depth and slope in the x-direction, with top and bottom pressure head ICs of -400 and -333 cm, respectively. These values were chosen based on the initial soil water content values obtained from the soil moisture sensors and their corresponding pressure head according to the soil water retention curves for the two horizons. The initial concentration of the solutes in the soil was set as 0 mg cm^{-3}, and the solute pulse concentration after application was calculated as follows:

$$C_{Br}\ (mg\ cm^{-3}) = \frac{120\ 000\ mg}{([(I + R\ )_a - (\vartheta * ET_o)_a] * 3848 cm^2)} \qquad [6]$$

where ϑ is a reduction factor (0 to 1) for potential evapotranspiration (ET_o) measured by the weather station, irrigation (I) and rainfall (R) are the water inputs obtained for the application day (a). A time-variable flux boundary condition was assigned to a 70-cm radius (3848 cm^2) in the center of the experimental plot (**Figure 3.3**). This variable flux was estimated for each day i as follows:

$$variable\ flux_i = (I + R)_i - (\vartheta \times ET_o)_{\ i} \quad [7]$$

Atmospheric boundary condition was assigned to the rest of the soil surface (65 cm downslope and 65 cm upslope), where HYDRUS 2D performs the corresponding calculations automatically using rainfall and evaporation.

A free drainage boundary condition was applied to the bottom of the soil domain, and no-flow boundary conditions were established along the vertical upslope edge of the domain. For the vertical downslope edge, a gradient boundary condition was assigned using a factor of 0.12, which was calculated using the following equation:

$$grad = \sin(\alpha) \quad [8]$$

where *grad* is the gradient factor, and α is the soil slope angle ($6.89° = 0.12\pi$ for this case).

For solute transport, a third-type boundary condition (Cauchy) code = 1 was assigned to the top and the bottom of the domain, except for the application area, where the third-type code = 2 was selected (Radcliffe and Šimůnek 2010).

All simulations were performed considering a period of 80 days, aiming to cover: 1) all the rainfall events since the soil moisture sensors were installed at day 1 (t_0), 2) the solute application 30 days after (t_0), 3) the two sampling dates after solute application, and 4) to have sufficient daily data for simulations.

Sensitivity analysis

Aiming to determine the contribution of individual model inputs to the total uncertainty for the target variable to predict, we conducted a global sensitivity analysis using a modification of the Morris method (Campolongo et al. 2007). This methodology computes elementary effects (EE_i) for the factor X_i generating trajectories (r) in the input factor space following the equations:

$$EE_i = \frac{[Y(X_1 + \Delta, X_2, + \Delta \ldots, X_{i-1}, X_i + \Delta, \ldots\ldots, X_k) - Y(X_1, X_2, \ldots., X_k)]}{\Delta} \quad [9]$$

$$\Delta = \left(\frac{1}{p-1}\right) \times \omega \quad [10]$$

where Δ is the change in the factor X_i calculated by Eq. [7], k is the total number of factors, p is the number of levels which factor X_i is allowed to move in the hyperparameter space, and ω is a scalar called "grid-jump" which is typically estimated as $p/2$ (Morris 1991; Pujol 2017). Cuntz et al. (2015) suggested that the number of trajectories (r) should be at least equal to the number of factors. Both the mean (μ) and the standard deviation (σ) were computed over all r values calculated for factor X_i according with the following equations:

$$\mu_i = \frac{1}{r}\sum_{j=1}^{r}\left(EE_i^j\right) \quad [11]$$

$$\sigma_i = \sqrt{\frac{1}{(r-1)}\sum_{j=1}^{r}(EE_i^j - \mu_i)^2} \quad [12]$$

Then, the overall effect of X_i in the output variation was computed by μ_i with σ_i indicating interactions between model inputs or factors. Saltelli et al. (2008) indicated that Eq. [9] has a limitation when positive and negative EE_i can cancel each other out, which indicates that the factor is not essential (Type II error). To overcome this issue, Campolongo et al. (2007) proposed the use the absolute values of EE in Eq. [11] as presented by:

$$\mu^*_i = \frac{1}{r}\sum_{j=1}^{r}\left|EE_i^j\right| \quad [13]$$

where μ^*_i is the overall effect. The statistics calculated by the Morris elementary effect method (μ_i, μ^*_i, and σ_i) create a ranking of the importance of factors regardless of the magnitude (Song et al. 2015), which can be considered a qualitative method.

The Morris elementary effect parameters used in the sensitivity analysis were r = 100, k = 11, Δ = 0.6; with p = 6 and ω = 3 (Eq. [9] and [10]). The Morris sampler generator and sensitivity index computation were performed with the R package "Sensitivity" (Pujol 2017).

The input factors in the model were analyzed visually from graphical representation of μ^* and σ. The importance of the parameters assessed in the sensitivity analysis and their further classification were evaluated following the guidelines described by Lagmmoglia et al. (2017). They defined three ranges of importance: 1) highly influential parameters if $\mu^* \geq 0.5\ \mu_{max}$; 2) influential if $0.1\ \mu_{max} < \mu^* < 0.5\ \mu_{max}$; and 3) non-influential if $\mu^* \leq 0.1\ \mu_{max}$.

The range of the values for the soil hydraulic parameters included in the analysis (θ_s, θ_r, α, n, K_s) was obtained from field measurements. The range evaluated for Br^- longitudinal dispersivity (D_l) was based on values recommended from a previous study (Boivin et al. 2006), and Br^- transversal dispersivity (D_t) was set as 10% of the value selected for D_l. The parameter ϑ was set arbitrarily between 0.25 and 0.75. This factor represents the uncertainty in the potential evaporation, which should be lower than the one estimated by the weather station due to dormant plant cover during the experimental period. The HYDRUS parameter ranges are presented in **Table 3.2**.

Model parameters calibration

After identifying the most influential parameters with the sensitivity analysis, a model calibration and parameter optimization process was conducted. The model-independent Parameter Estimation δ Uncertainty Analysis (PEST) package was employed for the calibration of the initial HYDRUS 2D/3D parameters following the guidelines of Doherty (2015). PEST performs a Gauss–Marquardt–Levenberg type algorithm to estimate potential values of parameters that minimize the weighted sum of squared deviations between the calculated and observed values. This Gauss–Marquardt–Levenberg type algorithm minimizes the objective function (ϕ) as follows:

$$\phi = \sum_{i}^{i=N_t} (w_i\, r_i)^2 \qquad [14]$$

where N_t is the total number of observations, w_i is the weight associated with the i^{th} observation and r_i is the i^{th} residual (difference between model output and measurement).

To obtain optimized parameters, PEST estimates the relationship among the measured data and model parameters throughout a Taylor series expansion, and further conforming a Jacobian matrix, which includes partial derivatives of the measured values with respect to the parameters. The iteration of the estimation of these partial derivatives with gradual changes in the model parameters from their original value generates a new set of parameters on each run. This set of parameters is revised as an updated vector at every run, based on the gradient of objective function as described by Marquardt (1963). The PEST algorithm ends the iteration when changes in the parameters are minimal.

Two datasets were used for the calibration. One corresponded to daily average volumetric water content obtained from the six soil moisture sensors (**Figure 3.3**) for 80 days, and the other

corresponded to Br^- soil concentration collected 5 and 46 days after application. Twelve observation groups were established, and weights (w_i) were generated with the condition that all groups contributed in the same way to the objective function. This approach has been successfully used for model calibration for solute and water movement in the soil using HYDRUS 2D/3D (Urbina et al. 2019; 2021).

PEST model calibration was performed using R Studio R version 4.0.4 (2021-02-15) "Lost Library Book" (R Studio Team 2015).

Statistical analysis

The model performance was evaluated with the Root Mean Square Error (*RMSE*) and the Willmott agreement index (*d*), and the Nash – Sutcliffe efficiency (*NSE*) index, which were calculated using the following equations:

$$RMSE = \sqrt{\frac{\sum_{i=1}^{n}(m_i - s_i)^2}{n}} \qquad [15]$$

$$d = 1 - \frac{\sum_{i=1}^{n}(m_i - s_i)^2}{\sum_{i=1}^{n}(|s_i - m_a| + |m_i - m_a|)^2} \qquad [16]$$

$$NSE = 1 - \frac{\sum_{i=1}^{n}(m_i - s_i)^2}{\sum_{i=1}^{n}(m_i - m_a)^2} \qquad [17]$$

where m_i corresponds to the observed value for *i* data point, s_i corresponds to the simulated value for *i* data point, and m_a corresponds to the average of observed values.

The bromide distribution within the plot graphs (contour maps) were produced using contour plot option of SigmaPlot 11.0 software (Systat Software Inc. GmbH, Germany), which performs a bicubic interpolation between the data points.

Results

Lateral movement of solutes: field measurements

Br^- distribution within the experimental plot 5 and 46 DASA is presented in **Figure 3.4**. In both evaluation dates, it was observed a pattern where Br concentrations decreased with soil depth. Interestingly, it was observed at 5 DASA lateral movement of the Br^- following the slope main direction, defined as a plume that moved up to 90 cm away from the application area (white circle). This movement was more evident within the first 15 cm depth, but a similar pattern was also observed within 15 – 30 cm depth.

When assessing the Br^- distribution at 45 DASA, a similar pattern of lateral movement was observed at 0 - 15 cm depth, but concentrations were considerably lower than those observed at 5 DASA (solute dissipation), and the plume direction changed slightly towards 315°, but kept the main slope direction. Br^- concentration and distribution increased within 15 - 30 and 30 - 40 cm, indicating vertical movement within the soil. However, results observed at 5 and 46 DASA confirmed prevalence of solute lateral movement with the soil slope direction.

Sensitivity analysis and model inputs

The Morris sensitivity analysis for HYDRUS 2D/3D inputs identified three main inputs from the soil water retention curve: α, n, and θ_s (van Genuchten equation's parameters) as highly influential according to the guidelines recommended by Lammoglia et al. (2017) for changes in soil water content predicted for the three observation points (**Figure 3.5** and **3.6**). In the case of the Ap horizon, α_1 and n_1 were classified as the most influential inputs in all observation points. For the Bt horizon, parameters n_2 and θ_{s2} were highly influential inputs for changes in predicted soil water content (**Figure 3.5**). Additionally, the parameters α_1 and α_2 were considered as influential for soil water content dynamics modelling.

For soil solute transport modelling (Br^- concentration), the sensitivity analysis determined α as a highly influential parameter in horizon Ap regardless of the distance from the application point (**Figure 3.6**). For sampling point 2 (located 60 cm away from the solute application area) in the Ap horizon, the reduction factor (ϑ) was also identified as highly influential factor for predicting Br^- concentration.

Model calibration and parameter optimization

The calibration improved the performance of the model describing the behavior of both water and Br^- movement, but this was more evident for the latter. For soil water content, the *RMSE* reduction was negligible when the model was calibrated (i.e., 0.030 to 0.027), and the Willmot agreement (*d*) and Nash-Sutcliffe efficiency (*NSE*) indices increased slightly by 0.010 and 0.036, respectively. Conversely, when the model to predict Br^- concentration was calibrated, *d* substantially increased by 0.33, and the *NSE* changed from -0.030 to 0.228. Therefore, the results indicated the need to calibrate the model, especially to describe Br^- movement.

Six parameters were not calibrated with the algorithm PEST (kept as a fixed value) because they were not considered influential according to the results from Morris sensitivity analysis, as observed in **Figure 3.5** and **3.6**.

In general, the values of calibrated parameters *n* and θ_s were lower than the calculated ones (initial values), but α was slightly higher than the initial value in both soil horizons. However, when comparing between initial and calibrated, they agreed, and the calibrated values varied within the uncertainty boundaries (i.e., 95% confidence limits) of the observed values.

Modeling soil water content dynamics in anisotropic soils

Soil water content was monitored in three observation points distributed along the central transect in the experimental plot for a period of 80 days. We compared these measured values with those predicted by the HYDRUS 2D/3D forward model (calculated) and with model calibration (calibrated) (**Figure S3.1**). However, little improvement was observed in the statistical parameters to assess model performance for soil water content modelling after the calibration (**Table 3.3**). Then, we focused on the comparisons among the measured values and their corresponding calibrated values, which are presented in **Figure 3.7**.

There was agreement between the calibrated and corresponding measured values of volumetric soil water content (**Figure 3.7**). Time series of the soil water content monitored in the Ap horizon presented higher variability than those in the Bt horizon. This was likely the result of the textural anisotropy observed for this soil (**Table 3.1**) and the proximity of the Ap horizon to the soil surface, which was subjected to more intense changes in atmospheric boundary conditions (e.g., rainfall) (**Figure 3.3**). The *RMSE* calculated for the time series of soil water content in the Ap horizon varied from 0.048 to 0.022 cm^3 cm^{-3}, whereas those measurements corresponding to the same dates in the Bt horizon ranged from 0.028 to 0.009 cm^3 cm^{-3}.

Modeling solute transport in anisotropic soils with sloped conditions

Samples were collected to monitoring solute movement along the soil profile and determine the existence of subsurface lateral movement under soils with textural anisotropic horizons, as observed in the Cecil series at Lake Wheeler, NC (**Table 3.1**).

The calibration significantly improved the model performance for predicting Br^- concentration in soil (**Table 3.2**; **Figure 3.8**). The *RMSE* of individual sampling points during the first sampling time (5 DASA) presented values ranging from 0.028 to 0.482 mg cm^{-3},

meanwhile the *RMSE* varied from 0.010 to 0.752 mg cm^{-3} for 46 DASA. The calibrated Br^- series was closer to the measured one, while the calculated series (obtained with forward model) overestimated Br^- concentration. This overestimation was more evident for 46 DASA, where the calibrated Br^- concentration values in observation point 3 were almost 4 times higher than the corresponding measured points throughout the soil profile (**Figure 3.8**).

The presence of Br^- in all sampling points confirmed movement from the application area to further positions downslope. This was more evident during the first sampling date (5 DASA), where the concentration at 10 cm depth for the sampling point 2 (46 DASA) was higher than that observed at the same depth in sampling point 1. Sampling at 46 DASA presented concentration values in the sampling point 2 lower than those observed at 5 DASA.

As observed for soil water content, calibration of HYDRUS 2D/3D inputs improved the prediction of Br^- concentration within the soil profile and its further distribution with time and space.

Lateral movement of solutes in anisotropic soils with sloped conditions

One of the main advantages of modelling with HYDRUS 2D/3D is its versatility to simulate the solute movement within the soil domain matrix under specific boundary conditions with a time progression. Using this approach, it was predicted that Br^- moved as a plume preferentially along the slope (**Figure 3.9**). For instance, in the forward model Br^- detection in the Ap horizon was shown at positions slightly outside the application area during 1 DASA, while Br^- traces were detected > 50 cm downslope from the application area at 5 DASA. Although in the first two evaluations, Br^- movement tended to move either parallel to the soil surface or towards deeper layers within the soil matrix, at 46 DASA, the direction of the

movement was horizontal or even opposite to slope inclination generating an increase in Br^- concentration at shallower depths reaching values from 0.4 and 0.5 mg cm^{-3}.

The forward model tended to overestimate solute concentration especially in the farthest point down slope of the experimental plot (**Figure 3.9**), where values calculated were almost twice as high as those of the calibrated model. Conversely, the calibrated model presented values that better fit field Br^- concentrations at 5 and 46 DASA while keeping a similar path for plume movement. One day after the solute application, the highest concentration was mostly located in the first 10 cm right below the application area. Over time, the plume moved both vertically and laterally, but with more intensity in the lateral movement. The calibrated model also predicted a resurfacing of Br^- traces when the plume was 110 cm away from the application center (**Figure 3.9**).

Discussion

Sensitivity analysis and model calibration to enhance performance

Sensitivity analysis has been widely recommended as a valuable tool for hydrology modelling during its development, calibration, and further model verification (McCuen 1973). However, the complexity of the model and its inputs will determine the selection of a given sensitivity analysis methodology (Iooss and Lemaître 2015; Devak and Dhanya 2017). In that regard, the modified screening method of Morris (Campolongo et al. 2007; Pujol 2009) is a sensitivity analysis with several advantages for models such as HYDRUS 2D/3D. These include lower computational cost for the iterations required in the identification of influential parameters and reliability while comparing with other types of inherently more complex sensitivity analysis (Brunetti et al. 2018; Urbina et al. 2020). This approach has been successfully used in other

modelling studies using HYDRUS (Zhou et al. 2012; Turco et al. 2017; Brunetti et al. 2018) or SWAP (Urbina et al. 2020).

Our results from the Morris sensitivity analysis provided valuable information while assessing the main parameters for model calibration using the PEST analysis. This resulted in a significant improvement of HYDRUS 2D performance for predicting soil water content dynamics and solute transport (**Table 3.2**), similarly to that mentioned by McCuen (1973) and Rogers et al. (1985) for hydrological modelling improvement after the implementation of sensitivity analysis. PEST analysis is versatile to use with any possible model because requires the initial inputs and the model outputs, avoiding direct changes to the structure of the model or the algorithms employed to perform the calculations (Deb et al. 2013; Urbina et al. 2021).

The role of parameters α, n, and θ_s (within the van Genuchten's equation) provide a rationale for differential results obtained for soil water content and Br^- movement after the model calibration with PEST. For instance, the input α describes the air entry potential, while n defines the water retention curve shape (Radcliffe and Šimůnek 2010); therefore, the soil water content dynamics. In this regard, small variations in both parameters (as observed in **Table 3.4**) in the calibration will not represent a significant change in the retention curve for the horizon assessed (**Figure S3.2**). Conversely, changes in α will produce significant variations into the shape of hydraulic conductivity function $K_{(h)}$ (Vogel et al. 2001) and further significant differences in Br^- concentration calculated with the HYDRUS model.

The model calibration performed with PEST was considered satisfactory, where the parameters α, n, and θ_s presented narrow uncertainty boundaries. In addition, the calibrated values were among the confidence limits obtained for those fitted from field observations (**Table 3.3**), indicating a good estimation by the PEST calibration approach (Urbina et al. 2021).

The use of PEST as an external parameter optimization package for HYDRUS has been mentioned by Šimůnek et al. (2012b), who indicated its flexibility for choosing the parameters to be optimized in addition to the target variable to be used within the objective function. Furthermore, there are several studies in which HYDRUS 2D/3D performance significantly improved as a result of optimization of parameters using PEST, which they are in agreement with our findings for modelling solute transport and soil water content dynamics after model calibration (Deb et al. 2013; Matteau et al. 2019; Liu et al. 2021; Urbina et al. 2021).

Modeling soil water dynamics and solute movement in turfgrass with HYDRUS 2D/3D

HYDRUS 2D/3D is a powerful tool for understanding soil water dynamics and solute fate and movement through the soil profile, covering multiple soil matrix and boundary conditions. This software has been tested under a wide range of scales, from laboratory assays to field conditions, the latter varying from a few to hundreds of meters (Šimůnek et al. 2012b). Monitoring of soil water content through indirect measurements (sensors and dataloggers) has contributed to improve simulation accuracy.

In multiple studies, HYDRUS 2D/3D simulations of temporal changes in soil water content have demonstrated to provide high levels of agreement between measured data and calculated values, reflected on low values of *RMSE*, like the one observed for our simulations in both soil horizons (McCoy and McCoy 2009; Bufon et al. 2012; Deb et al. 2013; Filipović et al. 2019; Domínguez-Niño et al. 2020). Furthermore, HYDRUS 2D/3D adequately predicted Br^- concentration both spatially and temporally within our experimental conditions.

Despite the existence of studies conducted to assess the use of HYDRUS 2D/3D as a tool to understand water and solute dynamics within natural soils or laboratory repacked columns (Pang et al. 2000; Boivin et al. 2006; Gärdenäs et al. 2006; de Oliveira et al. 2019; Grecco et al.

2019 Varvaris et al. 2021), none of them have been performed within anisotropic soils or positioned in sloping conditions. Consequently, the findings obtained in this study may become a useful baseline for further studies in soil modelling and pesticide fate, in both agricultural and non-agricultural settings.

HYDRUS 2D/3D can be a valuable tool in turfgrass management to perform simulations of soil water dynamics and predict the movement and fate of solutes, such as fertilizers and pesticides, under different weather and management scenarios (McCoy and McCoy 2009; Gannon et al. 2016). Furthermore, potential simulations to be performed with HYDRUS 2D/3D after a proper model calibration would become a cornerstone for assessing off target herbicide risk and opportunely implement best management practices.

For instance, these simulations would allow identification of critical values of soil water content or rainfall scenarios where the off-target herbicide movement is more likely to occur. Therefore, the monitoring of soil water content and previous assessment of weather data could generate decision making tools before the herbicide application (Mahoney et al. 2015), minimizing crop and environmental impacts.

Lateral movement of solutes in slope soils: HYDRUS 2D/3D modelling and applications

Under sloped conditions, the transport of solutes through soil lateral flow may represent an important process in edaphic contamination and solute fate, which magnitude depends on the water input amount (rainfall), and the initial and antecedent soil water content (Kim et al. 2005; Kahl e al. 2007). In addition, the magnitude and occurrence of anisotropy in soil hydraulic properties due to the presence of horizons with contrasting soil texture become crucial factors for subsurface lateral flow (McCord et al. 1991; Filipović et al. 2018). Our experimental plot exhibited both conditions favoring this subsurface lateral flow.

Studies of lateral flow and its modelling with HYDRUS are very scarce. Filipović et al. (2018) studied the potential subsurface lateral flow in sloped soils performing simulations with HYDRUS 2D to describe this phenomenon and observed relatively small lateral movement of tracer under rainstorm events. Even though their results are based on simulations from a "virtual experiment", the authors highlighted the importance of some factors involved in the subsurface lateral flow, such as anisotropy within soil horizons, timing and location of the tracer application, and presence of extreme rainfall events.

The Br^- movement described in this study, both observed and simulated, provide evidence for subsurface lateral flow under slope conditions and anisotropic soil horizons (**Table 3.1**) as it was hypothesized by Filipović et al. (2018). However, an unexpected and interesting observation was the temporal progression of the simulated Br^- distribution, which indicated solute flux resurfacing downslope from the application point (**Figure 3.9**). This behavior could be associated with upward solute movement caused by evaporation in the soil surface. For instance, when we performed the simulation using the calibrated model but excluded the evaporation into the initial conditions, Br^- moved mostly downward and without any resurface flux at 46 DASA (**Figure 3.10**). This last result reinforces the role of the evaporation on the surfacing flux and solute upward movement, as it has been reported for anionic solutes in soils (Mohammed et al. 2000; Jacques et al. 2008) under unsaturated conditions. Consequently, the subsurface lateral movement would play a fundamental role in the solute distribution and potential accumulation in downslope areas potentially reaching high concentrations at or close to the surface that could modify plant growth and integrity.

The lateral movement of solutes or pesticides in soil has been a subject of interest in turfgrass management. Leon et al. (2016) studied the effect of irrigation to incorporate the herbicide and reduce runoff lateral movement of pre-emergence herbicides in sandy soils with moderate slope (14%) under simulated storm events. This study highlighted the implications of off-target movement of herbicides in turfgrass landscapes, where ponds and creeks, as well as ornamental plants and turf species could be negatively affected in this commodity. Therefore, a properly calibrated HYDRUS 2D/3D model is a powerful tool for predicting subsurface lateral movement to complement information about runoff risk in turfgrass systems with irregular topography (e.g., golf courses, lawns, recreational areas) (Dann et al. 2006). Additionally, this predictive approach could be coupled with geographical information systems (GIS) to identify areas with high risk of pesticide off-target movement and accumulation, allowing the optimization of the pesticide use, as reported by Anlauf et al. (2018).

Conclusions

The results obtained in the present study corroborated the occurrence of subsurface water and solute lateral movement under sloped conditions and within anisotropic soils, as it was hypothesized previously in the literature. Simulations performed with HYDRUS 2D/3D allowed to visualize this lateral movement accurately.

Our findings indicate potential for the use of HYDRUS 2D/3D as valuable tool for management in turfgrass systems to predict pesticide transport and fate under adverse scenarios like rainstorm, as well as the identification of areas with potential pesticide off-target movement risk. This will ultimately inform the design and selection of management practices to mitigate that risk and prevent negative impacts on the turfgrass and the environment.

Further experiments, including pesticides application method in settings with different soil and landscape conditions, are recommend to provide more evidence of the lateral movement, where other management strategies like the use of biochar and soil water content monitoring could be evaluated.

Acknowledgements

We would like to thank Adam Howard for his valuable help with soil physical analyses. We also thank Dr. Raymond McCauley, Marty Parish, and Daniel Freund for their assistance and invaluable help at the Lake Wheeler Turf Field Laboratory.

References

Abit, S. M., Amoozegar, A., Vepraskas, M. J., Niewoehner, C. P. 2008. Fate of nitrate in the capillary fringe and shallow groundwater in a drained sandy soil. Geoderma 146(1-2): 209-215. https://doi.org/10.1016/j.geoderma.2008.05.015

Abdalla, N. A., Lear, B. 1975. Determination of inorganic bromide in soils and plant tissues with a bromide selective-ion electrode. Communications in Soil Science and Plant Analysis 6(5): 489-494. https://doi.org/10.1080/00103627509366585

Amoozegar, A. 1989. A compact constant-head permeameter for measuring saturated hydraulic conductivity of the vadose zone. Soil Science Society of America Journal 53(5): 1356-1361. https://doi.org/10.2136/sssaj1989.03615995005300050009x

Anlauf, R., Schaefer, J., Kajitvichyanukul, P. 2018. Coupling HYDRUS-1D with ArcGIS to estimate pesticide accumulation and leaching risk on a regional basis. Journal of Environmental Management 217: 980-990. https://doi.org/10.1016/j.jenvman.2018.03.099

Blake, G.R., Hartge, K.H. 1986. Bulk density. In: Klute, A. (ed.), Methods of soil analysis, part 1, Physical and mineralogical methods. Am. Soc. Agr. Madison, Wisconsin, USA, pp. 363–375. https://doi.org/10.2134/agronmonogr9.1.c30

Boivin, A., Šimůnek, J., Schiavon, M., van Genuchten, M.T. 2006. Comparison of pesticide transport processes in three tile-drained field soils using HYDRUS-2D. Vadose Zone Journal 5(3): 838-849. https://doi.org/10.2136/vzj2005.0089

Brunetti, G., Šimůnek, J., Turco, M., Piro, P. 2018. On the use of global sensitivity analysis for the numerical analysis of permeable pavements. Urban Water Journal 15(3): 269-275. https://doi.org/10.1080/1573062X.2018.1439975

Bufon, V.B., Lascano, R.J., Bednarz, C., Booker, J.D., Gitz, D. C. 2012. Soil water content on drip irrigated cotton: comparison of measured and simulated values obtained with the Hydrus 2-D model. Irrigation Science 30(4): 259-273. https://doi.org/10.1007/s00271-011-0279-z

Campolongo, F., Cariboni, J., Saltelli, A. 2007. An effective screening design for sensitivity analysis of large models. Environmental Modelling Software 22(10): 1509-1518. https://doi.org/10.1016/j.envsoft.2006.10.004

Cuntz, M., Mai, J., Zink, M., Thober, S., Kumar, R., Schäfer, D., Schrön, M., Craven, J., Rakovec, O., Spieler, D., Prykhodko, V., Dalmasso, G., Musuuza, J., Langenberg, B., Attinger, S., Samaniego, L. 2015. Computationally inexpensive identification of noninformative model parameters by sequential screening. Water Resources Research 51(8): 6417-6441. https://doi.org/10.1002/2015WR016907

Dane, J. H., Hopmans, J. W. 2002. 3.3.2 Laboratory. In: J.H. Dame, G.C. Topp (Eds.), Methods of Soil Analysis, Part 4 – Physical Methods. Soil Science Society of America. Madison, Wisconsin, USA, pp. 675-720. https://doi.org/10.2136/sssabookser5.4.c25

Dann, R.L., Close, M.E., Lee, R., Pang, L. 2006. Impact of data quality and model complexity on prediction of pesticide leaching. Journal of Environmental Quality 35(2): 628-640. https://doi.org/10.2134/jeq2005.0257

de Oliveira, L.A., Grecco, K.L., Tornisielo, V.L., Woodbury, B.L. 2019. Atrazine movement in corn cultivated soil using HYDRUS-2D: A comparison between real and simulated data. Journal of Environmental Management 248: 109311. https://doi.org/10.1016/j.jenvman.2019.109311

Deb, S. K., Shukla, M. K., Šimůnek, J., Mexal, J. G. 2013. Evaluation of spatial and temporal root water uptake patterns of a flood-irrigated pecan tree using the HYDRUS (2D/3D) model. Journal of Irrigation and Drainage Engineering 139(8): 599-611. https://doi.org/10.1061/(ASCE)IR.1943-4774.0000611

Devak, M., Dhanya, C.T. 2017. Sensitivity analysis of hydrological models: review and way forward. Journal of Water and Climate Change 8(4): 557-575. https://doi.org/10.2166/wcc.2017.149

Doherty, J. 2015. Calibration and uncertainty analysis for complex environmental models. Brisbane, Australia: Watermark Numerical Computing.

Domínguez-Niño, J.M., Arbat, G., Raij-Hoffman, I., Kisekka, I., Girona, J., Casadesús, J. 2020. Parameterization of soil hydraulic parameters for HYDRUS-3D simulation of soil water dynamics in a drip-irrigated orchard. Water 12(7): 1858. https://doi.org/10.3390/w12071858

Filipović, V., Coquet, Y., Gerke, H.H. 2019. Representation of plot-scale soil heterogeneity in dual-domain effective flow and transport models with mass exchange. Vadose Zone Journal 18(1): 1-14. https://doi.org/10.2136/vzj2018.09.0174

Filipović, V., Gerke, H.H., Filipović, L., Sommer, M. 2018. Quantifying subsurface lateral flow along sloping horizon boundaries in soil profiles of a hummocky ground moraine. Vadose Zone Journal 17(1): 1-12. https://doi.org/10.2136/vzj2017.05.0106

Gannon, T.W., Jeffries, M.D., Ahmed, K.A. 2016. Irrigation and soil surfactants affect abamectin distribution in soil. Crop Science 57(2): 573-580. https://doi.org/10.2135/cropsci2016.05.0320

Gärdenäs, A.I., Šimůnek, J., Jarvis, N., van Genuchten, M.T. 2006. Two-dimensional modelling of preferential water flow and pesticide transport from a tile-drained field. Journal of Hydrology, 329(3-4): 647-660. https://doi.org/10.1016/j.jhydrol.2006.03.021

Gee, G.W., Orr, D. 2002. 2.4 Particle-size analysis. In: J.H. Dame, G.C. Topp (Eds.), Methods of Soil Analysis, Part 4 – Physical Methods. Soil Science Society of America. Madison, Wisconsin, USA, pp. 255-293. https://doi.org/10.2136/sssabookser5.4.c9

Grecco, K.L., de Miranda, J.H., Silveira, L.K., van Genuchten, M. T. 2019. HYDRUS-2D simulations of water and potassium movement in drip irrigated tropical soil container cultivated with sugarcane. Agricultural Water Management 221: 334-347. https://doi.org/10.1016/j.agwat.2019.05.010

Grossman, R. B., Reinsch, T. G. 2002. 2.4 Particle-size analysis. In: J.H. Dame, G.C. Topp (Eds.), Methods of Soil Analysis, Part 4 – Physical Methods. Soil Science Society of America. Madison, Wisconsin, USA, pp. 201-228. https://doi.org/10.2136/sssabookser5.4.c9

Haith, D.A., Rossi, F.S. 2003. Risk assessment of pesticide runoff from turf. Journal of environmental quality 32(2): 447-455. https://doi.org/10.2134/jeq2003.4470

Iooss B., Lemaître P. 2015. A Review on Global Sensitivity Analysis Methods. In: Dellino G., Meloni C. (eds), Uncertainty Management in Simulation-Optimization of Complex Systems. Operations Research/Computer Science Interfaces Series, vol 59. Springer, Boston, Massachusetts, USA. pp 101-122. https://doi.org/10.1007/978-1-4899-7547-8_5

Jacques, D., Šimůnek, J., Mallants, D., van Genuchten, M.T. 2008. Modelling coupled water flow, solute transport and geochemical reactions affecting heavy metal migration in a podzol soil. Geoderma 145(3-4): 449-461. https://doi.org/10.1016/j.geoderma.2008.01.009

Kahl, G., Ingwersen, J., Nutniyom, P., Totrakool, S., Pansombat, K., Thavornyutikarn, P., Streck, T. 2007. Micro-trench experiments on interflow and lateral pesticide transport in a sloped soil in Northern Thailand. Journal of Environmental Quality 36(4): 1205-1216. https://doi.org/10.2134/jeq2006.0241

Kim, H.J., R.C. Sidle, Moore, R.D. 2005. Shallow lateral flow from a forested hillslope: Influence of antecedent wetness. Catena 60:293–306. https://doi.org/10.1016/j.catena.2004.12.005

Klute, A. 1986. Water Retention: Laboratory Methods. In: Klute, A. (ed.), Methods of soil analysis, part 1, Physical and mineralogical methods. Am. Soc. Agr. Madison, Wisconsin, USA, pp. 635–662. https://doi.org/10.2136/sssabookser5.1.2ed.c26

Klute, A., Dirksen, C. 1986. Hydraulic Conductivity and Diffusivity: Laboratory Methods. In: Klute, A. (ed.), Methods of soil analysis, part 1, Physical and mineralogical methods. Am. Soc. Agr. Madison, Wisconsin, USA, pp. 687–674. https://doi.org/10.2136/sssabookser5.1.2ed.c28

Lammoglia, S. K., Makowski, D., Moeys, J., Justes, E., Barriuso, E., Mamy, L. 2017. Sensitivity analysis of the STICS-MACRO model to identify cropping practices reducing pesticides losses. Science of the Total Environment 580: 117-129. https://doi.org/10.1016/j.scitotenv.2016.10.010

Lee, S.J., Mehler, L., Beckman, J., Diebolt-Brown, B., Prado, J., Lackovic, M., Calvert, G.M. 2011. Acute pesticide illnesses associated with off-target pesticide drift from agricultural applications: 11 States, 1998–2006. Environmental health perspectives 119(8): 1162-1169. https://doi.org/10.1289/ehp.1002843

Leij, F. J., van Genuchten, M. T., Yates, S. R., Russell, W. B. 1991. RETC: A computer program for analyzing soil water retention and hydraulic conductivity data. In: van Genuchten, M. Th., Leij, F. J. Lund, L. J. (eds.), Proc. Int. Workshop, Indirect Methods for Estimating the Hydraulic Properties of Unsaturated Soils. University of California, Riverside. pp. 263-272.

Leon, R.G., Unruh, J.B., Brecke, B.J. 2016. Relative lateral movement in surface soil of amicarbazone and indaziflam compared with other preemergence herbicides for turfgrass. Weed Technology 30(1): 229-237. https://doi.org/10.1614/WT-D-15-00126.1

Liu, Y., Ao, C., Zeng, W., Srivastava, A.K., Gaiser, T., Wu, J., Huang, J. 2021. Simulating water and salt transport in subsurface pipe drainage systems with HYDRUS-2D. Journal of Hydrology 592: 125823. https://doi.org/10.1016/j.jhydrol.2020.125823

Marquardt, D.W. 1963. An algorithm for least-squares estimation of nonlinear parameters. Journal of the Society for Industrial and Applied Mathematics 11(2): 431-441.

Mahoney, D.J., Gannon, T.W., Jeffries, M.D., Matteson, A.R., Polizzotto, M.L. 2015. Management considerations to minimize environmental impacts of arsenic following monosodium methylarsenate (MSMA) applications to turfgrass. Journal of Environmental Management 150: 444-450. https://doi.org/10.1016/j.jenvman.2014.12.027

Matteau, J.P., Gumiere, S.J., Gallichand, J., Létourneau, G., Khiari, L., Gasser, M.O., Michaud, A. 2019. Coupling of a nitrate production model with HYDRUS to predict nitrate leaching. Agricultural Water Management 213: 616-626. https://doi.org/10.1016/j.agwat.2018.10.013

McCoy, E.L., McCoy, K.R. 2009. Simulation of putting-green soil water dynamics: implications for turfgrass water use. Agricultural water management 96(3): 405-414. https://doi.org/10.1016/j.agwat.2008.09.006

McCord, J.T., D.B. Stephens, Wilson, J.L. 1991. Hysteresis and state dependent anisotropy in modeling unsaturated hillslope hydrologic processes. Water Resour. Res. 27:1501–1518. https://doi.org/10.1029/91WR00880

McCuen, R.H. 1973. The role of sensitivity analysis in hydrologic modeling. Journal of Hydrology 18(1): 37-53. https://doi.org/10.1016/0022-1694(73)90024-3

Mohamed, A.A., Sasaki, T., Watanabe, K. 2000. Solute transport through unsaturated soil due to evaporation. Journal of Environmental Engineering 126(9): 842-848. https://doi.org/10.1061/(ASCE)0733-9372(2000)126:9(842)

Morris, M.D. 1991. Factorial sampling plans for preliminary computational experiments. Technometrics 33: 161–174. https://doi.org/10.2307/1269043

Munsell (Munsell Color Company). 2004. Munsell soil color charts. Maryland, USA.

Oerke, E.C. 2006. Crop losses to pests. The Journal of Agricultural Science 144(1): 31-43. https://doi.org/10.1017/S0021859605005708

Pang, L., Close, M.E., Watt, J.P., Vincent, K.W. 2000. Simulation of picloram, atrazine, and simazine leaching through two New Zealand soils and into groundwater using HYDRUS-2D. Journal of Contaminant Hydrology 44(1): 19-46. https://doi.org/10.1016/S0169-7722(00)00091-7

Pujol, G. 2009. Simplex-based screening designs for estimating metamodels. Reliability Engineering and System Safety 94: 1156–1160. https://doi.org/10.1016/j.ress.2008.08.002

Pujol, G. 2017. Sensitivity: Global sensitivity analysis of model out-puts. Comprehensive R Archive Network. Retrieved from https://CRAN.R-project.org/package=sensitivity

Racke, K. 2000. Pesticides for turfgrass pest management uses and environmental issues. In: Clark, J.M.; Kenna, M.P (eds). Fate and management of turfgrass chemicals, ACS Symposium Series 743. American Chemical Society, Washington, DC. pp 45–64

Radcliffe, D.E., Šimůnek, J. 2010. Soil physics with HYDRUS: Modeling and applications. CRC press. Boca Raton, Fl. USA. 373 p. https://doi.org/10.1201/9781315275666

R Studio Team. 2015. R Studio: integrated development for R. R Studio, Inc., Boston Available in http://www.rstudio.com/. Accessed 30 Jul 2021.

Rogers, C.C.M., Beven, K.J., Morris, E.M., Anderson, M.G. 1985. Sensitivity analysis, calibration and predictive uncertainty of the Institute of Hydrology Distributed Model. Journal of Hydrology, 81(1-2): 179-191. https://doi.org/10.1016/0022-1694(85)90175-1

Saltelli, A., Ratto, M., Andres, T., Campolongo, F., Cariboni, J., Gatelli, D., Tarantola, S. 2008. Global sensitivity analysis: the primer. John Wiley & Sons. Chichester, UK. 292 p.

Šejna, M., Šimůnek, J., & Van Genuchten, M. T. 2018. The HYDRUS Software Package for Simulating Two- and Three-Dimensional Movement of Water, Heat, and Multiple Solutes in Variably-Saturated Media. User Manual. Version 3.01. PC-Progress, Prague, Czech Republic. 322 p.

Shinde, D., Savabi, M. R., Nkedi–Kizza, P., & Vazquez, A. (2001). Modeling transport of atrazine through calcareous soils from south Florida. Transactions of the ASAE 44(2): 251. doi: 10.13031/2013.4686

Šimůnek, J., & van Genuchten, M. T., Šejna, M. 2012a. The HYDRUS Software Package for Simulating Two- and Three-Dimensional Movement of Water, Heat, and Multiple Solutes in Variably-Saturated Media. User Manual. Version 2.0. PC-Progress, Prague, Czech Republic. 230 p.

Šimunek, J., van Genuchten, M.T., Šejna, M. 2012b. HYDRUS: Model use, calibration, and validation. Transactions of the ASABE 55(4): 1263-1274.

Šimůnek, J., van Genuchten, M. T., Šejna, M. 2016. Recent developments and applications of the HYDRUS computer software packages. Vadose Zone Journal 15(7): 1-25. https://doi.org/10.2136/vzj2016.04.0033

Šimůnek, J., Sejna, M., van Genuchten, M. T. 2018. New features of version 3 of the HYDRUS (2D/3D) computer software package. Journal of Hydrology and Hydromechanics 66(2): 133-142. https://doi.org/10.1515/johh-2017-0050

Song, X., Zhang, J., Zhan, C., Xuan, Y., Ye, M., Xu, C. 2015. Global sensitivity analysis in hydrological modeling: Review of concepts, methods, theoretical framework, and applications. Journal of Hydrology 523: 739-757. https://doi.org/10.1016/j.jhydrol.2015.02.013

Topp, G.C., Ferré, P.A. 2002. 3.1 Water Content. In: J.H. Dame, G.C. Topp (Eds.), Methods of Soil Analysis, Part 4 – Physical Methods. Soil Science Society of America. Madison, Wisconsin, USA, pp. 417-545. https://doi.org/10.2136/sssabookser5.4.c19

Turco, M., Kodešová, R., Brunetti, G., Nikodem, A., Fér, M., Piro, P. 2017. Unsaturated hydraulic behaviour of a permeable pavement: Laboratory investigation and numerical analysis by using the HYDRUS-2D model. Journal of Hydrology 554: 780-791. https://doi.org/10.1016/j.jhydrol.2017.10.005

Urbina, C. A. F., van Dam, J. C., Hendriks, R. F. A., van Den Berg, F., Gooren, H. P. A., Ritsema, C. J. 2019. Water flow in soils with heterogeneous macropore geometries. Vadose Zone Journal 18(1): 1-17. https://doi.org/10.2136/vzj2019.02.0015

Urbina, C. A. F., van den Berg, F., van Dam, J. C., Tang, D. W. S., Ritsema, C. J. 2020. Parameter sensitivity of SWAP–PEARL models for pesticide leaching in macroporous soils. Vadose Zone Journal 19(1): e20075. https://doi.org/10.1002/vzj2.20075

Urbina, C. A. F., van Dam, J., Tang, D., Gooren, H., Ritsema, C. 2021. Estimating macropore parameters for HYDRUS using a meta-model. European Journal of Soil Science. https://doi.org/10.1111/ejss.13103

van Genuchten, M. T. 1980. A closed-form equation for predicting the hydraulic conductivity of unsaturated soils. Soil Science Society of America Journal 44(5): 892-898. https://doi.org/10.2136/sssaj1980.03615995004400050002x

Varvaris, I., Pittaki-Chrysodonta, Z., Børgesen, C.D., Iversen, B.V. 2021. Parameterization of two-dimensional approaches in HYDRUS-2D. Part 2: Solute transport on field and column-scale. Soil Science Society of America Journal. https://doi.org/10.1002/saj2.20262

Vogel T., van Genuchten, M.Th., Cislerová, M. 2001. Effect of the shape of the soil hydraulic functions near saturation on variably-saturated flow predictions, Advances in Water Resources 24(2): 133-144. https://doi.org/10.1016/S0309-1708(00)00037-3

Zhou, J., Cheng, G., Li, X., Hu, B. X., Wang, G. 2012. Numerical modeling of wheat irrigation using coupled HYDRUS and WOFOST models. Soil Science Society of America Journal 76(2): 648-662. https://doi.org/10.2136/sssaj2010.0467

Figures

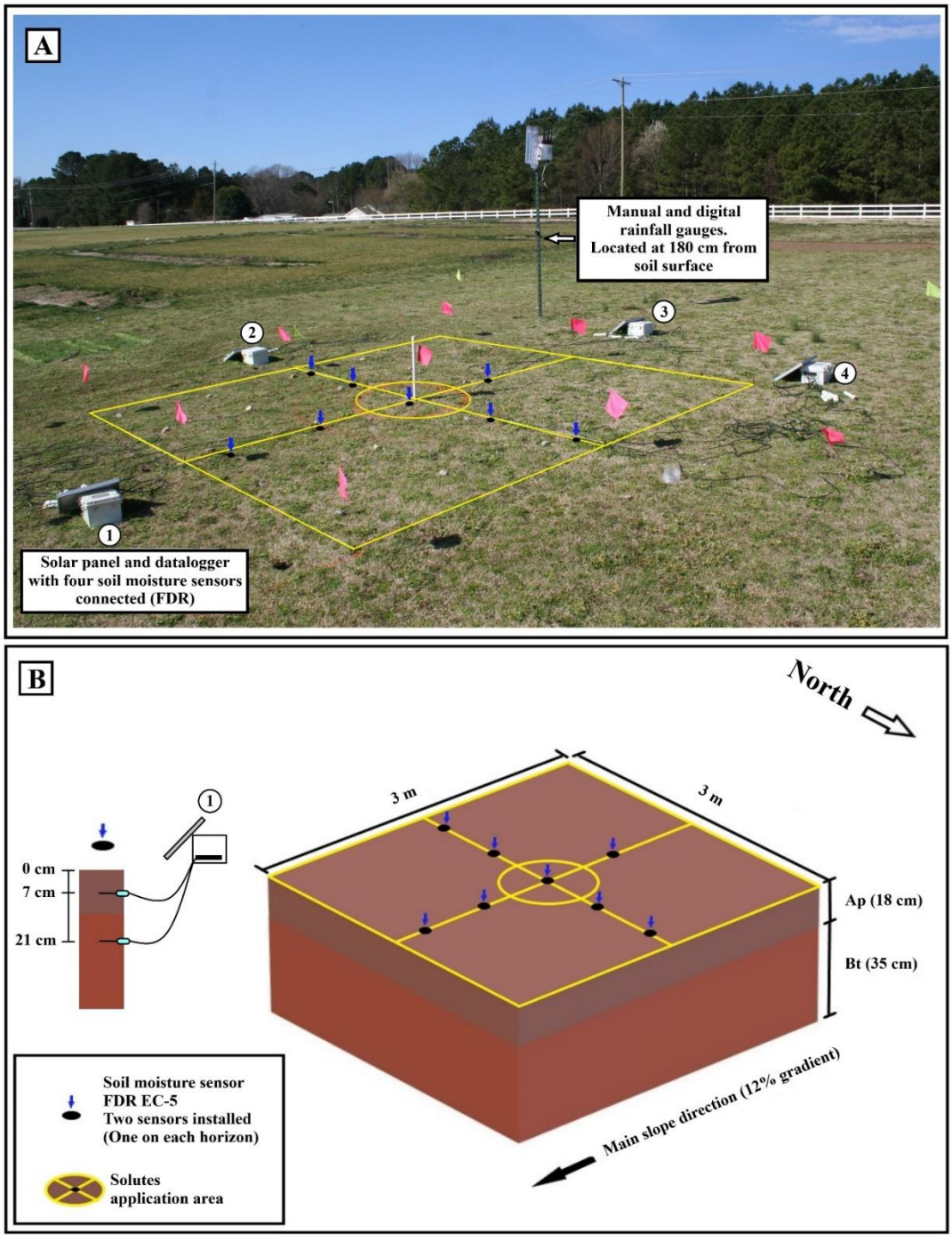

Figure 3.1 Experimental plot establishment in the field (A) and 3D soil profile diagram (B) with dimensions, soil horizons depth, and soil moisture sensor locations within the plot at Raleigh, NC. Number 1-4 inside the circles represent the unique id of the dataloggers. Soil profile colors according with Munsell (2004).

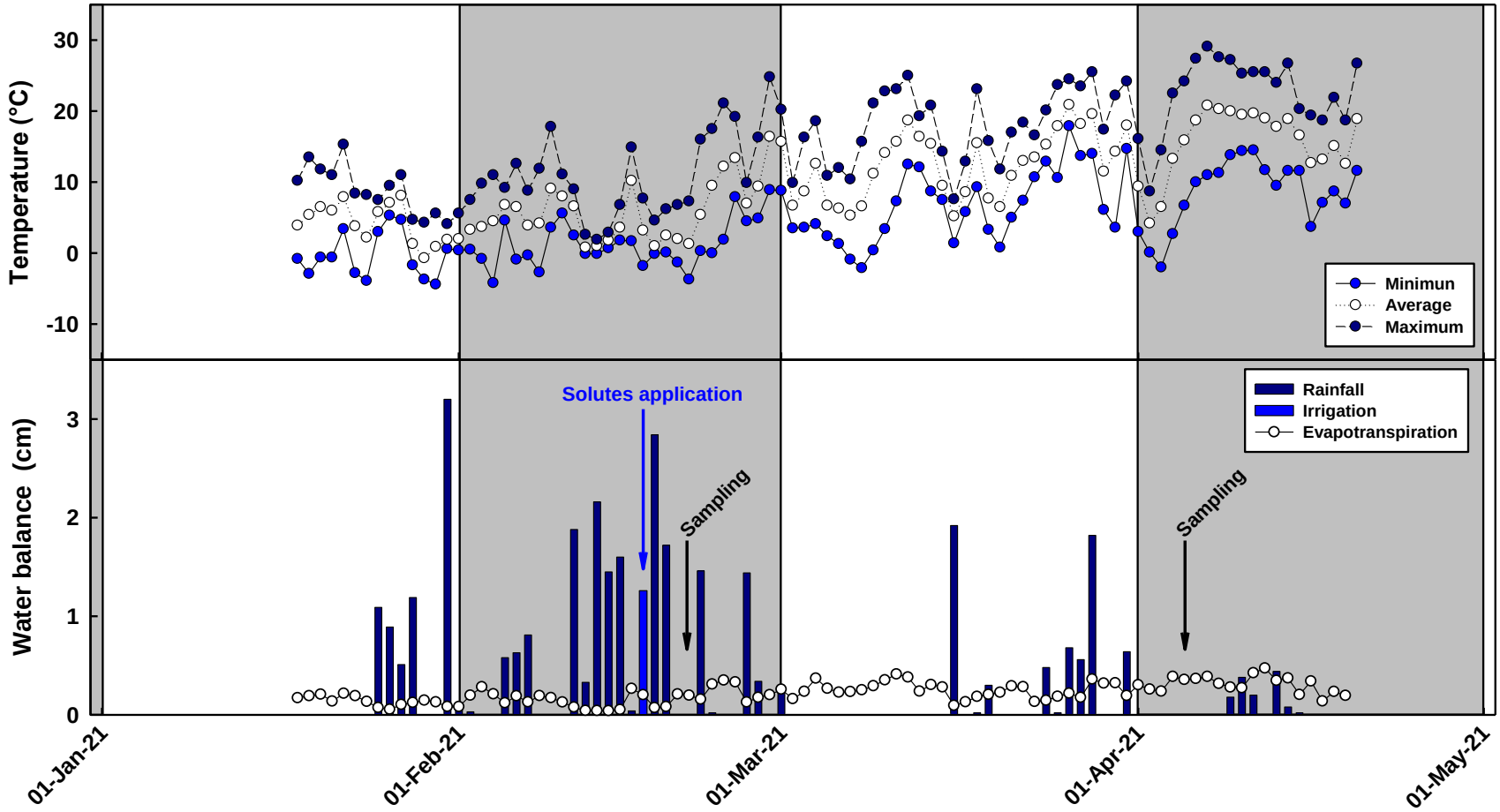

Figure 3.2 Air temperature and atmospheric water balance assessed during the tracer experiment in Raleigh, NC. Black arrows represent the soil sampling moments. Gray and white background used to contrast consecutive months. Blue arrow represents the solute application.

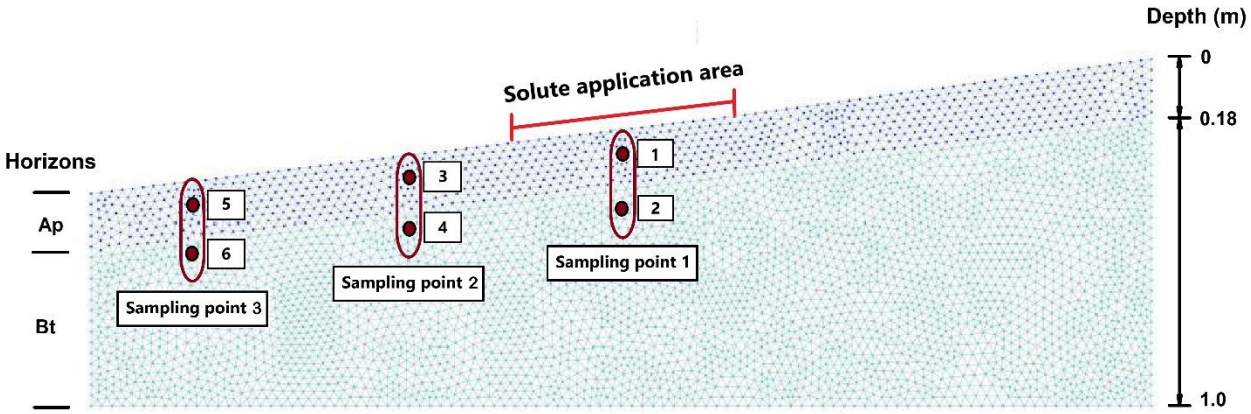

Figure 3.3 Finite element grid representing the soil domain assessed to evaluate soil water content dynamics and solute lateral movement in Cecil series located at Raleigh, NC. Grid contains 8147 triangular elements and 4202 nodes. Red dots correspond to FDR sensors and dark red ovals correspond to the soil sampling points.

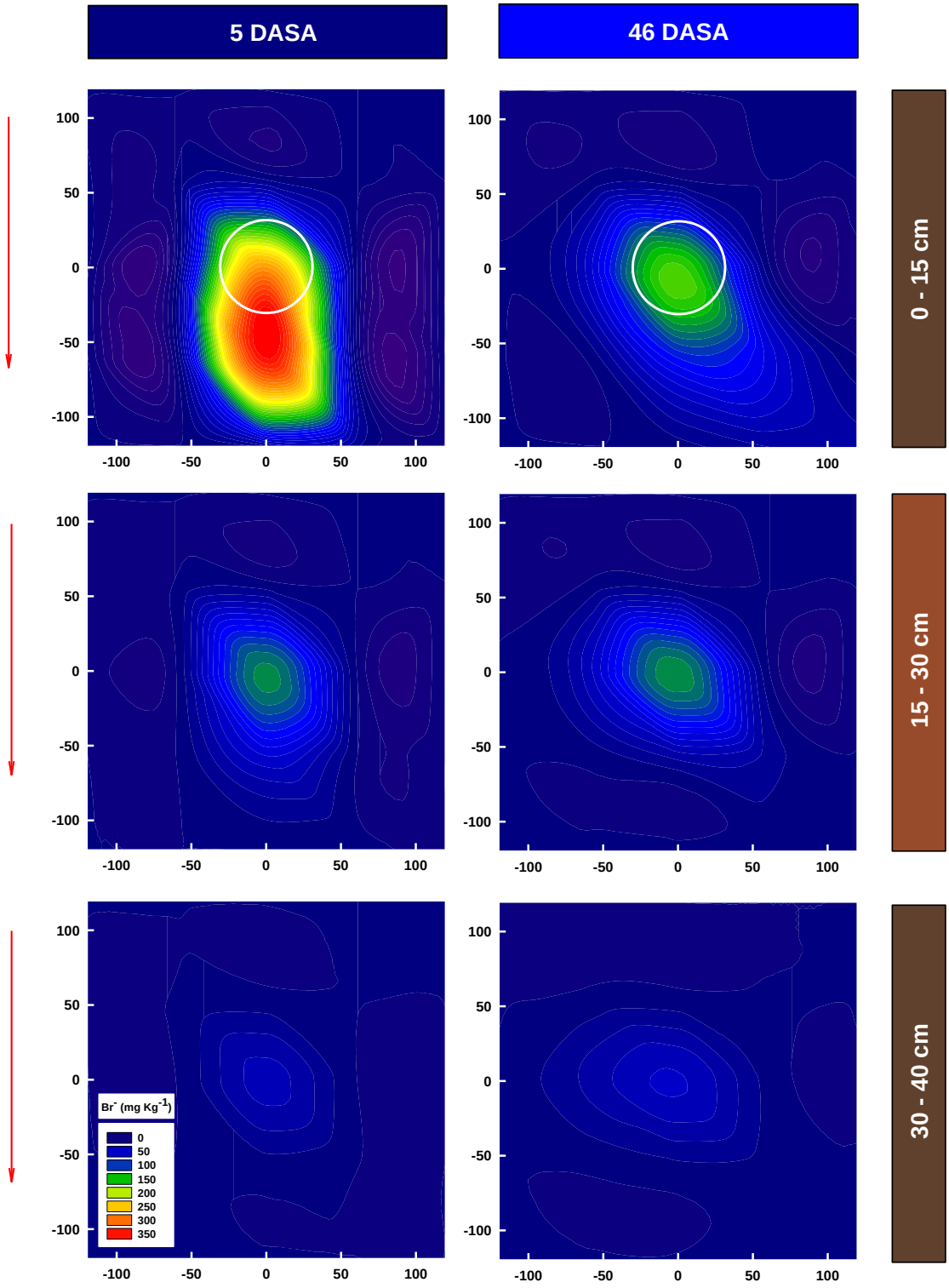

Figure 3.4 Bromide distribution along the surface of experimental plot assessed for three soil depths at two different sampling times in Raleigh, NC. Bromide values (mg Kg^{-1}) were obtained from soil samples from the field. Numbers in *x* and *y* axis represent the coordinates within the plot. White circle located in the center of the plot represents the solute application area. Red arrows show the main slope direction.

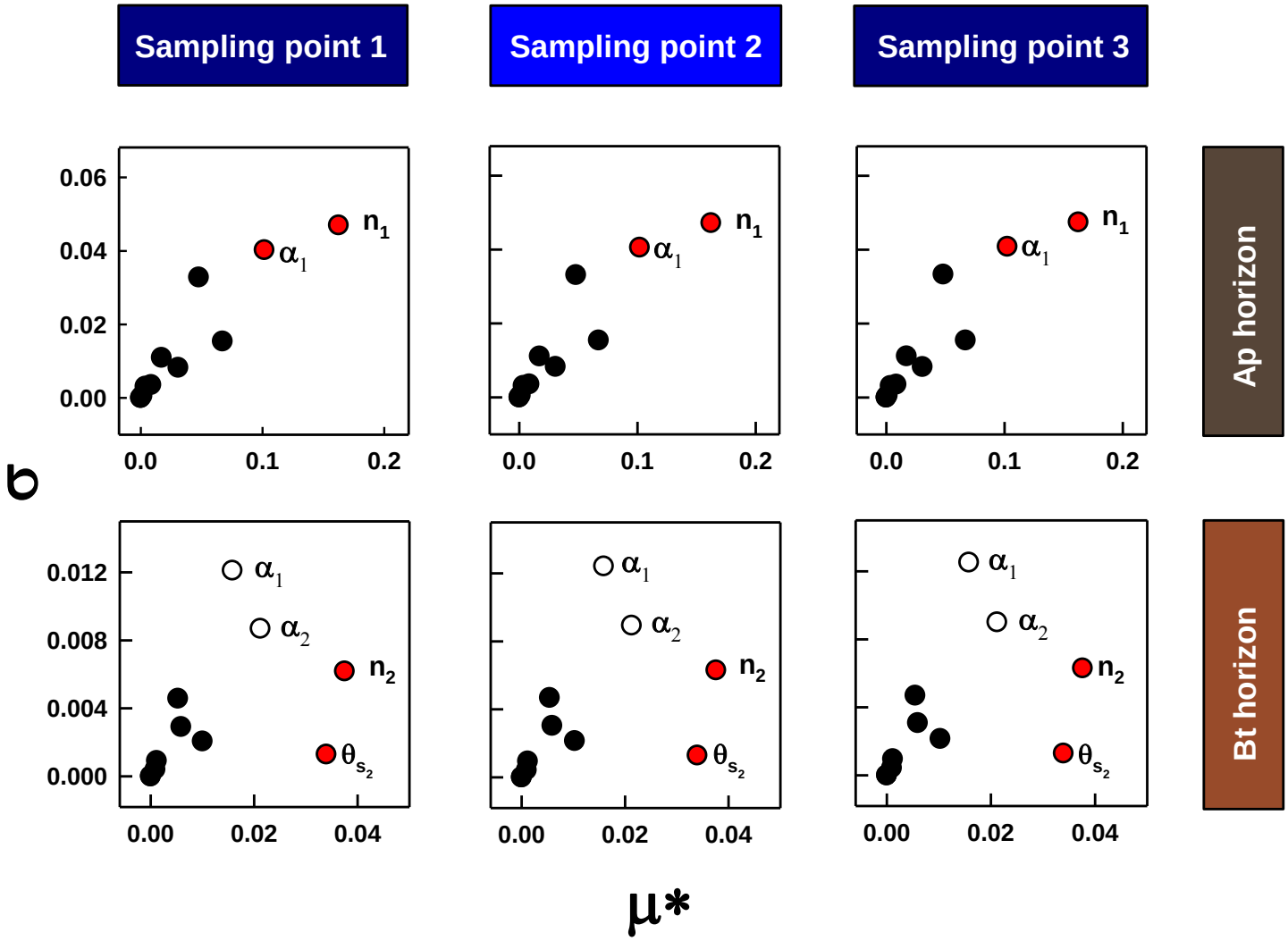

Figure 3.5 Morris one-factor at time sensitivity analysis performed for modelling soil water content ($cm^3\ cm^{-3}$) with HYDRUS 2D/3D for three observation points in Raleigh, NC. Tagged red and white dots in bold font are described respectively as the highly influential and influential parameters according with Lammoglia et al. (2017). Subscripts 1 and 2 represent parameters were measured in the Ap and Bt, respectively.

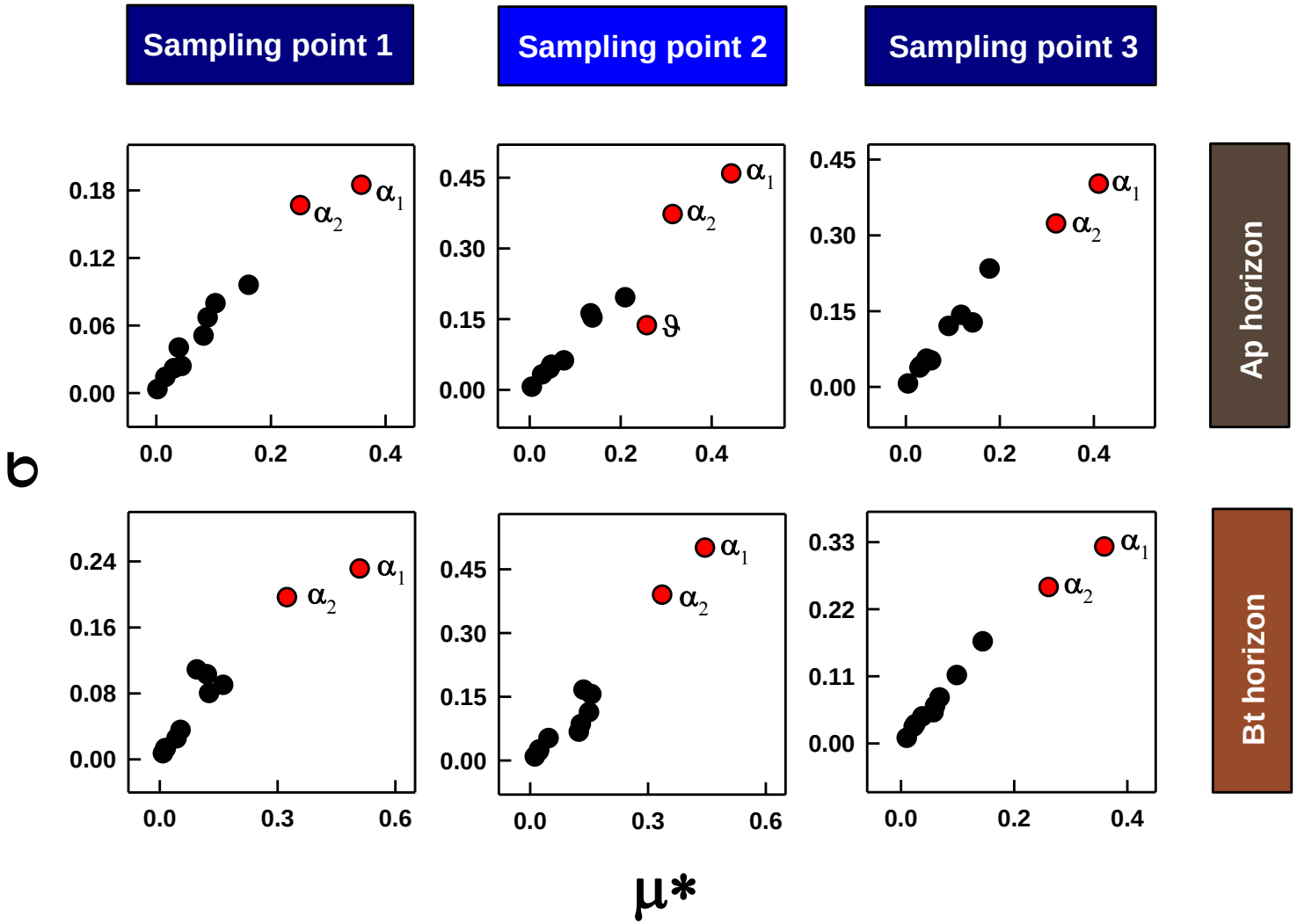

Figure 3.6 Morris one-factor at time sensitivity analysis performed for modelling bromide concentration (mg cm^{-3}) with HYDRUS 2D/3D for six different observation nodes in Raleigh, NC. Tagged red and white dots in bold font are described respectively as the highly influential and influential parameters according with Lammoglia et al. (2017). Subscripts 1 and 2 represent parameters were measured in the Ap and Bt, respectively.

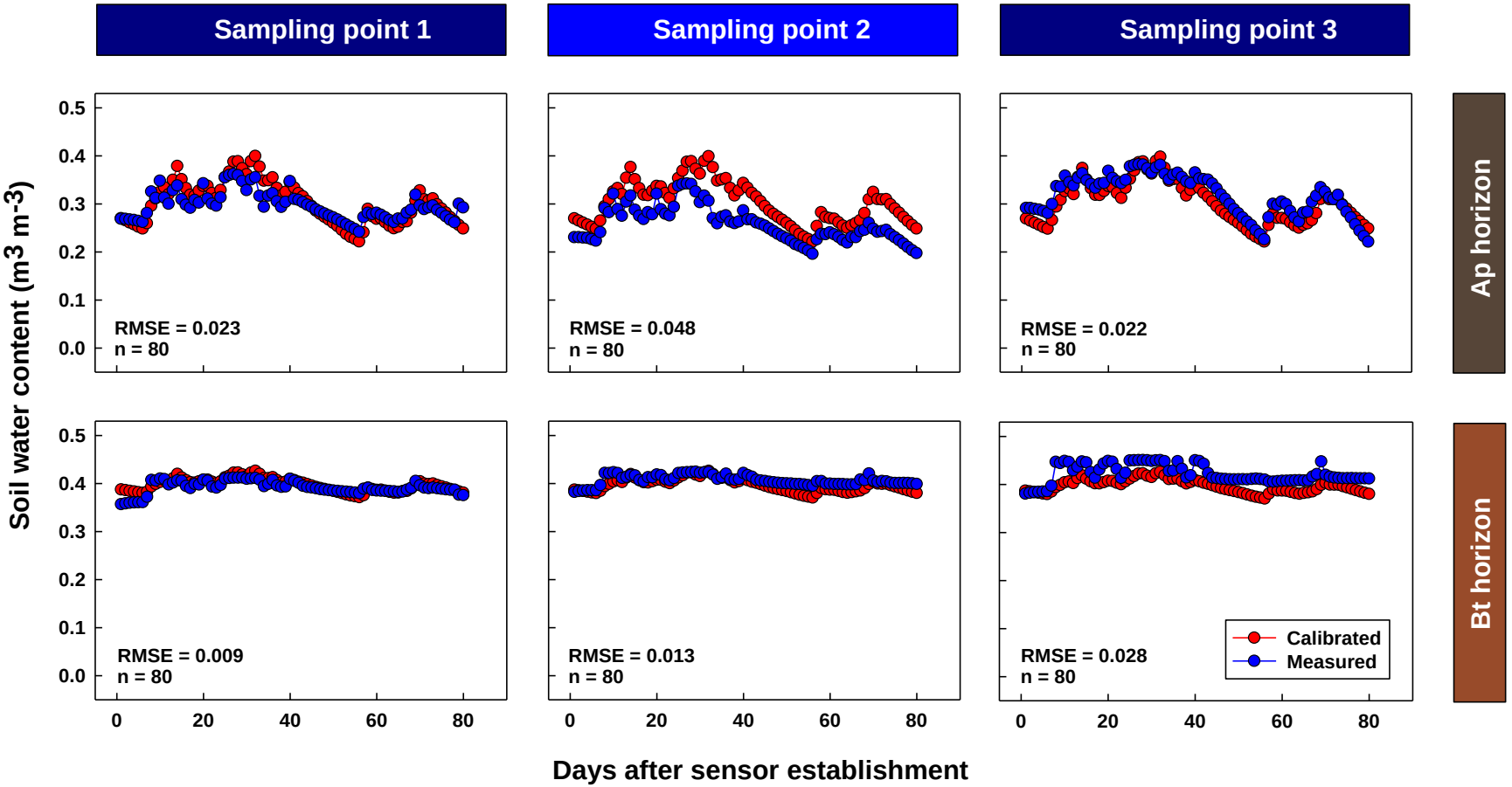

Figure 3.7 Measured and calibrated daily time series of soil volumetric water content assessed during period of 80 days at Raleigh, NC.

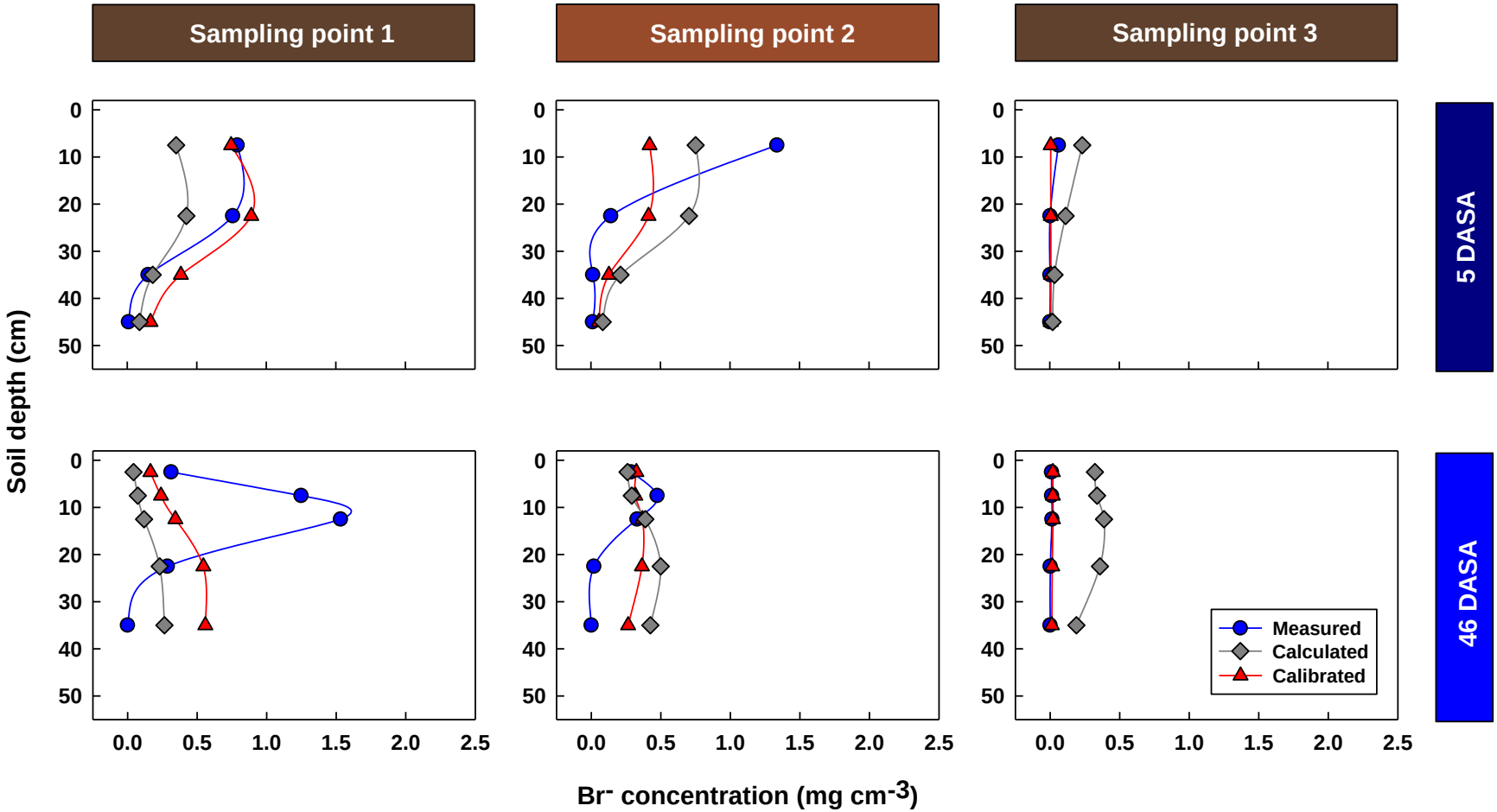

Figure 3.8 Bromide distribution along soil depth assessed for three sampling points in the experimental plot at two sampling times in Raleigh, NC. Bromide values were obtained from soil samples from the field (measured), simulated with HYDRUS 2D/3D with the initial model parameters (calculated), and simulated with HYDRUS 2D/3D after calibration (calibrated). Sampling times were conducted 5 and 46 days after solute application (DASA).

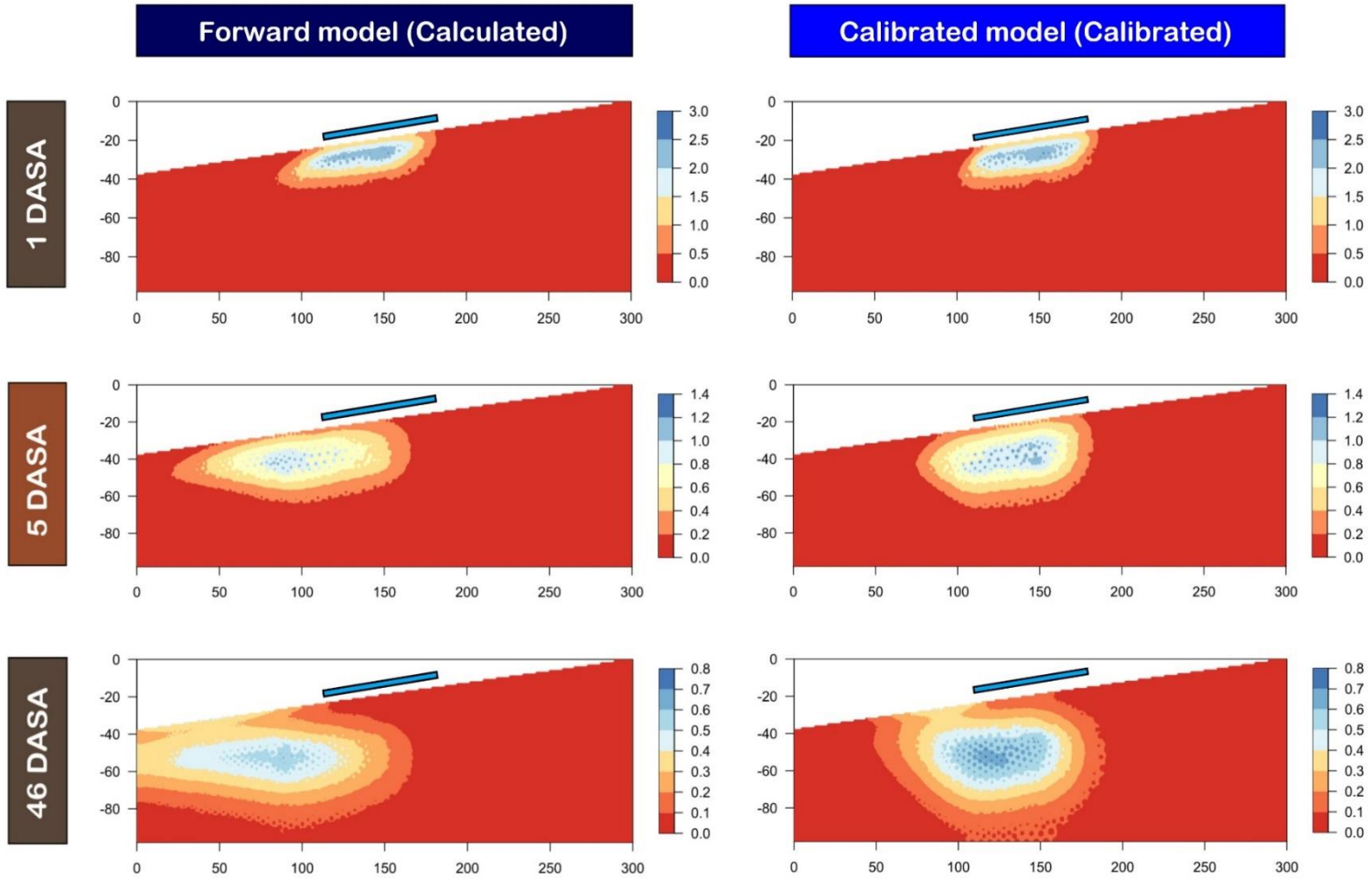

Figure 3. 9 Simulations for Br^- distribution and movement within soil domain during three different dates at Raleigh, NC. Simulations were conducted at 1, 5 and 46 days after solute application (DASA). Br^- values were simulated with HYDRUS 2D/3D with the initial model parameters (calculated), and after calibration (calibrated). Units for axis x and y in the soil domain are cm. Light blue bar above the soil surface indicates the solute application area. Color scale bar units for $Br^-$are in mg cm^{-3}.

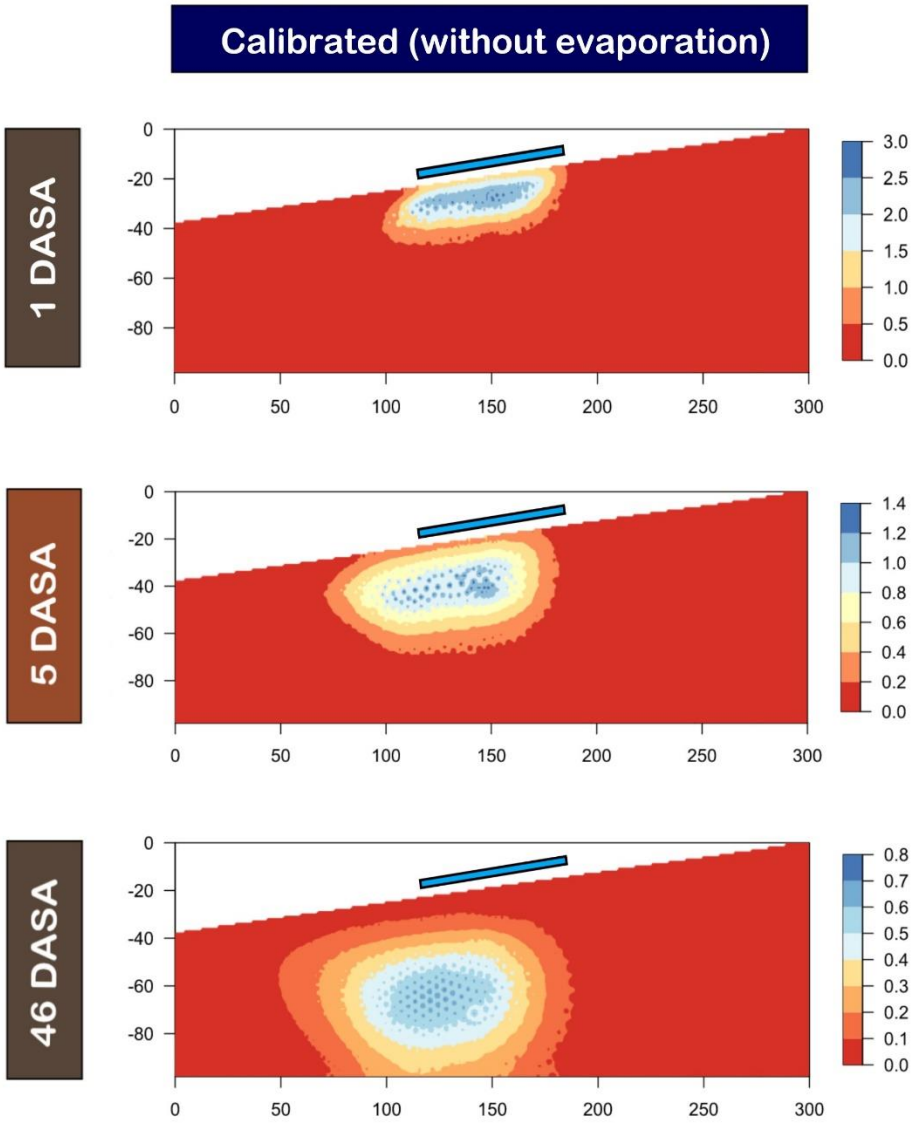

Figure 3.10 Simulations for Br^- distribution and movement within soil domain during three different dates at Raleigh, NC. Simulations were conducted at 1, 5 and 46 days after solute application (DASA). Br^- values were simulated with HYDRUS 2D/3D after calibration assuming no evaporation. Units for axis x and y in the soil domain are cm. Light blue bar above the soil surface indicates the solute application area. Color scale bar units for $Br^-$are in mg cm^{-3}.

Tables

Table 3.1 Soil physical properties assessed for Cecil series in the experimental plot in Raleigh, NC.

Horizon	Depth	K_s* ($cm\ h^{-1}$)	Bulk density* ($g\ cm^{-3}$)	Porosity* ($cm^3\ cm^{-3}$)	Sand (%)	Silt (%)	Clay (%)	α	n	Θ_s	Θ_r
Ap	0-18	36.32 ± 4.48	1.20 ± 0.04	0.55 ± 0.01	91	5	4	0.006	1.460	0.47	0.08
Bt	18-60	3.28 ± 1.25	1.32 ± 0.03	0.50 ± 0.01	21	11	68	0.015	1.085	0.46	0.27

* Average values ± standard error (n= 6).

Table 3.2 HYDRUS 2D/3D parameters and range values assessed in the sensitivity analysis.

Horizon	Parameter	Min	Max	Units
Ap	θ_s	0.420	0.520	cm^3cm^{-3}
	α	0.002	0.013	cm^{-1}
	n	1.150	1.770	*
	K_s	764.160	979.200	cm day^{-1}
	D_l	5.000	20.000	cm
Bt	θ_s	0.440	0.480	cm^3cm^{-3}
	α	0.008	0.037	cm^{-1}
	n	1.060	1.110	*
	K_s	48.720	108.720	cm day^{-1}
	D_l	5.000	20.000	cm
All	ϑ	0.250	0.750	*

* Unitless

Table 3.3 Overall statistical parameters to assess overall model performance (before and after calibration) while predicting soil water content and bromide concentration with HYDRUS 2D/3D.

Predicting variable	Statistical parameter*	Forward model	Calibrated model
Soil water content (cm^3 cm^{-3})	RMSE	0.030	0.027
	d	0.941	0.951
	NSE	0.802	0.838
Bromide concentration (mg cm^{-3})	RMSE	0.453	0.389
	d	0.247	0.576
	NSE	-0.030	0.228

* RMSE: Root mean square error; d: Willmott agreement index; NSE: Nash – Sutcliffe efficiency.

Table 3.4 Initial and calibrated parameters used in HYDRUS 2D/3D for modelling soil water content and subsurface lateral movement of solutes in Raleigh, NC.

Horizon	Parameter	Transformation	Initial value	Lower limit*	Upper limit*	Calibrated value	Lower limit*	Upper limit*
Ap	θ_s	Fixed	0.470	**	**	0.470	**	**
	α	log	0.006	0.002	0.127	0.012	0.009	0.016
	n	log	1.460	1.010	1.770	1.288	1.266	1.311
	K_s	Fixed	871.680	**	**	871.680	**	**
	D_l	Fixed	5.000	**	**	5.000	**	**
Bt	θ_s	log	0.460	0.340	0.580	0.450	0.441	0.460
	α	log	0.015	0.002	0.077	0.020	0.014	0.026
	n	log	1.090	1.010	1.110	1.064	1.051	1.077
	K_s	Fixed	78.720	**	**	78.720	**	**
	D_l	Fixed	5.000	**	**	5.000	**	**
All	ϑ	Fixed	0.500	**	**	0.500	**	**

* 95% percent confidence limits

** Parameters were not included into the calibration process due the results obtained in the Morris sensitivity analysis (**Figs. 1** and **2**).

Supplementary material

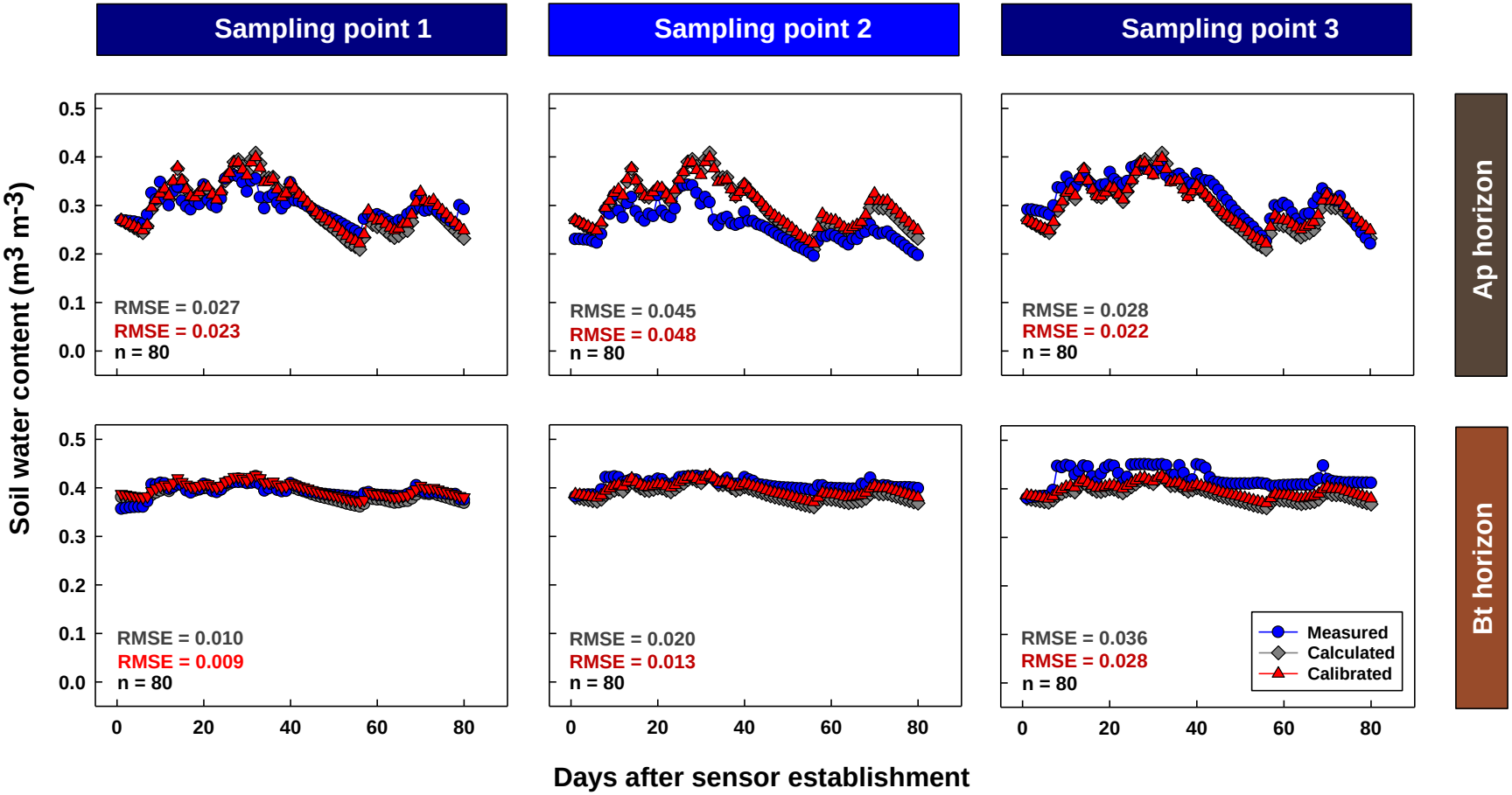

Figure S3.1 Measured, calculated, and calibrated daily time series of soil volumetric water content assessed during period of 80 days at Lake Wheeler, NC. RMSE values correspond to calculated (in gray) and calibrated (in red).

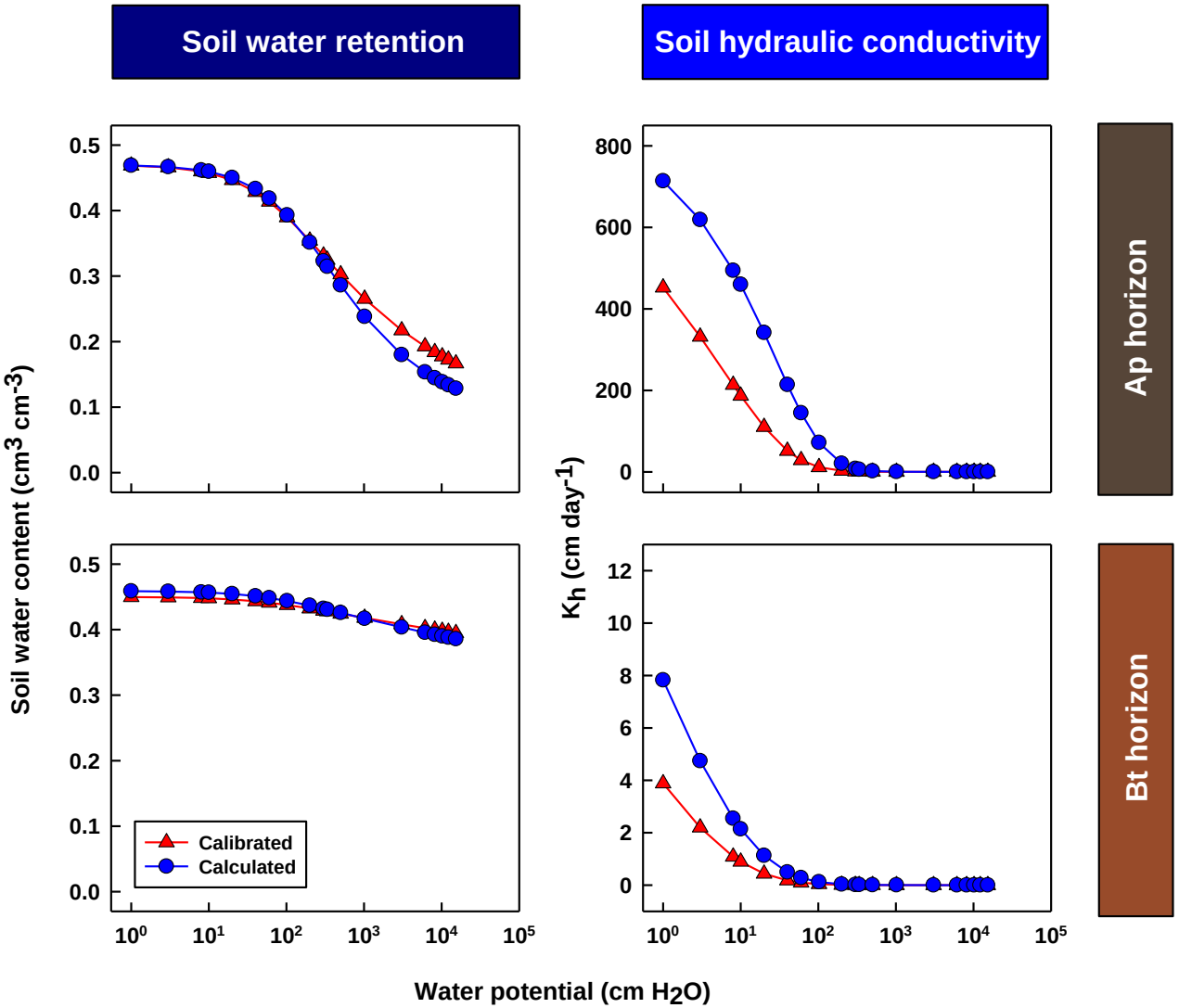

Figure S3.2 Soil hydraulic properties estimated using the van Genuchten parameters after calibration (calibrated) and without calibration (calculated) for the soil horizons assessed.

CHAPTER 4: Evaluation of imazapic and flumioxazin carryover risk for Brassica carinata establishment

Formatted for *Field Crops Research*

Manuel E. Camacho[1,2]; Michael J. Mulvaney[3]; Joshua L. Heitman[2]; Travis W. Gannon[2]; Aziz Amoozegar[2]; Ramon G. Leon[2,4,5*]

1 Centro de Investigaciones Agronómicas (CIA), Universidad de Costa Rica, 11503-2060 San Pedro, Costa Rica.

2 Department of Crop and Soil Sciences, North Carolina State University, Campus Box 7620, Raleigh, NC 27695, USA.

3 Agronomy Department, University of Florida, Institute of Food and Agricultural Sciences, Jay, FL 32565.

4 Center for Environmental Farming Systems, North Carolina State University, Campus Box 7609, Raleigh, NC 27695, USA.

5 Genetic Engineering and Society Center, North Carolina State University, Campus Box 7565, Raleigh, NC 27695, USA.

Abstract

Carinata (*Brassica carinata* A. Braun) has become a promising alternative crop for biofuel production in the Southeastern USA. However, there are concerns of carryover issues caused by soil persistent herbicides used in rotational crops and to which carinata is susceptible. The present study evaluated the potential carryover risk for carinata of imazapic and flumioxazin. Field trials were established in two different sites (Clayton and Jackson Springs) in North Carolina, USA. Applications were conducted to bare soil using the recommended label rate of imazapic (70 g ai ha^{-1}) and flumioxazin (107 g ai ha^{-1}) at 24, 18, 12, 6 and 3 months before carinata planting (MBP). Additionally, those same herbicides were applied in preemergence (PRE) right after carinata planting at 1X, 0.5X, 0.25X, 0.125X and 0.063X of the label rate. A non-treated control was included for comparison. In addition, undisturbed soil cores were taken for further herbicide residue analysis and greenhouse bioassay. No differences with the nontreated control were observed for plant density when applications for both herbicides were done over 3 months before planting, regardless the site. Plant damage observed in carinata was less than 25% when flumioxazin or imazapic were applied at least 6 MBP in a sandy loam, while in a coarser textured soil this value changed to 12 MBP. In addition, it was observed that the application of 0.063X of either herbicide in preemergence was enough to produce a decrease of 40% in plant density and damage values higher than 25%. Quantification of herbicide residues in soils showed that imazapic moved deeper in the soil profile than flumioxazin. This behavior was more evident in Jackson Springs, where imazapic was detected between 15 and 20 cm depth. In addition, it was estimated that to cause a minimum of 25 % plant damage in carinata, threshold values for herbicide concentration in soils of 7.78 and 6.90 ng g^{-1} (for imazapic and flumioxazin, respectively) should be detected.

Introduction

Weed presence in cropping systems and its corresponding management is one of the main challenges for a productive and profitable agriculture (Bridges 1994), and herbicides have become the most common and widely used tool to address these problems in the United States of America (USA), mostly because of their effectiveness and implementation ease. However, its misuse has resulted in other economic and ecological issues such as herbicide resistance evolution (Heap 2014). Also, the persistence of herbicide residues in soil and potential carryover (Hollaway et al. 2003; Palhano et al. 2018) could result in plant toxicity and significant economic losses (Rector et al. 2020), especially when considering the establishment of non-traditional or alternative crops.

Carinata (*Brassica carinata* A. Braun) has become an attractive winter rotational crop for the Southeastern region of the USA due to its potential uses for livestock feed and large-scale biofuel production (Mulvaney et al. 2019; Kumar et al. 2020). This crop presents desirable agronomic characteristics such as abiotic stress tolerance, plant pathogens and seed shattering resistance (Kumar et al. 1984; Rakow and Getinet 1997; Yang et al. 2010; Zanetti et al. 2013; Raman et al. 2017). In addition, comparing other seed-oil species used in industry, carinata seeds present higher quantities of long-chain fatty acids (e.g., erucic acid), preferred to generate high-energy fuels with less energy inputs (Mulvaney et al. 2019; Kumar et al. 2020).

Carinata was originally cultivated in Northeast Africa and recently introduced into other countries including Canada (Rakow and Getinet 1997), Australia and New Zealand (Rahman et al. 2018), Italy (Cardone et al. 2003), Spain (Gasol et al. 2007; Martínez-Lozano et al. 2009), and India (Thakur et al. 2019).

Due to its recent introduction as a rotational winter crop in the USA, there is limited information about the agronomic practices needed to attain high yields sustainably (Mulvaney et al. 2019). Specifically, there are few reports about weed control and carinata tolerance to herbicides (Leon et al. 2017; Ethridge et al. 2021).

Currently, in the southeastern USA, crop rotations include soybean (*Glycine max* L. Merr.), peanut (*Arachis hypogaea* L.), or cotton (*Gossypium hirsutum* L.) grown from Spring to Fall (Johnson et al. 2001). In these rotational systems, the use of preemergent herbicides imazapic (ALS inhibitor family) and flumioxazin (PPO inhibitor family) has been widely implemented for effective control of dicotyledonous species and to ensure target crop yields (Ferrell and Vencill 2003; Matocha et al. 2003; Berger et al. 2012). Nevertheless, their soil persistence and further adverse effects in crop establishment are of concern to growers. For instance, plant injury and yield reduction have been reported for cotton due to imazapic carryover after peanut (York et al. 2000). In addition, this carryover effect of imazapic and flumioxazin has been reported for winter cover crops planted after peanut-cotton rotation (Price et al. 2020) and those reports agree with anecdotal information from growers, who have observed uneven carinata stands and plant damage at later stages of the winter growing season (e.g., plant stunting, chlorosis, flower abortion). Despite those reports and concerns, there are no studies about herbicide carryover effects and their impact on carinata. Therefore, the present study was conducted to address three objectives to: 1) study the potential carryover risk of two residual herbicides (imazapic and flumioxazin) widely used in crop rotations in the southeastern USA on carinata establishment, 2) characterize their movement and behavior within the soil, and 3) relate soil herbicide concentration with carinata planting and establishment safety.

Materials and Methods

Field experiments

Field experiments were conducted between 2017 and 2019 at the Central Crop Research Station in Clayton, North Carolina, USA (35.670°N, 78.490° W) and the Sandhills Research Station in Jackson Springs, North Carolina, USA (35.186° N, 79.669°W). Soils series were Norfolk loamy sand (fine-loamy, kaolinitic, thermic Typic Kandiudults) and Candor sand (sandy, kaolinitic, thermic Grossarenic Kandiudults), respectively.

Risk of *B. carinata* injury due to carry over was studied for imazapic (Cadre®; BASF Co., Research Triangle Park, NC) and flumioxazin (Valor® SX; Valent U.S.A Co., Walnut Creek, CA). Imazapic was applied to bare ground at 70 g ai ha^{-1} and flumioxazin at 107 g ai ha^{-1} at 24, 18, 12, 6 and 3 months before *B. carinata* planting. In addition, those herbicides were applied at planting time at 1X (respectively 70 and 107 g ai ha^{-1}), 0.5X, 0.25X, 0.125X and 0.068X. Herbicides were applied using a CO_2 pressurized backpack sprayer flat-fan spray nozzles (XR; TeeJet®, XR11002VS, Spraying Systems Co., Wheaton, IL). This equipment was calibrated to deliver 187 L ha^{-1} of solution at 214 kPa of pressure. A non-treated control was included for comparison.

Each individual treatment mentioned above was applied to four plots (9 m^2 each), randomly distributed in the field. The plots were planted with 100 seeds of *B. carinata* var "Avanza 641" along a 1.0 m long furrow in the middle of the plot. Stand counts were performed one, two and three and half months after planting to evaluate the effect of the herbicides on crop emergence and survival.

One week after planting, two undisturbed soil cores (4.45 cm diameter and 121.9 cm length) were taken from each plot and inserted in clear polyethylene sleeves using a hydraulic

probe equipped with a cutting head (Giddings Machine Company, Windsor, CO) installed on a Polaris Ranger (Polaris, Roseau, MN). Soil cores were split into two groups: 1) cores for the greenhouse bioassay and 2) cores for residue analysis. Both groups were stored separately at -12° C.

Greenhouse bioassay

One hundred and two days after collection, soil cores from the first group were transferred to the greenhouse and placed horizontally and fixed to a specially designed bench to avoid rolling. A 2 cm wide opening was carefully cut along the sleeve without disturbing the soil. A 0.5 cm depth furrow was dug into the exposed soil, and *B. carinata* seeds were planted every 2 cm, starting from 0 cm depth to the end of the core. Soil cores were irrigated three times per day to maintain soil moisture at favorable levels for seed germination and plant growth. Daily mean temperature in the greenhouse was 24° C, ranging from 19° C to 29° C.

Plant injury due to herbicide residues was evaluated 45 days after planting. Three variables were used: 1) closest distance from the soil surface in which injury was observed, 2) farthest distance from the soil surface in which injury was observed, and 3) visual estimated plant injury in the region between points 1 and 2 with 0% = no damage, 100% = deformed, missing or death plant.

Soil samples preparation

Soil cores from the second group were moved to a lab bench and let to thaw for 8 h. These soil cores were horizontally dissected into 4 segments: 0 to 5 cm, 5 to 10 cm, 10 to 15, and 15 to 20 cm soil depths. Segmenting equipment (paddy knives) was decontaminated every time used with an ammonia: water (2:1 vol vol^{-1}) solution and dried with disposable towel paper to avoid residue cross contamination.

These soil segments were placed into labelled Ziploc bags and stored at -12° C until sample homogenization, which was carried out by adding 200 g pulverized dry ice and passing them through a soil grinder SA-45 with a 2.0 mm sieve screen (Global Gilson, Lewis Center, OH).

Herbicide residue analysis

Flumioxazin was extracted from corresponding samples combining 20 g of processed soil with 25 mL of acetonitrile (Optima® LC/MS, Fisher Chemical, Fair Lawn, NJ) in high-density polyethylene conic containers (225 mL). These containers were shaken for 45 minutes at 200 rpm in a KS501 digital orbital laboratory shaker (IKA Works Inc., Wilmington, NC) and further centrifuged for 10 minutes at 3500 rpm using an Allegra 6KR centrifuge (Beckman Coulter Inc., Indianapolis, IN). A 10 mL aliquot of supernatant was collected for each soil sample, and 1 mL of this aliquot was filtered with a 0.45 µm PTFE membrane (VWR International, Radnor, PA), and further analyzed through high performance liquid chromatography–mass spectrometry methodology (Agilent-6120 Infinity; Agilent Technologies, Inc., Wilmington, DE) coupled with a rapid resolution high-definition column (Agilent ZORBAX RRHD SB-C18; Agilent Technologies, Inc., Wilmington, DE). For imazapic extraction, the same protocol was implemented, but using 25 mL of methanol (Optima® LC/MS, Fisher Chemical, Fair Lawn, NJ) instead of acetonitrile.

The corresponding analyte concentrations were quantified using peak area measurements (OpenLAB CDS ChemStation, version C.01.04; Agilent Technologies Inc., Wilmington, DE). For both herbicides, the limit of quantification was 1.25 ng mL^{-1}, and the limit of detection was 0.625 ng mL^{-1}. Fortification recovery control of imazapic for soil samples ranged from 89 to

103% for Jackson Springs, and from 93 to 99% for Clayton. Meanwhile, the recovery controls of flumioxazin varied from 90 to 103% for Jackson Springs, and from 84 to 95% for Clayton.

In addition, 20 g of soil were taken from each processed sample to estimate gravimetric soil moisture content ($g\ g^{-1}$) following Topp and Ferré (2002) procedures, aiming to calculate the soil solids mass in the samples, and correct the final pesticide residue concentration to soil dry mass basis.

Experimental design and statistical analysis

For the herbicide residues assessed in the soils samples, a factorial analysis of variance (ANOVA) was performed using PROC GLIMMIX, where location (L), herbicide (H), time of application before planting (MBP), soil depth (SD) and their corresponding interactions were considered fixed effects, while block was set up as random. Means were separated using Bonferroni-Test ($p \leq 0.05$).

The field study and the greenhouse bioassay were conducted as a randomized complete block designs with four replications in both locations. Results were analyzed separately by the two main components of the study: the herbicide carryover risk treatments and increasing fractions to the recommended rate (1X) at planting. For the carryover experiment, a factorial analysis of variance (ANOVA) was performed using PROC GLIMMIX, where location (L), herbicides (H), time of application (T), and their corresponding interactions were considered fixed effects, while block was random. Treatments were compared to the nontreated control using Dunnett-Test ($p \leq 0.05$).

For the increasing fractions to the recommended rate (1X) at planting, a factorial analysis of variance (ANOVA) was performed using PROC GLIMMIX, where location (L), herbicide (H), and increasing fractions to the recommended rate (1X) at planting (D), and their

corresponding interactions were considered fixed effects, while block was set up as random. Treatments were compared to the nontreated control using Dunnett-Test ($p \leq 0.05$). Data were analyzed with Statistical Analysis Systems (SAS), version 9.4, Cary, NC 27513.

Nonlinear regression models were fit for the main component time of application (T) under field and greenhouse conditions. For the herbicide carryover risk treatments, plant density in the field and plant damage in the greenhouse bioassay were selected as dependent variables (*y*) and the herbicide time application before planting (MBP) as the independent variable (*x*). For the herbicide increasing fractions, the same dependent variables were used, but in this case the independent variable (*x*) corresponded to the incremental fractions to reach the recommended doses (1X).

In addition, plant damage and plant density data were grouped by herbicide with their corresponding recovered concentration (ng of herbicide g of $soil^{-1}$). Nonlinear regression models were fit to describe the behavior of plant damage or plant density as dependent variable (*y*) due changes in the soil herbicide concentration (ng g^{-1}) as independent variable (*x*). From these models, herbicide concentration threshold values were established for a 25% plant damage and 25% decrease in plant density for carinata. This percent was arbitrarily chosen because it is within the range of tolerable density reductions without impacting yield (Mulvaney et al. 2019) and plants suffering 25% damage tend to recover to levels similar to the nontreated (Leon et al. 2017).

All regression models were fitted using the package *easynls* in R Studio R version 4.0.4 (2021-02-15) “Lost Library Book” (R Studio Team 2015), and further optimized using PROC NLIN in SAS.

Results

Total herbicide recovery from soils for imazapic and flumioxazin

When imazapic or flumioxazin were applied at 12 and 18 MBP, recovered herbicide amounts from both location soils were < 2% of the corresponding total applied (i.e., the herbicide recommended doses 1X). As the application interval decreased to 6 and 3 MBP, the recovery values in the soil profile increased for both herbicides, and vertical movement was observed with imazapic reaching deeper layers within the soil than flumioxazin at 3 and 6 MBP (**Table 4.1**). This vertical movement was more evident in the sandy soil from Jackson Springs, where imazapic was detected between 15 and 20 cm depth, and recovered amounts were 7.96 ± 2.12 % and 3.61 ± 0.67 %, for 3 and 6 MBP, respectively (**Table 4.1**). Conversely, flumioxazin remained in the top 5 cm of soil, with a small movement down to 10 cm depth as observed for 3 and 6 MBP in both locations. In the loamy sand at Clayton, flumioxazin residues at 5 - 10 cm soil depth were 2.08 ± 0.81% 3 MBP and 3.05 ± 0.39 % 6 MBP. Meanwhile flumioxazin recovery in Jackson Springs ranged from 3.90 ± 0.43 % to 2.14 ± 0.59% for 3 and 6 MBP, respectively (**Table 4.1**).

Carryover herbicide effects on *B. carinata* under field and greenhouse conditions

The carryover of imazapic and flumioxazin on carinata reduced plant density under field conditions but only in a few treatments (**Figure 4.1**). Carinata exhibited self-thinning evidenced as a marked reduction in plant density during the three evaluation dates even in the nontreated control. This reduction was more evident in Clayton, where plant density was less than 40 plants m^{-1} for both herbicides after 103 days after planting (DAP).

Flumioxazin applied 0 MBP in both Clayton and Jackson Springs (assessed 30 DAP) presented the lowest plant density, 0.33 ± 0.33 and 8 ± 6.11 plants m^{-1}, respectively, which were

considerably lower than the corresponding nontreated control (62.25 ± 5.80 plants m^{-1} in Clayton and 67.75 ± 7.13 plants m^{-1} in Jackson Springs; Dunnett test $p < 0.0001$). Interestingly, 27 days later (57 DAP), it was observed that imazapic presented the same behavior as flumioxazin in both locations. Thus, both herbicides applied at 0 MBP exhibited the lowest carinata density (**Figure 4.1**) after two months with values < 5.00 plants m^{-1} (both Jackson Springs and Clayton) for flumioxazin, and 8.00 ± 4.35 and 6.66 ± 2.72 plants m^{-1} (Jackson Springs and Clayton, respectively) for imazapic. Those crop densities represented considerable reductions compared with their respective nontreated controls (53.25 ± 3.04 plants m^{-1} in Clayton and 54.25 ± 6.53 plants m^{-1} in Jackson Springs; Dunnett test $p < 0.0001$). Also, it was observed that when imazapic or flumioxazin were applied 3 MBP or at longer intervals, plant density values did not differ from the nontreated control, regardless of location (**Figure 4.1**).

In addition to plant density, herbicide carryover effects on carinata injury were also assessed under greenhouse conditions (**Figure 4.2**). The highest values for plant damage were observed for both herbicides when they were applied at 0 MBP, regardless of location. In Clayton, imazapic and flumioxazin caused 48 ± 4 % and 31 ± 6 % damage, respectively. Meanwhile, in Jackson Springs for these same herbicides damage assessed for 0 MBP was 59 ± 10 % and 60 ± 13 %, respectively (**Figure 4.2**).

Plant damage decreased with the increment in the time interval between application and planting for both herbicides and location. This behavior was described using quadratic plateau regression models, which R^2 ranged from 0.40 to 0.58 for flumioxazin, and 0.50 to 0.64 for imazapic (**Table 4.2**). Our results allowed identifying critical preplant intervals for application, so carinata would not be negatively affected by herbicide residues. For example, carinata density remained high and stable when the herbicides assessed were applied > 6 MBP, in both locations

(**Figure 4.2**). In Clayton, the preplant interval to avoid a 25 % damage by imazapic or flumioxazin was 6 MBP, while in Jackson Springs it was 12 MBP (**Figure 4.2**).

Preemergence herbicide doses effects on *B. carinata* under field and greenhouse conditions

Except for imazapic assessed 30 DAP in both locations, there was a decrease in carinata density as herbicide dose increased for both herbicides (**Figure 4.3**). Unlike flumioxazin, imazapic effect on plant density was evident only until 57 DAP in both locations, clearly showing that imazapic effect on carinata plants is slower than that of flumioxazin. This decreasing trend in plant density in response to herbicide dose was best described with quadratic plateau regression models, with R^2 ranging from 0.80 to 0.90 for flumioxazin, and 0.52 to 0.78 for imazapic (**Table 4.3**). These regression models included the critical inflection point indicating the dose above which, plant density reached a maximum and did not change with further increases in herbicide dose. For instance, in Jackson Springs at 57 DAP, the critical doses for imazapic and flumioxazin were 48.3 g ai ha^{-1} (0.69X) and 21.4 g ai ha^{-1} (0.20X), respectively. The critical values in Clayton were 14.7 g ai ha^{-1} (0.21X) and 18.19 g ai ha^{-1} (0.17X) for imazapic and flumioxazin, respectively at this same evaluation date (**Figure 4.3**). However, even at the lowest evaluated dose (6.68 and 4.38 g ai ha^{-1} for imazapic and imazapic, respectively), both herbicides caused 50 - 60% reductions in plant density compared with the nontreated control (**Figure 4.3**).

Carinata damage increased exponentially as dose increased for both herbicides (**Figure 4.4**) until reaching a point in which further increments did not change damage. Regression models fitted to describe this pattern presented R^2 values from 0.69 to 0.36 for imazapic, and for flumioxazin from 0.57 to 0.36 (**Table 4.4**). Herbicide dose to reach an arbitrary threshold of 25 % damage were 5.25 and 6.30 g ai ha^{-1} (0.075X and 0.09X) for imazapic in Clayton and Jackson

Springs, respectively. Meanwhile, for flumioxazin the thresholds were 5.35 and 10.70 g ai ha^{-1} (0.05X and 0.10X) for Clayton and Jackson Springs, respectively (**Figure 4.4**).

Herbicide residue levels for injury and survival thresholds in *B. carinata*

As concentration of herbicide residues recovered from the soil (ng g^{-1}) increased, there was a corresponding increase in plant damage for both imazapic and flumioxazin (**Figure 4.5**). Regression models fitted to describe this pattern in plant damage presented R^2 values of 0.42 and 0.35 for imazapic and flumioxazin, respectively. Using these models, it was estimated that the minimum value concentration to cause 25 % plant damage was 7.78 and 6.90 ng g^{-1} for imazapic and flumioxazin, respectively.

This same approach was performed to identify herbicide concentration thresholds that would decrease carinata density by 25 % compared with the nontreated control. The corresponding regression models fitted to describe this decrease in plant density, presented R^2 values of 0.36 and 0.39 for imazapic and flumioxazin, respectively (**Figure 4.6**). For flumioxazin, it was estimated that at 12.7 ng g^{-1}, the plant density will drop from 43 to 33 plant m^{-1} (corresponding to 25% decrease in plant density). Meanwhile, this threshold corresponded to 14.7 ng g^{-1} for imazapic (**Fig 4.6**).

Discussion

Imazapic and flumioxazin movement and behavior in soils

The herbicides from the imidazolinone family are very persistent in the soil and under optimum conditions they can remain in the soil for extended periods ranging from 371 to 705 days after application (Marchesan et al. 2010). Imazapic has been described as a highly persistent herbicide in soils, with slow rates of degradation and minimal volatilization (Aichele and Penner 2005; Ulbrich et al. 2005).

Furthermore, the soil adsorption affinity (expressed as K_d) for imazapic ranged from 0.23 to 0.10 in soils with textural classes ranging from clay to loamy sand (Goldwasser et al. 2021). In weathered soils from Brazil (Ultisols and Oxisols), reported K_d for imazapic was 0.25 to 0.052 for sandy clay loam and loamy sand, respectively (de Assis et al. 2021). These low K_d values added to high solubility (2150 mg L^{-1}) make possible imazapic downward movement into the soil profile deeper than flumioxazin, especially under coarse-textured soils with low organic matter content (Neto et al. 2017; de Assis et al. 2021), as observed in our results of herbicide recovery from soils in Jackson Springs (sand textured soil). Conversely, flumioxazin has higher adsorption affinity when compared with imazapic. For instance, K_d values of 3.8 to 0.4 have been reported for soils with textural classes ranging from sandy clay loam to loamy sand (Ferrell and Vencill 2003). In addition, flumioxazin presents lower mobility within the soil, with a tendency to remain in the first 5 cm within the soil surface (Chen et al. 2021). Furthermore, its persistence in the soil is considerably lower than that reported for imazapic (Ferrell and Vencill 2003; Alister et al 2008). Flumioxazin degradation rate is affected by temperature, soil moisture and organic matter (OM), influencing microorganism activity, which is critical for the stability of this herbicide in the soil (Ferrell and Vencill 2003; Chen et al. 2021). As microbial activity increases, flumioxazin's half-life and persistence decrease.

Herbicide carryover risk, soil residues and further implications for carinata

Carinata crop stands under field conditions exhibited a decreasing trend during the three evaluations performed after planting. This behavior has been previously described for this plant species as "self-thinning" due to intraspecific competition among the emerged plants (Mulvaney et al. 2019; Seepaul et al. 2021). Reductions in population density are not necessarily a major problem for production because carinata has a high degree of compensatory ability to deal with

changes in density by modifying the level of branching of the plant. Thus, maximum yield can be achieved under a variety of plant densities (Seepaul et al. 2021). High densities will have more plants with less branching and inflorescences, while low densities will exhibit fewer plants with abundant branching and reproductive structures. Therefore, as long as growers use high planting densities, yield goals can still be achieved even if there is some level of reduction in carinata crop stand resulting from herbicide carryover. However, it is the combined effect of herbicides on plant density and plant damage, what represents the highest risk to production as observed for imazapic in other rotational crops in southeastern U.S. (York et al. 2000) and Brazil (Ulbrich et al. 2005). Imazapic residues its corresponding concentration thresholds for plant damage and reduction in plant density in the present study were similar to those reported in the literature for yield reductions in cotton with other herbicides of the imidazolinone family such as imazaquin (Barnes et al. 1989).

These results have implications for carinata crop management. For instance, if carinata is planted at a low density, although there might be good crop establishment early on, negative effects on plant growth can occur later during the growing season. This scenario is likely to occur due to: 1) the persistence and mobility reported for the ALS-inhibitor herbicide family (Marchesan et al. 2010; de Assis et al. 2021), 2) subsequent root growth and interception of the metabolite at deeper soil positions (Souza et al. 2020), and 3) the slow rate of the mechanism of action which must first deplete amino acid seed reserves before symptoms of herbicide toxicity affect the plant (Webster and Masson 2001). This might explain why, unlike flumioxazin, reductions in plant density due imazapic were not observed at 30 DAP but at 57 DAP.

Flumioxazin is a protoporphyrinogen oxidase (PPO) inhibiting preemergence herbicide. This mechanism of action is the result of the inhibition of the enzyme responsible for

protoporphyrin (Proto) synthesis, leading to an uncontrolled accumulation of Proto and further blocking synthesis of chlorophylls and heme (Duke et al. 1991). Because this pathway involves photodynamic compounds, this herbicide effect is more likely to occur during the first 3 weeks after the application (Leon et al. 2017; Glaspie et al. 2021), which was faster than that observed for imazapic when applied into the same soils and at the same doses (**Figure 4.3**).

Practical considerations for imazapic and flumioxazin use in carinata cropping systems

Some practical implications that can be taken from our results are the consideration of divergent behavior, persistence, and mobility of imazapic and flumioxazin when assessing plant damage and carryover effects on carinata. For instance, if a bioassay is intended to determine if the residues of imidazolinone herbicides are low enough to ensure safe carinata planting, it is crucial to consider soil properties and sampling depth (Horowitz 1976; Winton and Weber 1996). For example, if imazapic was applied previously in a sandy soil, planting bioindicators and determining safety just based on the number of emerged seedlings could be misleading because of the vertical movement of this herbicide in the soil. A better approach would be to collect soils from different depths and running the bioassay with those different soil depths.

Imazapic and flumioxazin are registered for preemergence control of dicotyledoneous weed species in soybean, peanut, and cotton, and their use in the southeastern U.S. has been both extensive and intensive (Ferrell and Vencill 2003; Matocha et al. 2003; Berger et al. 2012). Therefore, if carinata is incorporated as a winter crop to an existing peanut–cotton rotation, selection of the appropriate preemergence herbicide will be critical to avoid herbicide carryover issues as those described in the present study. For instance, the risk of carinata damage and reductions in plant density would be lower if flumioxazin was employed as the preemergence herbicide during the peanut or cotton cycle in the previous spring-summer season. This type of

rotational consideration has been used to ensure the safety other Brassicaceae species. For example, daikon radish (*Raphanus sativus* L.) planted as a cover crop was affected by residual herbicides in peanut-cotton rotations, but imazapic reduced plant height more than flumioxazin (Price et al. 2020).

Soil properties should be also considered when selecting the proper herbicides as part of a well-designed crop rotation. For example, flumioxazin persistence in soil is highly dependent on OM and water content, which are directly involved in the microbial-mediated degradation of this herbicide (Chen et al. 2021; Glaspie et al. 2021). In addition, soil texture plays a role on sorption to soil particles and herbicide bioavailability. As the clay fraction increases, the herbicide binds to clay, and its availability for microbial decomposition and mineralization decreases. Therefore, there will be considerable differences among sandy clay loam, loam, and sandy loam soils for flumioxazin persistence (Ferrell and Vencill 2003). Conversely, a loamy sand or sandy soil with low OM content will propitiate suitable conditions for persistence of imidazolinone herbicides such as imazapic (Marchesan et al. 2010).

Therefore, when planning to grow carinata as a winter crop after rotational cotton or peanut, it is important to address both soil physical-chemical properties as well as herbicide behavior in soil. Our results provide a baseline for residue levels and application intervals that can be used to determine the risk to carinata of flumioxazin and imazapic carryover in sand or loamy sand textured soils. We encourage to extend this approach to areas with finer textured soils (loam, silty loam, clay loam) and further research development. It is important to caution that the present study focused on carinata seedling establishment. It will be necessary to confirm the safety of residue levels identified here during the entire growing season to make sure that yield is not adversely affected.

Conclusions

Carinata has been recently introduced as an alternative winter crop in the southeastern USA show promise to diversify crop rotations. However, concerns among growers about the risk of carryover of commonly used residual herbicides have hampered the adoption of this crop.

In sand and loamy sand soils, imazapic was more persistent and moved to deeper layers within the soil representing a risk to carinata plants even when applied 6 MBP or at shorter intervals. Our results suggested that carinata can be planted safely if either imazapic or flumioxazin were applied at a 12 MBP interval or longer. When a peanut–cotton rotation incorporates carinata as winter crop, special caution must be taken to identify edaphic conditions as well as preemergence herbicide selection to avoid herbicide carryover and damage to carinata. Based on our results, the use of flumioxazin as a preemergence herbicide in the preceding summer crop is a better alternative than imazapic to ensure carinata safety. Although, fields should be safe to grow carinata after 12 months of imazapic treatment.

Founding

Present research was supported by the U.S. Department of Agriculture–National Institute of Food and Agriculture grant 2017-6505- 26807 and by Hatch Projects FLA-WFC-005843, FLA-WFC-005953, and NC02653. A special gratitude goes to Southeast Partnership for Advanced Renewables from Carinata (SPARC).

Acknowledgements

The authors would like to thank Adam Howard for his valuable help with soil physical analyses, Dr. Theresa Reinhardt Piskackova, Sandy Ethridge, and Alyssa Zsido for technical assistance during the crop establishment and treatment applications. Also, our gratitude goes to Ashley Pouncey, Alex Veverka and Haley Woolard for their support and help with the greenhouse bioassay and soil samples preparation.

In a very special way, we thank Daniel Freund and Khalied Ahmed for their assistance and invaluable advises and help with the sampling homogenization and the pesticide residue analysis.

This project wouldn't be possible without Dr. Alan J. Franzluebbers help, who kindly lent us the hydraulic probe equipment. We appreciate your goodwill.

Literature cited

Aichele, T.M., Penner, D. 2005. Adsorption, desorption, and degradation of imidazolinones in soil. Weed Technology 19(1): 154-159. https://doi.org/10.1614/WT-04-057R

Alister, C., Rojas, S., Gómez, P., Kogan, M. 2008. Dissipation and movement of flumioxazin in soil at four field sites in Chile. Pest Management Science 64(5): 579-583. https://doi.org/10.1002/ps.1533

Barnes, C.J., Goetz, A.J., Lavy, T.L. 1989. Effects of imazaquin residues on cotton (*Gossypium hirsutum*). Weed Science 37(6): 820-824. https://doi.org/10.1017/S0043174500072908

Berger, S., Ferrell, J., Brecke, B., Faircloth, W., Rowland, D. 2012. Influence of flumioxazin application timing and rate on cotton emergence and yield. Weed Technology 26(4): 622-626. https://doi.org/10.1614/WT-D-12-00044.1

Bridges, D.C. 1994. Impact of weeds on human endeavors. Weed Technology 8(2): 392-395. https://doi.org/10.1017/S0890037X00038987

Cardone, M., Mazzoncini, M., Menini, S., Rocco, V., Senatore, A., Seggiani, M., Vitolo, S. 2003. *Brassica carinata* as an alternative oil crop for the production of biodiesel in Italy: agronomic evaluation, fuel production by transesterification and characterization. Biomass and Bioenergy 25(6): 623-636. https://doi.org/10.1016/S0961-9534(03)00058-8

Chen, Y., Han, J., Chen, D., Liu, Z., Zhang, K., Hu, D. 2021. Persistence, mobility, and leaching risk of flumioxazin in four Chinese soils. Journal of Soils and Sediments 21(4): 1743-1754. https://doi.org/10.1007/s11368-021-02904-3

de Assis, F.X., Maciel, A., Xavier, B.T.D. L., Lima, V.F.D., Silva, J.P.S.D. 2021. Imazapic interaction and mobility in soil cultivated with sugarcane in northeast Brazil. Revista Brasileira de Recursos Hídricos 26 e16. https://doi.org/10.1590/2318-0331.262120210007

Duke, S.O., Lydon, J., Becerril, J.M., Sherman, T.D., Lehnen, L.P., Matsumoto, H. 1991. Protoporphyrinogen oxidase-inhibiting herbicides. Weed Science 39(3): 465-473. https://doi.org/10.1017/S0043174500073239

Ethridge, S.R., Post, A., Devkota, P., Mulvaney, M.J., Leon, R.G. 2021. Characterization of carinata tolerance to select herbicides using field dose-response studies. Weed Technology 1-10. https://doi.org/10.1017/wet.2021.57

Ferrell, J.A., Vencill, W.K. 2003. Flumioxazin soil persistence and mineralization in laboratory experiments. Journal of Agricultural and Food Chemistry 51(16): 4719-4721. https://doi.org/10.1021/jf0342829

Gasol, C.M., Gabarrell, X., Anton, A., Rigola, M., Carrasco, J., Ciria, P., Rieradevall, J. 2007. Life cycle assessment of a *Brassica carinata* bioenergy cropping system in southern Europe. Biomass and Bioenergy 31(8): 543-555. https://doi.org/10.1016/j.biombioe.2007.01.026

Glaspie, C.F., Jones, E.A.L., Penner, D., Pawlak, J.A., Everman, W.J. 2021. Effect of clay, soil organic matter, and soil pH on initial and residual weed control with flumioxazin. Agronomy 11(7): 1326. https://doi.org/10.3390/agronomy11071326

Goldwasser, Y., Rabinovitz, O., Gerstl, Z., Nasser, A., Paporisch, A., Kuzikaro, H., Rubin, B. 2021. Imazapic herbigation for Egyptian broomrape (*Phelipanche aegyptiaca*) control in processing tomatoes—laboratory and greenhouse studies. Plants 10(6): 1182. https://doi.org/10.3390/plants10061182

Heap, I. 2014. Global perspective of herbicide-resistant weeds. Pest Management Science 70(9): 1306-1315. https://doi.org/10.1002/ps.3696

Hollaway, K.L., Kookana, R.S., Noy, D.M., Smith, J.G., Wilhelm, N. 2006. Crop damage caused by residual acetolactate synthase herbicides in the soils of south-eastern Australia. Australian Journal of Experimental Agriculture 46(10): 1323-1331. https://doi.org/10.1071/EA05053

Horowitz, M. 1976. Application of bioassay techniques to herbicide investigations. Weed Research 16(4): 209-215. https://doi.org/10.1111/j.1365-3180.1976.tb00404.x

Johnson III, W.C., Brenneman, T.B., Baker, S.H., Johnson, A.W., Sumner, D.R., Mullinix Jr, B. G. 2001. Tillage and pest management considerations in a peanut–cotton rotation in the southeastern Coastal Plain. Agronomy Journal 93(3): 570-576. https://doi.org/10.2134/agronj2001.933570x

Kumar, S., Seepaul, R., Mulvaney, M.J., Colvin, B., George, S., Marois, J.J. Small, I.M. 2020. *Brassica carinata* genotypes demonstrate potential as a winter biofuel crop in South East United States. Industrial Crops and Products 112353. https://doi.org/10.1016/j.indcrop.2020.112353

Kumar, A., Singh, P., Singh, D. P., Singh, H., Sharma, H. C. 1984. Differences in osmoregulation in *Brassica* species. Annals of Botany 54(4): 537-542. https://doi.org/10.1093/oxfordjournals.aob.a086824

Leon, R.G., Ferrell, J.A., Mulvaney, M.J. 2017. Carinata tolerance to preemergence and postemergence herbicides. Weed Technology 31(6): 877-882. https://doi.org/10.1017/wet.2017.62

Marchesan, E., dos Santos, F.M., Grohs, M., de Avila, L.A., Machado, S.L., Senseman, S.A., Massoni, P.F.S., Sartori, G.M. 2010. Carryover of imazethapyr and imazapic to nontolerant rice. Weed Technology 24(1): 6-10. https://doi.org/10.1614/WT-08-153.1

Martínez-Lozano, S., Gasol, C.M., Rigola, M., Rieradevall, J., Anton, A., Carrasco, J., Gabarrell, X. 2009. Feasibility assessment of *Brassica carinata* bioenergy systems in Southern Europe. Renewable Energy 34(12): 2528-2535. https://doi.org/10.1016/j.renene.2009.05.023

Matocha, M.A., Grichar, W.J., Senseman, S.A., Gerngross, C.A., Brecke, B.J., Vencill, W.K. 2003. The persistence of imazapic in peanut (*Arachis hypogaea*) crop rotations. Weed Technology 17(2): 325-329. https://doi.org/10.1614/0890-037X(2003)017[0325:TPOIIP]2.0.CO;2

Mulvaney, M.J., Leon, R.G., Seepaul, R., Wright, D.L., Hoffman, T.L. 2019. *Brassica carinata* seeding rate and row spacing effects on morphology, yield, and oil. Agronomy Journal 111(2): 528-535. https://doi.org/10.2134/agronj2018.05.0316

Neto, M.D.D.C., Souza, M.D.F., Silva, D.V., Faria, A.T., da Silva, A.A., Pereira, G.A.M., de Freitas, M.A.M. 2017. Leaching of imidazolinones in soils under a Clearfield system. Archives of Agronomy and Soil Science 63(7): 897-906. https://doi.org/10.1080/03650340.2016.1249471

Palhano, M.G., Norsworthy, J.K., Barber, T. 2018. Sensitivity and likelihood of residual herbicide carryover to cover crops. Weed Technology 32(3): 236-243. https://doi.org/10.1017/wet.2018.7

Price, K.J., Li, X., Price, A. 2020. Cover crop response to residual herbicides in peanut-cotton rotation. Weed Technology 34(4): 534-539. https://doi.org/10.1017/wet.2020.5

R Studio Team. 2015. R Studio: integrated development for R. R Studio, Inc., Boston Available in http://www.rstudio.com/. Accessed 30 August 2021.

Rahman, M., Khatun, A., Liu, L., Barkla, B.J. 2018. Brassicaceae mustards: traditional and agronomic uses in Australia and New Zealand. Molecules 23(1): 231. https://doi.org/10.3390/molecules23010231

Rakow, G., Getinet, A. 1997. *Brassica carinata* an oilseed crop for Canada. *In* International Symposium Brassica 97, Xth Crucifer Genetics Workshop 459 (pp. 419-428).

Raman, R., Qiu, Y., Coombes, N., Song, J., Kilian, A., Raman, H. 2017. Molecular diversity analysis and genetic mapping of pod shatter resistance loci in *Brassica carinata* L. Frontiers in Plant Science 8: 1765. https://doi.org/10.3389/fpls.2017.01765

Rector, L.S., Pittman, K.B., Beam, S.C., Bamber, K.W., Cahoon, C.W., Frame, W.H., Flessner, M.L. 2020. Herbicide carryover to various fall-planted cover crop species. Weed Technology 34(1): 25-34. https://doi.org/10.1017/wet.2019.79

Seepaul, R., Kumar, S., Iboyi, J.E., Bashyal, M., Stansly, T.L., Bennett, R., Wright, D.L. 2021. *Brassica carinata*: Biology and agronomy as a biofuel crop. GCB Bioenergy 13(4): 582-599. https://doi.org/10.1111/gcbb.12804

Souza, A.D.S., Leal, J.F.L., Langaro, A.C., Carvalho, G.S.D., Pinho, C.F.D. 2020. Leaching and carryover for safrinha corn of the herbicides imazapyr+ imazapic in soil under different water conditions. Revista Caatinga 33 (2): 287-298. https://doi.org/10.1590/1983-21252020v33n202rc

Thakur, A.K., Singh, K.H., Sharma, D., Parmar, N., Nanjundan, J. 2019. Breeding and genomics interventions in Ethiopian mustard (*Brassica carinata* A. Braun) improvement–A mini review. South African Journal of Botany 125: 457-465. https://doi.org/10.1016/j.sajb.2019.08.002

Topp, G.C., Ferré, P.A. 2002. 3.1 Water Content. In: J.H. Dame, G.C. Topp (Eds.), Methods of Soil Analysis, Part 4 – Physical Methods. Soil Science Society of America. Madison, Wisconsin, USA, pp. 417-545. https://doi.org/10.2136/sssabookser5.4.c19

Ulbrich, A.V., Souza, J.R.P., Shaner, D. 2005. Persistence and carryover effect of imazapic and imazapyr in Brazilian cropping systems. Weed Technology 19(4): 986-991. https://doi.org/10.1614/WT-04-208R2.1

Webster, E.P., Masson, J.A. 2001. Acetolactate synthase-inhibiting herbicides on imidazolinone-tolerant rice. Weed Science 49(5): 652-657. https://doi.org/10.1614/0043-1745(2001)049[0652:ASIHOI]2.0.CO;2

Winton, K., Weber, J.B. 1996. A review of field lysimeter studies to describe the environmental fate of pesticides. Weed Technology 10(1): 202-209. https://doi.org/10.1017/S0890037X00045929

Yang, B., Rahman, M.H., Liang, Y., Shah, S., Kav, N.N. 2010. Characterization of defense signaling pathways of *Brassica napus* and *Brassica carinata* in response to *Sclerotinia sclerotiorum* challenge. Plant Molecular Biology Reporter 28(2): 253-263. https://doi.org/10.1007/s11105-009-0149-5

York, A.C., Jordan, D.L., Batts, R.B., Culpepper, A.S. 2000. Cotton response to imazapic and imazethapyr applied to a preceding peanut crop. Journal of Cotton Science 4: 210-216.

Zanetti, F., Monti, A., Berti, M. T. 2013. Challenges and opportunities for new industrial oilseed crops in EU-27: A review. Industrial Crops and Products 50: 580-595. https://doi.org/10.1016/j.indcrop.2013.08.030

Tables

Table 4.1 Effect of the herbicide application interval before carinata planting on total recovery of two herbicides in soils from two locations of North Carolina.

Location	Herbicide	Depth (cm)	Recovery of the total applied (%)*									
			0 MBP†		3 MBP		6 MBP		12 MBP		18 MBP	
Clayton	Flumioxazin	0 – 5	79.34	B‡	4.15	HI	1.77	I	0.00	I	0.00	I
		5 – 10	0.00	I	2.08	I	3.05	HI	0.03	I	0.00	I
		10 – 15	0.00	I	0.00	I	0.01	I	0.00	I	0.00	I
		15 – 20	0.00	I	0.00	I	0.00	I	0.00	I	0.00	I
	Imazapic	0 – 5	93.72	A	23.86	E	8.74	GHI	0.46	I	0.00	I
		5 – 10	1.81	I	32.86	D	11.50	FGH	1.88	I	0.00	I
		10 – 15	0.00	I	0.70	I	1.65	I	1.15	I	0.28	I
		15 – 20	0.00	I	0.00	I	0.00	I	0.13	I	0.00	I
Jackson Springs	Flumioxazin	0 – 5	57.67	C	4.10	HI	2.28	I	0.00	I	0.00	I
		5 – 10	19.71	EF	3.90	HI	2.14	I	0.05	I	0.00	I
		10 – 15	0.00	I	0.17	I	0.05	I	0.00	I	0.00	I
		15 – 20	0.00	I	0.00	I	0.00	I	0.00	I	0.00	I
	Imazapic	0 – 5	73.28	B	8.49	GHI	1.42	I	0.48	I	0.00	I
		5 – 10	18.33	EF	14.35	FG	3.67	HI	0.91	I	0.00	I
		10 – 15	2.13	I	13.09	FG	3.30	HI	1.79	I	0.15	I
		15 – 20	0.00	I	7.96	GHI	3.61	HI	0.70	I	0.14	I

* Percent of nominal application rates for each herbicide: 70 and 107 g ai ha^{-1} for imazapic and flumioxazin, respectively.

† MBP: Months before planting carinata.

‡ Means followed by same letter are not significantly different according to Bonferroni test ($p < 0.05$).

Table 4.2 Regression model and fit parameters to predict carinata damage in response to interval between applications and planting. Regression model fit was quadratic plateau.

Location	Herbicides	a	b	c	R^2	F	pr > F	AIC‡
Clayton	Imazapic	49.67 ± 6.11†	-6.62 ± 1.17	0.09 ± 0.08	0.50	7.2	0.0042	198.41
	Flumioxazin	31.94 ± 3.48	-1.81 ± 0.27	0.04 ± 0.01	0.40	10.49	0.0007	184.54
Jackson Springs	Imazapic	55.70 ± 5.30	-4.33 ± 0.40	0.09 ± 0.01	0.64	17.58	<0.0001	194.56
	Flumioxazin	60.95 ± 8.34	-10.06 ± 1.61	0.46 ± 0.11	0.58	14.38	0.0001	213.38

Quadratic plateau: y = (a + b * x + c * (x^2)) * (x <= -0.5 * b/c) + (a + (-b^2/(4 * c))) * (x > -0.5 * b/c)"

† Model parameter ± standard error

‡ Akaike information criterion (AIC)

Table 4.3 Regression model and fit parameters to predict carinata density in response to herbicide dose in two North Carolina locations. Regression model fit was quadratic plateau.

Evaluation	Location	Herbicides	a	b	c	R^2	F	pr > F	AIC‡
30 DAP	Clayton	Imazapic**							
		Flumioxazin	60.37 ± 4.97†	-523.60 ± 69.44	1171.80 ± 73.49	0.82	46.82	<0.00001	179.47
	Jackson Springs	Imazapic**							
		Flumioxazin	66.09 ± 4.76	-332.40 ± 46.02	469.20 ± 64.08	0.80	41.22	<0.00001	183.20
57 DAP	Clayton	Imazapic	50.84 ± 4.01	-379.80 ± 55.87	886.00 ± 58.16	0.78	34.64	<0.0001	169.63
		Flumioxazin	53.05 ± 3.21	-604.00 ± 44.02	1743.40 ± 42.74	0.90	88.56	<0.0001	159.45
	Jackson Springs	Imazapic	44.99 ± 4.22	-101.10 ± 33.54	73.17 ± 78.48	0.52	10.63	0.0007	188.77
		Flumioxazin	53.52 ± 4.42	-491.70 ± 61.09	1253.80 ± 61.56	0.80	40.61	<0.0001	174.43
103 DAP	Clayton	Imazapic	24.24 ± 3.06	-176.70 ± 42.93	370.10 ± 46.73	0.62	16.23	<0.0001	157.08
		Flumioxazin	27.15 ± 2.24	-303.50 ± 30.76	861.20 ± 30.01	0.83	47.52	<0.0001	142.91
	Jackson Springs	Imazapic	52.50 ± 6.91	-1097.10 ± 162.50	8082.30 ± 141.10	0.54	11.98	0.0004	190.90
		Flumioxazin	52.50 ± 4.13	-947.80 ± 98.29	4669.40 ± 88.30	0.84	53.8	<0.0001	167.17

Quadratic plateau: y = (a + b * x + c * (x^2)) * (x <= -0.5 * b/c) + (a + (-b^2/(4 * c))) * (x > -0.5 * b/c)

** Indicates that no regression model presented good fit for this data

† Model parameter ± standard error

‡ Akaike information criterion (AIC)

Table 4.4 Regression model and fit parameters to estimate carinata damage in response to herbicide dose when applied preemergence. Regression model fit was quadratic plateau.

Location	Herbicides	a	b	c	R^2	F	pr > F	AIC‡
Clayton	Imazapic	6.14 ± 4.01†	299.67 ± 35.94	-590.05 ± 44.47	0.69	23.66	<.0001	183.90
	Flumioxazin	5.63 ± 7.12	597.70 ± 168.90	-3323.24 ± 148.60	0.36	5.71	0.0109	192.23
Jackson Springs	Imazapic	7.24 ± 8.83	232.86 ± 85.96	-320.10 ± 120.00	0.36	6.48	0.0064	220.55
	Flumioxazin	-1.41 ± 9.70	289.08 ± 108.60	-321.81 ± 176.80	0.57	13.42	0.0002	214.23

Quadratic plateau: y = (a + b * x + c * (x^2)) * (x <= -0.5 * b/c) + (a + (-b^2/(4 * c))) * (x > -0.5 * b/c)"

† Model parameter ± standard error

‡ Akaike information criterion (AIC)

Figures

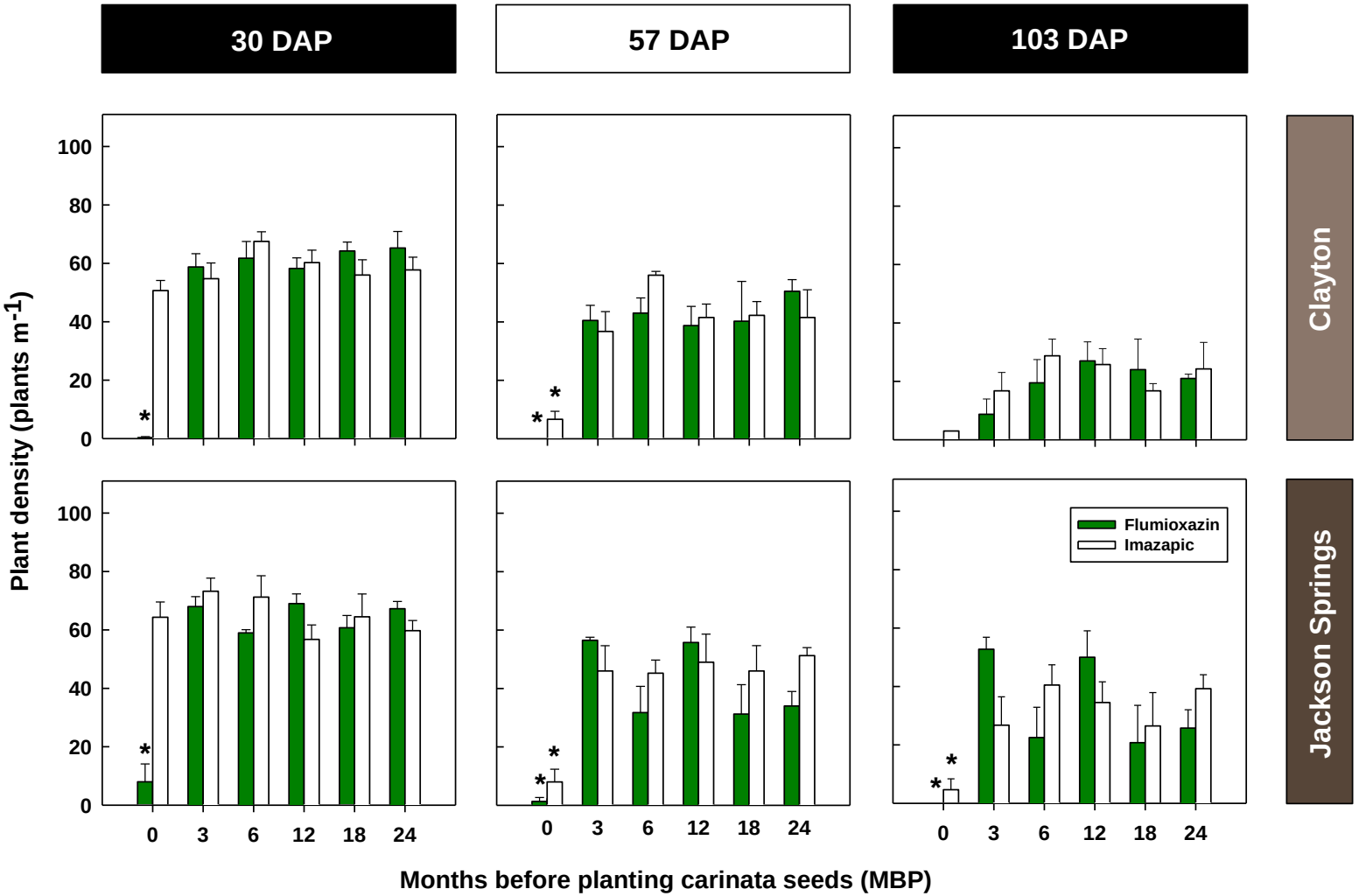

Figure 4.1 Carinata population density in response to application interval before planting for two herbicides in *B. carinata* in two locations of North Carolina. The evaluations were done 30, 57, and 103 days after carinata planting (DAP). Error bars represent the standard error of the mean (n=4). * Indicates significant differences with the control without herbicide, according with Dunnett-Test (p-value < 0.05).

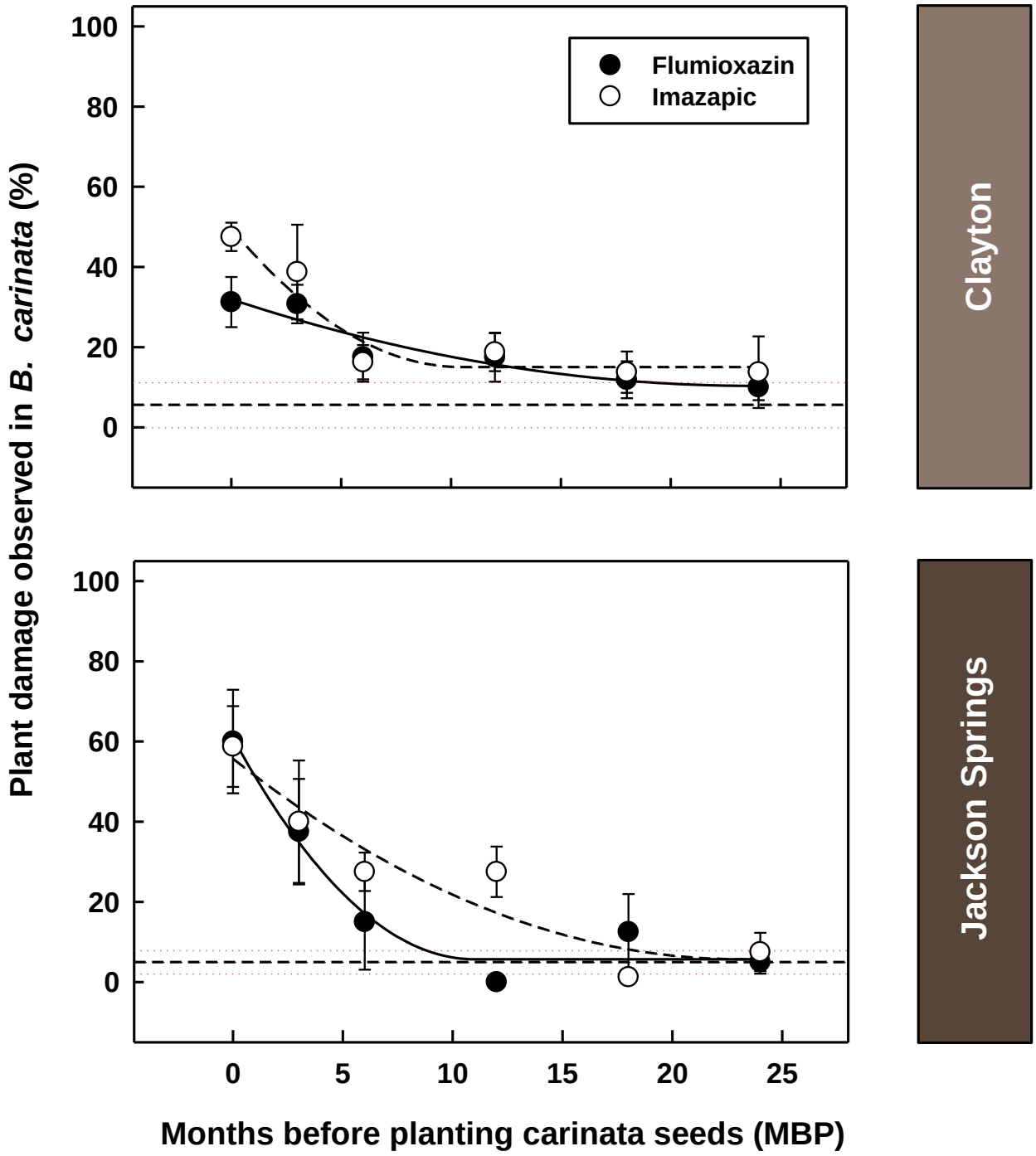

Figure 4.2 Plant damage at different soil depths in soil cores collected from two locations of North Carolina in response to application interval before carinata planting for two herbicides in *B. carinata*. Black solid and discontinuous lines represent the best-fit model for imazapic and flumioxazin, respectively. Error bars represent the standard error of the mean (n=4). Continuous red lines indicate the average plant damage observed in the control treatment and discontinuous red lines represent standard error.

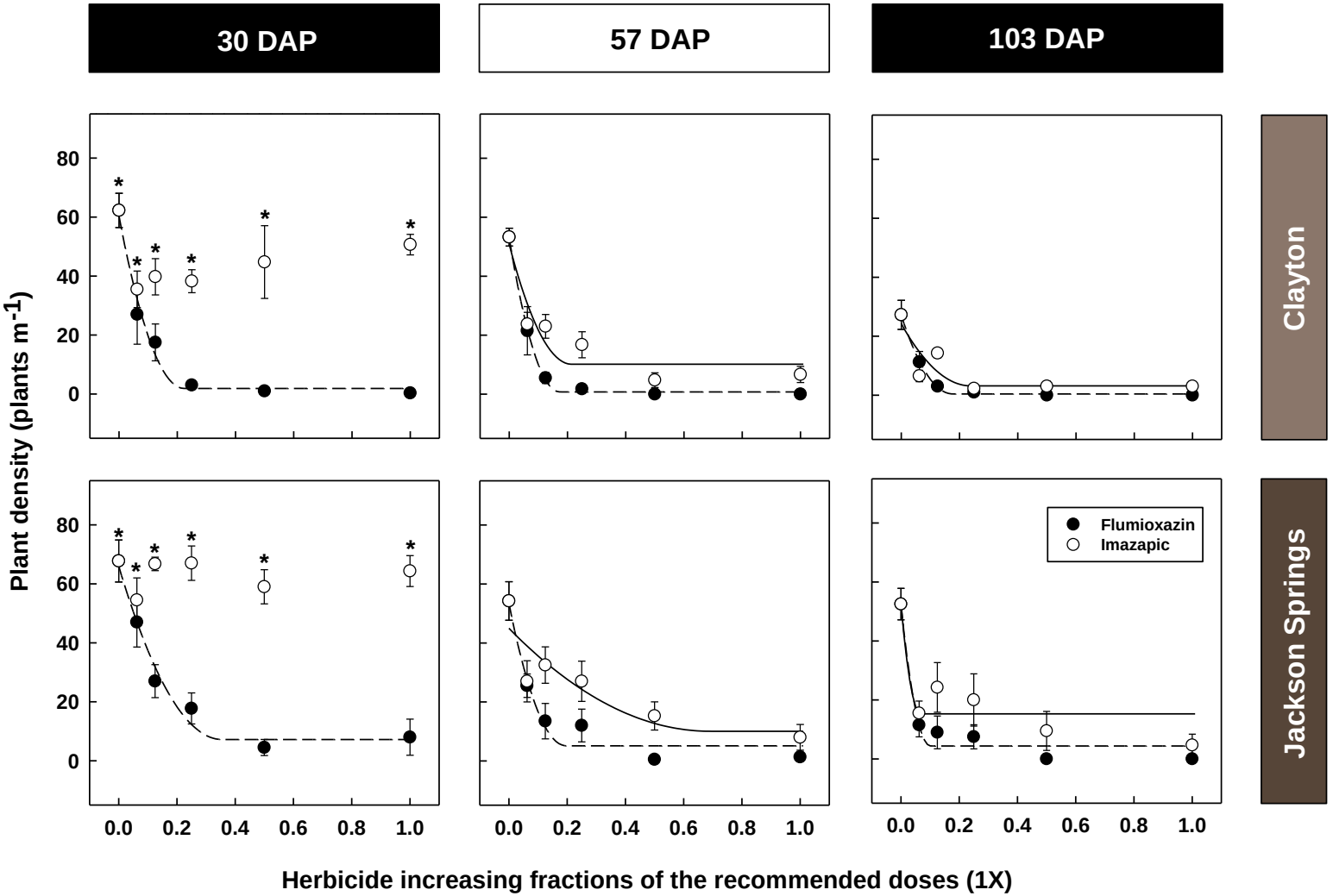

Figure 4.3 Effect of increasing doses of two herbicides on *B. carinata* population evaluated in two locations of North Carolina. Black solid and discontinuous lines represent the best-fit model for imazapic and flumioxazin, respectively. The evaluations were done 30, 57, and 103 days after carinata planting (DAP) * indicates that no regression model presented good fit for this data. Error bars represent the standard error of the mean (n=4). Full doses (1X) for imazapic and flumioxazin were applied at time zero using recommended label rates of 70 g ai ha^{-1} and 107 g ai ha^{-1}, respectively.

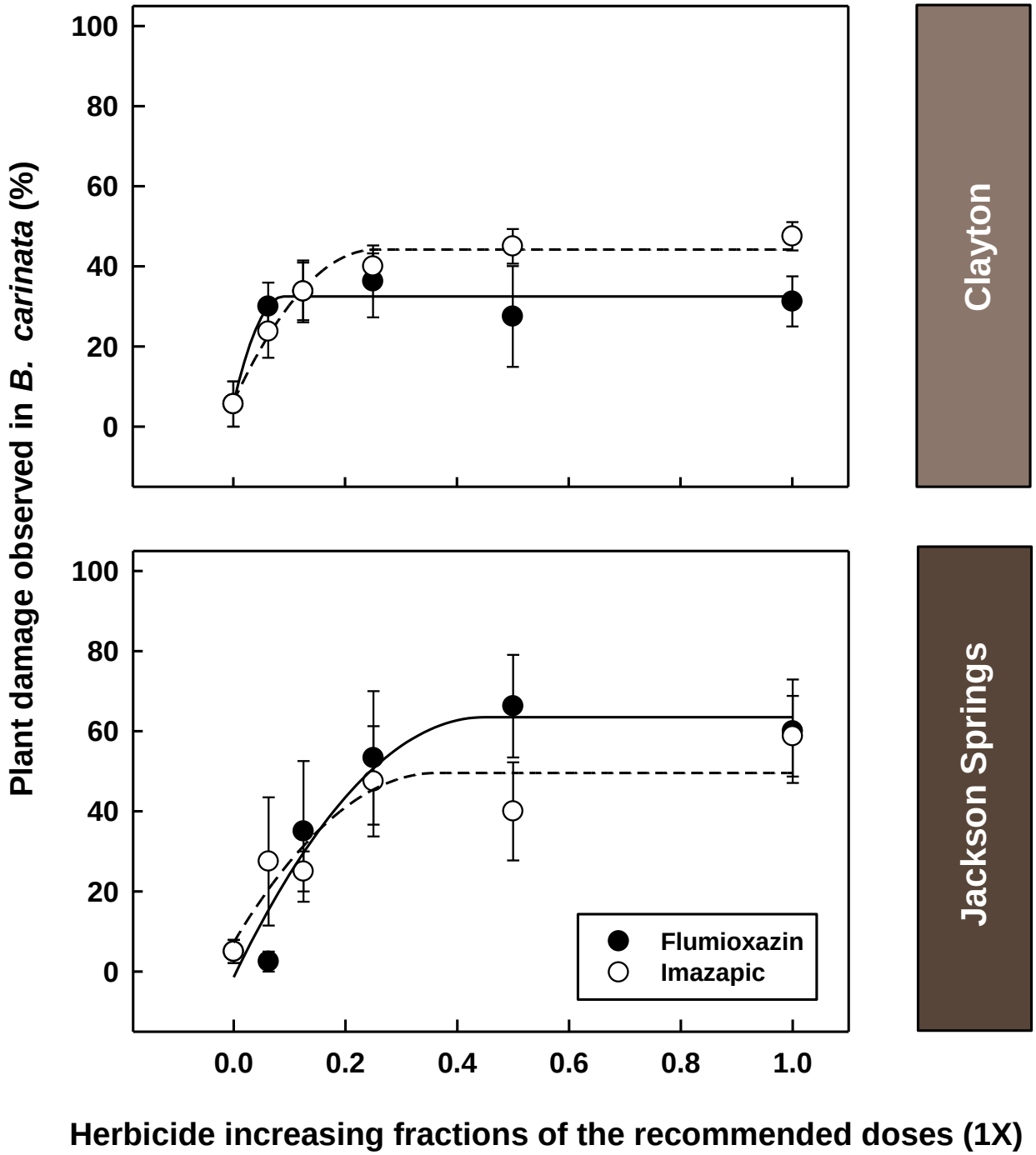

Figure 4.4 Plant damage at different soil depths in soil cores collected from two locations of North Carolina to evaluate the effect of increasing doses of two herbicides in *B. carinata*. Black solid and discontinuous lines represent the best-fit model for imazapic and flumioxazin, respectively. Error bars represent the standard error of the mean (n=4). Full doses (1X) for imazapic and flumioxazin were applied using recommended label rates of 70 g ai ha^{-1} and 107 g ai ha^{-1}, respectively.

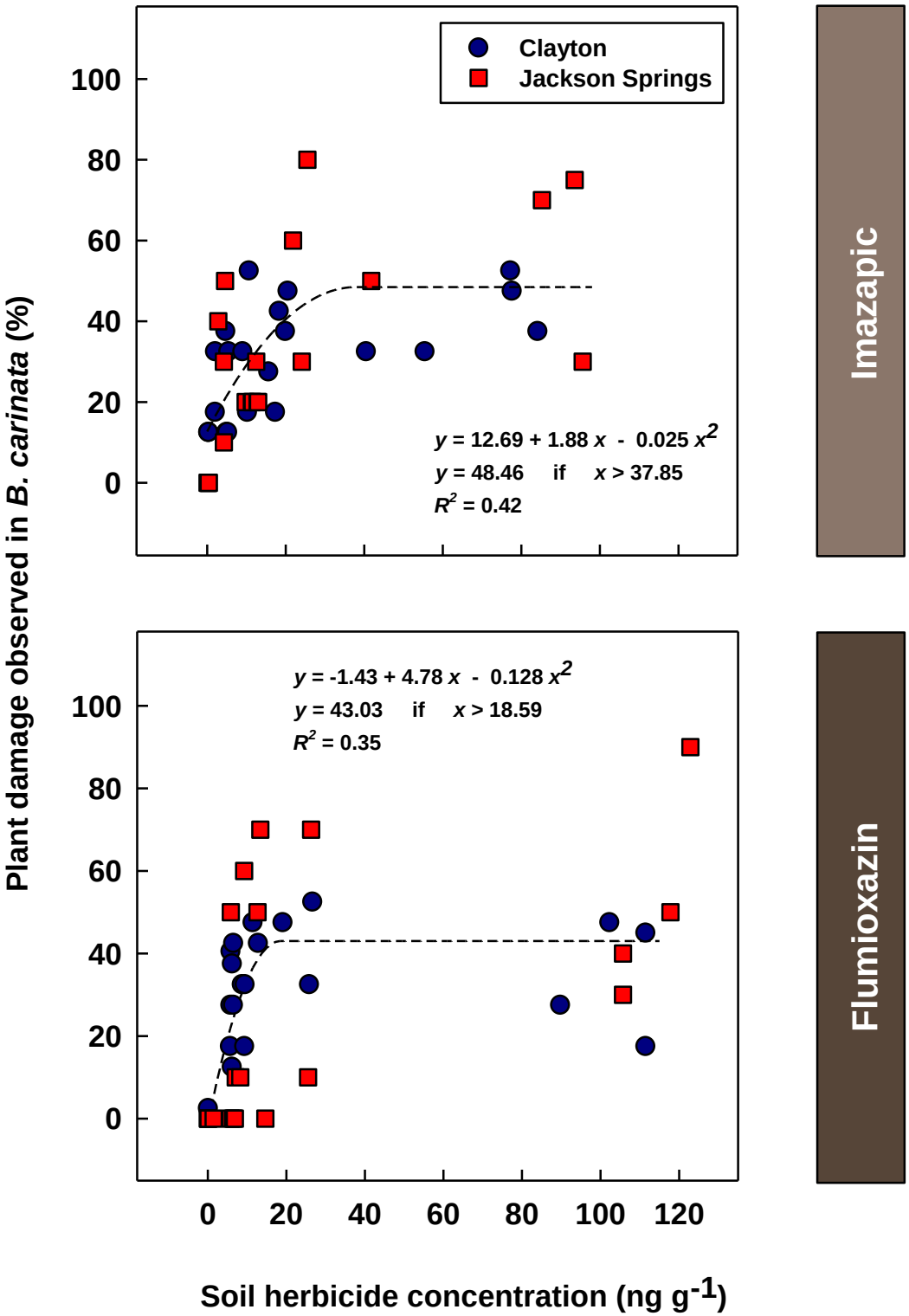

Figure 4.5 Soil herbicide recovered amount (expressed as concentration) and its effect on carinata plant damage observed in two locations of North Carolina. Black discontinuous lines represent the best-fit model selected for each herbicide.

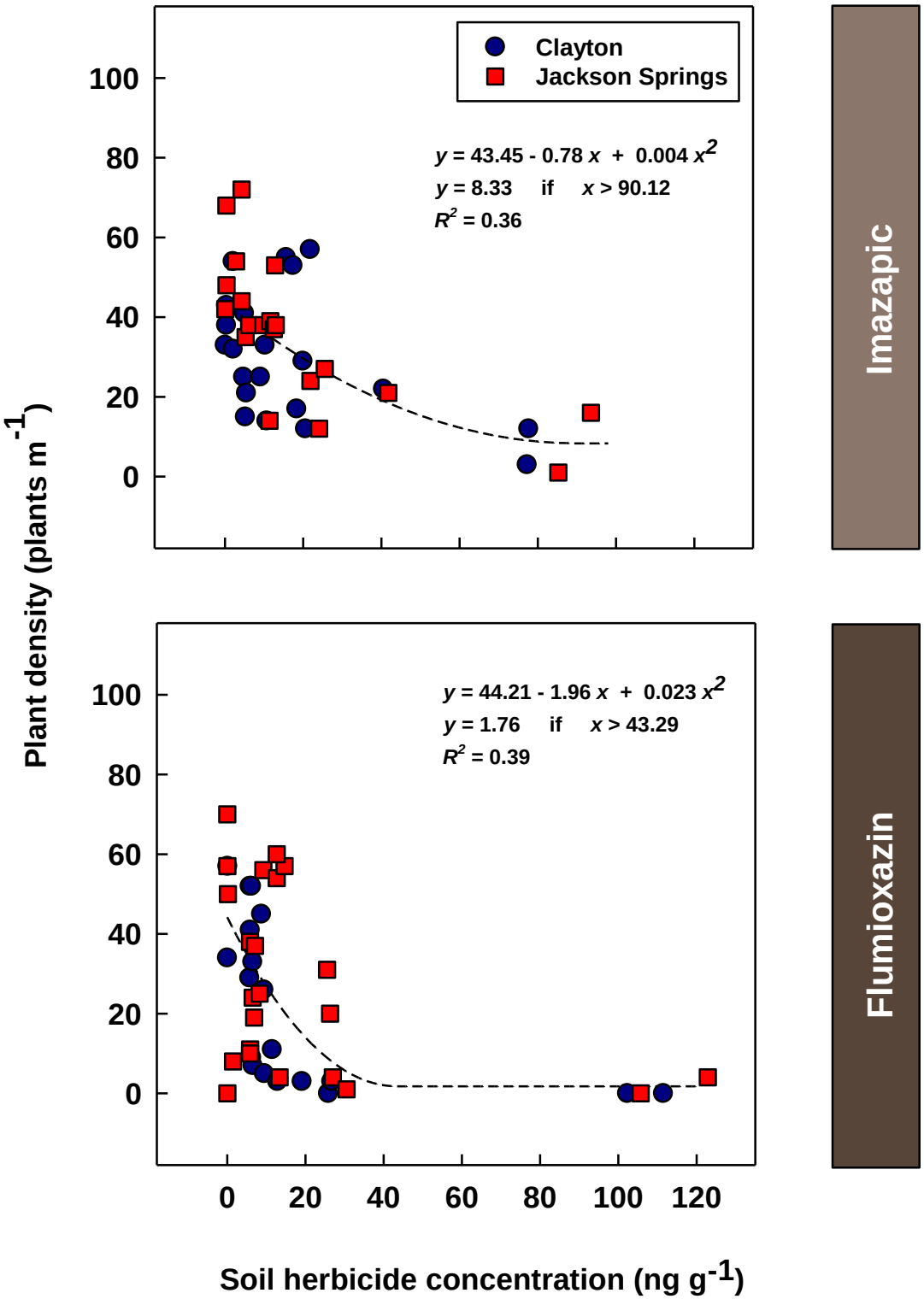

Figure 4.6 Soil herbicide recovered amount (expressed as concentration) and its effect on carinata plant density assessed in two locations of North Carolina. Black discontinuous lines represent the best-fit model selected for each herbicide.

CHAPTER 5: General conclusions and recommendations

The integration of soil physics to address weed management problems in agriculture is still an uncommon practice. In the previous three chapters of this dissertation, I was studied the effect of soil physical properties such as water potential and soil hydraulic conductivity on weed germination rate and seed total germination, fundamental biological processes controlling weed population dynamics. In addition, after conducting a field trial with a texture-anisotropic soil, I demonstrated the existence of solute lateral movement following the slope main direction using a conservative tracer, which represents a potentially important form off-target movement of pesticides. Furthermore, the dynamics of this lateral movement were described based on soil physical properties using numerical models. HYDRUS 2D/3D demonstrated to be a valuable tool to simulate solute fate as a result of lateral movement and has the potential for assessing herbicide fate in weed management. Finally, I described how carryover and leaching of two herbicides affecting carinata were associated to soil physical properties and the rainfall distribution, and how this information can be used to inform crop and weed management decisions such as crop rotation sequence and intervals.

Despite the practical advantages of using osmotic solutions as germination substrate to determine water potential requirements for germination, the present research clearly demonstrated that they do not accurately reproduce the how the edaphic environment supplies water to the seed during germination. For instance, PEG has been widely used to keep stable water potentials in germination studies but is limited just to represent a specific component within the complexity of the soil water dynamics and further effects on seed germination under filed conditions. Indeed, the seed germination variability in present study was better explained by soil unsaturated hydraulic conductivity. Consequently, assuming that an osmotic solution will

accurately represent the effect of soil conditions could lead to erroneous conclusions in further studies about population dynamics and plant ecology. Future studies contrasting the use of osmotic solutions and soils as germination substrate are recommended, extending this research approach to soils with textural class like clay or loamy sand, which were not covered in present study.

As it was hypothesized previously in the literature, the field experiment performed in the present dissertation to study lateral movement of solutes in soils with textural anisotropy provided empirical evidence for this type of movement. The results obtained in this field experiment remarks a new scope for solute movement and edaphic contamination, which studies traditionally have described the predominancy of soil vertical flow and its subsequent solute transport. In addition to the field observations, the use of numerical modeling was a valuable tool to describe and analyzed lateral movement in depth. In this respect, the simulations performed using HYDRUS 2D/3D were considered satisfactory because they approximated the values obtained from field measurements. Therefore, this software should be considered in further studies of lateral movement. Because the present study used a conservative tracer, it is necessary to expand our knowledge of solute lateral movement of organic molecules by conducting experiments that use actual pesticides as solute and different soil and landscape conditions. This information will greatly improve risk assessment studies for pesticide off-target movement by complementing existing models for leaching and runoff.

The results obtained in the carryover herbicide study revealed the pivotal role of soil physical properties in concurrence with the climatic conditions for crop safety after herbicide applications evidenced as differences observed in herbicide movement and persistence for the herbicides assessed under two different-textured soils. Therefore, special attention should be paid

to soil properties like organic matter content and texture before selecting the proper herbicides within the weed management strategy, as part of a well-designed crop rotation system. For instance, in coarser soils with low organic matter imazapic persistence will be greater than flumioxazin, which could present repercussions in further crop development, as observed in present study for carinata plants already established. It is recommended to replicate this experiment in other soils with textures such as clay (fine textural class) or soils with higher organic matter content, aiming to better describe how solute-soil particle interactions and soil water dynamics affect the persistence, distribution, and bioavailability of the herbicide. Finally, the carryover experiment conducted did not evaluate actual yield. Therefore, the results must be considered carefully in the context of safety during crop establishment. It is still possible that the rates identified here as injurious or safe might have a different impact on yield. However, this is unlikely because smaller plants are more susceptible to herbicides, and as time progresses the amount decreases in the soil as shown here. In any case, it will be important to confirm the impact of those rates on carinata yield with further herbicide carryover field studies.